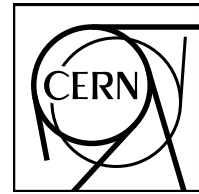


EUROPEAN ORGANISATION FOR NUCLEAR RESEARCH (CERN)



CERN-PH-EP-2012-052

Submitted to: Physical Review D

Search for supersymmetry in pp collisions at $\sqrt{s} = 7$ TeV in final states with missing transverse momentum and b -jets with the ATLAS detector

The ATLAS Collaboration

Abstract

The results of a search for supersymmetry in events with large missing transverse momentum and heavy flavour jets using an integrated luminosity corresponding to 2.05 fb^{-1} of pp collisions at $\sqrt{s} = 7 \text{ TeV}$ recorded with the ATLAS detector at the Large Hadron Collider are reported. No significant excess is observed with respect to the prediction for Standard Model processes. Results are interpreted in a variety of R -parity conserving models in which scalar bottoms and tops are the only scalar quarks to appear in the gluino decay cascade, and in an SO(10) model framework. Gluino masses up to 600–900 GeV are excluded, depending on the model considered.

Search for supersymmetry in pp collisions at $\sqrt{s} = 7$ TeV in final states with missing transverse momentum and b -jets with the ATLAS detector

The ATLAS Collaboration

The results of a search for supersymmetry in events with large missing transverse momentum and heavy flavour jets using an integrated luminosity corresponding to 2.05 fb^{-1} of pp collisions at $\sqrt{s} = 7$ TeV recorded with the ATLAS detector at the Large Hadron Collider are reported. No significant excess is observed with respect to the prediction for Standard Model processes. Results are interpreted in a variety of R -parity conserving models in which scalar bottoms and tops are the only scalar quarks to appear in the gluino decay cascade, and in an SO(10) model framework. Gluino masses up to 600–900 GeV are excluded, depending on the model considered.

PACS numbers: 12.60.Jv

I. INTRODUCTION

Supersymmetry (SUSY) [1–9] is a framework that provides an extension of the Standard Model (SM) and naturally resolves the hierarchy problem [10–13] by introducing supersymmetric partners of the known bosons and fermions. In the MSSM [14–18], which is an R -parity conserving minimal supersymmetric extension of the SM, SUSY particles are produced in pairs and the lightest supersymmetric particle (LSP) is stable, providing a possible candidate for dark matter. In a large variety of models, the LSP is the lightest neutralino, $\tilde{\chi}_1^0$. The coloured superpartners of quarks and gluons, the squarks (\tilde{q}) and gluinos (\tilde{g}), are expected to be produced in strong interaction processes at the centre-of-mass energy of the Large Hadron Collider (LHC). Their decays via cascades ending with the LSP would produce striking experimental signatures. The undetected LSP results in missing transverse momentum (its magnitude is referred to as E_T^{miss} in the following). The final states also contain multiple jets and possibly leptons. In the MSSM, the scalar partners of right-handed and left-handed quarks, \tilde{q}_R and \tilde{q}_L , can mix to form two mass eigenstates. The mixing effect is proportional to the corresponding SM fermion masses and therefore becomes important for the third generation. Large mixing can yield scalar bottom (sbottom, \tilde{b}_1) and scalar top (stop, \tilde{t}_1) mass eigenstates which are significantly lighter than other squarks. Consequently, \tilde{b}_1 and \tilde{t}_1 could be produced with large cross sections at the LHC, either directly in pairs, or through $\tilde{g}\tilde{g}$ production with subsequent $\tilde{g} \rightarrow \tilde{b}_1 b$ or $\tilde{g} \rightarrow \tilde{t}_1 t$ decays (gluino-mediated production).

In this paper, a search for scalar top and bottom quarks using an integrated luminosity corresponding to 2.05 fb^{-1} of $\sqrt{s} = 7$ TeV proton-proton collisions at the LHC, is presented. Events are selected by requiring large E_T^{miss} , several jets, including b -quark jets (b -jets), and either vetoing (0-lepton channel) or requiring (1-lepton channel) charged leptons. The search is mostly sensitive to the gluino-mediated production of third generation squarks. Results are interpreted in the framework of various simplified models in which scalar bottoms and tops are the only squarks that appear in the gluino decay cascade, and

in specific Grand Unification Theories (GUTs) based on the gauge group SO(10) [19, 20]. The GUT group SO(10) is especially compelling since it allows for gauge and matter unification. In the two SO(10) models considered in this paper, we also expect $t - b - \tau$ third generation Yukawa coupling unification at $Q = M_{\text{GUT}}$.

The paper is an update of a search presented by the ATLAS collaboration using 35 pb^{-1} of data collected in 2010 [21], with a number of improvements. The analysis has been extended by including more signal regions which profit from the increased available integrated luminosity and maximise the sensitivity to a large variety of SUSY scenarios. Data-driven methods are employed to estimate the contributions of SM background processes. Searches for scalar bottom quarks via $\tilde{g}\tilde{g}$ production have been also reported by the CMS [22] collaboration. Searches sensitive to direct scalar bottom production irrespective of gluino mass have been published by the ATLAS collaboration [23] using the same data-set employed in this paper.

II. THE ATLAS DETECTOR

The ATLAS detector [24] comprises an inner detector surrounded by a thin superconducting solenoid and a calorimeter system. Outside the calorimeters is an extensive muon spectrometer in a toroidal magnetic field.

The inner detector system is immersed in a 2 T axial magnetic field and provides tracking information for charged particles in a pseudorapidity range $|\eta| < 2.5$ [25]. The highest granularity is achieved around the vertex region using silicon pixel and microstrip (SCT) detectors. These detectors allow for an efficient tagging of jets originating from b -quark decays using impact parameter measurements and the reconstruction of secondary decay vertices. The transition radiation tracker (TRT), which surrounds the silicon detectors, contributes to track reconstruction up to $|\eta| = 2.0$ and improves electron identification by the detection of transition radiation.

The calorimeter system covers the pseudorapidity range $|\eta| < 4.9$. The highly-segmented electromagnetic calorimeter consists of lead absorbers with liquid argon

(LAr) as the active material and covers the pseudorapidity range $|\eta| < 3.2$. In the region $|\eta| < 1.8$, a pre-sampler detector using a thin layer of liquid argon is used to correct for the energy lost by electrons and photons upstream of the calorimeter. The hadronic tile calorimeter is a steel/scintillating-tile detector and is situated directly outside the envelope of the electromagnetic calorimeter. The two hadronic end-cap calorimeters have liquid argon as the active material, and copper absorbers. The calorimeter coverage is completed by forward calorimeters with liquid argon and copper and tungsten absorber material.

Muon detection is based on the deflection of muon tracks in the large superconducting air-core toroid magnets. Three eight-coil toroids, a barrel and two end-caps, generate the field for the muon spectrometer in the range $|\eta| < 2.7$. The toroids are instrumented with separate trigger and high-precision chambers.

III. MONTE CARLO SIMULATION

Simulated event samples are used to aid in the description of the background and to model the SUSY signal. Top quark pair and single top quark production are simulated with MC@NLO [26], fixing the top quark mass at 172.5 GeV, and using the next-to-leading-order (NLO) parton density function (PDF) set CTEQ6.6 [27]. Additional Monte Carlo (MC) samples generated with POWHEG [28] and ACERMC [29] are used to estimate the event generator systematic uncertainties. Samples of $W+\text{jets}$, $Z+\text{jets}$ with light and heavy flavour jets, and $t\bar{t}$ with additional b -jets, $t\bar{t}bb$, are generated with ALPGEN [30] and the PDF set CTEQ6L1 [31]. The fragmentation and hadronisation for the ALPGEN and MC@NLO samples are performed with HERWIG [32], using JIMMY [33] for the underlying event. Samples of $Zt\bar{t}$ and $Wt\bar{t}$ are generated with MADGRAPH [34] interfaced to PYTHIA [35]. Di-boson (WW , WZ , ZZ) samples are generated with HERWIG. The signal samples are generated using the HERWIG++ [36] v2.4.2 Monte Carlo program. The SUSY sample yields are normalised to the results of NLO calculations, as obtained using the PROSPINO [37] v2.1 program and the parameterisation of the PDFs is done with CTEQ6.6M [38]. The MC samples are produced using parameters tuned as described in Ref. [39, 40] and are processed through a detector simulation [41] based on GEANT4 [42]. The collision events considered in this search contain on average five proton-proton interactions per bunch crossing. This effect is included in the simulation, and MC events are reweighted to reproduce the mean expected number of collisions per bunch crossing estimated for data.

The background predictions, normalised to theoretical cross sections, including higher-order QCD corrections when available, are compared to data in control regions. The cross sections times branching ratio in the relevant final states used for each Standard Model background pro-

Physics process	$\sigma \cdot \text{BR}$ [nb] (perturbative order)	
$W \rightarrow \ell\nu$	31.4 (NNLO)	[45–47]
$Z/\gamma^* \rightarrow \ell^+\ell^-$	3.20 (NNLO)	[45–47]
$Z \rightarrow \nu\bar{\nu}$	5.82 (NNLO)	[45–47]
$t\bar{t}$	0.165 (NLO+NNLL)	[48–50]
Single top	0.085 (NLO+NNLL)	[48–50]
$t\bar{t}bb$	0.9×10^{-3} (LO)	[30]
$t\bar{t}+W/Z$	0.4×10^{-3} (LO)	[34]
WW , WZ , ZZ	0.071 (NLO)	[43, 44]

TABLE I: The most important background processes and their production cross sections, multiplied by the relevant branching ratios (BR). The ℓ indicates all three types of leptons (e , μ , τ) summed together. Contributions from higher order QCD corrections are included for W and Z boson production, for $t\bar{t}$ production and for di-boson production. The $Z/\gamma^* \rightarrow \ell^+\ell^-$ cross section is given for events with a di-lepton invariant mass of at least 40 GeV. The cross sections for $t\bar{t}bb$ and $t\bar{t}+W/Z$ production are given at leading order.

cess are listed in Table I. The W and Z/γ^* production processes are normalised to the next-to-next-to-leading order (NNLO) cross sections while the $t\bar{t}$ and single top production are normalised to the NLO+NNLL (next-to-next-to-leading logarithms) cross sections. The normalisation of the di-boson production is based on cross sections determined at NLO using MCFM [43, 44]. The $t\bar{t}$ production in association with W/Z or bb is normalised to LO.

For background from jet production from parton scattering processes (multi-jet in the following), no reliable prediction can be obtained from a leading-order Monte Carlo simulation and data-driven methods are used to determine the residual contributions of this background to the selected event samples, as discussed in Section VI.

IV. OBJECT RECONSTRUCTION

A pre-selection of electron and muon candidates is used to estimate the contribution from non-isolated leptons and misidentified electrons, to veto on additional leptons in the event when required, and to calculate the value of $E_{\text{T}}^{\text{miss}}$. More stringent identification criteria are then applied for the final selections.

Electrons are reconstructed from energy clusters in the electromagnetic calorimeter matched to a track in the inner detector. Candidates for the electron pre-selection must satisfy the “medium” [51] selection based on calorimeter shower shape, inner-detector track quality, and track-to-calorimeter cluster matching. Electrons used in the final selection are required to pass the “tight” [51] electron definition, which adds requirements on the ratio E/p between the calorimeter cluster energy E and the track momentum p , on the detection of tran-

sition radiation in the TRT, and on the isolation of the candidate. The scalar transverse momentum (p_T) sum of tracks within a cone in the η , ϕ plane of radius $\Delta R = 0.2$ around the electron candidate (excluding the electron track p_T itself), Σ_{p_T} , must be less than 10% of the electron p_T . Medium electrons are required to pass kinematic requirements of $p_T > 20$ GeV and $|\eta| < 2.47$, while the p_T threshold is raised to 25 GeV for tight electrons. In addition, electrons with a distance to the closest jet of $0.2 < \Delta R < 0.4$ are discarded.

Muons are identified as a match between an extrapolated inner detector track and one or more track segments in the muon spectrometer. A requirement on the minimum number of hits in each tracking device ensures the quality of the inner detector track reconstruction. Muons with a distance to the closest jet of $\Delta R < 0.4$ are discarded. In order to reject muons resulting from cosmic rays, tight criteria are applied on the proximity of the muon trajectories to the primary vertex (PV) [52]: $|z_\mu - z_{\text{PV}}| < 1$ mm and $|d_0| < 0.2$ mm, where z_μ is the z coordinate of the extrapolated muon track at the point of closest approach to the PV, z_{PV} is the coordinate of the PV, and $|d_0|$ is the magnitude of the impact parameter of the muon in the transverse plane. Pre-selected muons are required to satisfy all these requirements, and in addition to have $p_T > 10$ GeV and $\eta < 2.4$. For muons in the final selection, the p_T requirement is raised to 20 GeV and the muon is required to be isolated with $\Sigma_{p_T} < 1.8$ GeV.

Jets are reconstructed from three-dimensional calorimeter energy clusters by using the anti- k_t jet algorithm [53, 54] with a radius parameter of 0.4. The measured jet energy is corrected for inhomogeneities and for the non-compensating nature of the calorimeter by using p_T - and η -dependent correction factors [55]. Jets are required to have $p_T > 20$ GeV and $|\eta| < 2.8$. Events with jets failing jet quality criteria against noise and non-collision backgrounds are rejected. The quality criteria used are the same as in Ref. [55]. Additionally, in the 0-lepton channel the three leading jets, if central ($|\eta| < 2$), are required to have a jet charged fraction (defined as the scalar sum of the transverse momenta of the tracks associated with the jet divided by the jet p_T) of at least 5%. Jets within a distance of $\Delta R = 0.2$ of a pre-selected electron are rejected, since these jets are likely to be electrons also reconstructed as jets. For jets in the signal regions, the p_T requirement is tightened to 50 GeV to remove jets that are not associated with the hard scattering of interest.

A b -tagging algorithm exploiting both impact parameter and secondary vertex information [56] is used to identify jets containing a b -hadron decay. This algorithm has a 60% efficiency for tagging b -jets in a MC sample of $t\bar{t}$ events, with a mis-tag rate for light quarks and gluons of less than 1% and for c quarks of less than 10%. These b -jets are identified within the nominal acceptance of the inner detector ($|\eta| < 2.5$) and they are required to have $p_T > 50$ GeV.

The value of E_T^{miss} [57] is the magnitude of the vec-

tor \vec{E}_T^{miss} , which is calculated as the vector sum of the transverse momenta of all reconstructed jets with $p_T > 20$ GeV and $|\eta| < 4.5$, all preselected electrons and muons, and calorimeter energy clusters which do not belong to other reconstructed objects.

During a fraction of the data-taking period (about 40% of the total integrated luminosity), a localised electronics failure in the LAr barrel calorimeter created a dead region in the second and third calorimeter layers ($\Delta\eta \times \Delta\phi \simeq 1.4 \times 0.2$) in which on average 30% of the incident jet energy is not measured. Negligible impact is found on the reconstruction efficiency for jets with $p_T > 20$ GeV. For events selected during this data period, if any jet with $p_T > 50$ GeV falls in the aforementioned region, the event is rejected. The loss in signal acceptance is smaller than 10% in the affected period for the models considered.

In the event selection, a number of variables derived from the reconstructed objects are used. The transverse mass m_T formed by E_T^{miss} and the p_T of the lepton is defined as:

$$m_T = \sqrt{2p_T^{\text{lep}} E_T^{\text{miss}} - 2\vec{p}_T^{\text{lep}} \cdot \vec{E}_T^{\text{miss}}} \quad (1)$$

The effective mass m_{eff} is obtained as the scalar p_T sum of all selected objects in the event:

$$m_{\text{eff}} = \sum_i (p_T^{\text{jet}})_i + E_T^{\text{miss}} + \sum_j (p_T^{\text{lep}})_j \quad (2)$$

where the sums are over the number of jets, i , and the zero or one leptons, j , in a given signal region.

Finally, $\Delta\phi_{\min}$ is defined as the minimum azimuthal separation between the selected jets in a given signal region and the \vec{E}_T^{miss} direction.

V. EVENT SELECTION

This search uses proton-proton collisions recorded from March to August 2011 at a centre-of-mass energy of 7 TeV. After the application of beam, detector and data quality requirements, the data set consists of a total integrated luminosity of $2.05 \pm 0.08 \text{ fb}^{-1}$ [58, 59]. Two groups of signal regions are defined based on the presence, or otherwise, of a charged lepton ($\ell = e, \mu$) in the final state and are further referred to as 0-lepton and 1-lepton channels. In the 0-lepton channel, a veto on pre-selected leptons is applied, while exactly one lepton is required in the 1-lepton channel. Events containing two or more leptons are the subject of a different study [60].

The data are selected with a three-level trigger system. A trigger requiring a high transverse momentum jet and missing transverse momentum is used to select events for the 0-lepton channel. The plateau efficiency is reached for jets with $p_T > 130$ GeV and $E_T^{\text{miss}} > 130$ GeV. A single electron trigger, reaching the plateau efficiency for offline

electrons with $p_T \geq 25$ GeV, and a combined muon-jet trigger, reaching the plateau efficiency for muons with $p_T \geq 20$ GeV and jets with $p_T \geq 60$ GeV are used for the 1-lepton channel.

Events are required to have a reconstructed primary vertex associated with five or more tracks with $p_T > 0.4$ GeV, and must pass basic quality criteria against detector noise and non-collision backgrounds.

For the 0-lepton selection, at least one jet with $p_T > 130$ GeV, at least two additional jets with $p_T > 50$ GeV and $E_T^{\text{miss}} > 130$ GeV are required. At least one of the selected jets is required to be b -tagged. To reduce the amount of multi-jet background, where E_T^{miss} results from mis-reconstructed jets or from neutrinos emitted close to the direction of the jet axis, additional requirements of $\Delta\phi_{\min} > 0.4$ and $E_T^{\text{miss}}/m_{\text{eff}} > 0.25$ are applied.

Six signal regions are defined in order to obtain good signal sensitivity for the various models and parameter values studied. The regions are chosen by optimising the expected significance in models in which pair-produced gluinos decay with 100% branching ratio to on- and/or off-shell scalar bottom quarks. The signal regions are characterised by the minimum number of b -jets in the final state and by different thresholds on m_{eff} . The regions are labelled with the prefix SR0, and are listed in the upper section of Table II, together with a summary of the full selection applied.

For the 1-lepton channel, events are required to have exactly one lepton, a leading jet with $p_T > 60$ GeV, three further jets with $p_T > 50$ GeV, and $E_T^{\text{miss}} > 80$ GeV. At least one jet is required to be b -tagged. SM background processes that lead to the production of a W boson in the final state are rejected by requiring $m_T > 100$ GeV. Two signal regions, labelled with the prefix SR1 and summarised in Table II, are defined, based on different thresholds applied on the effective mass and the missing transverse momentum.

VI. BACKGROUND ESTIMATION

Standard Model processes contributing to the total background in the signal regions are top quark production (single and in pairs), the production of a W or a Z boson in association with heavy-flavour quarks (mostly b , but also c), and multi-jet production. The last enters in the signal regions if missing transverse momentum is produced in the final state, either because of the mismeasurement of one or more of the jets in the event, or because of the semileptonic decay of a heavy-flavour hadron.

Top and W/Z background estimation: The dominant SM background contributions to the signal regions are evaluated using control regions with low expected yields from the targeted SUSY signals. They are defined by selecting events containing exactly one lepton, large m_{eff} and low m_T . The background estimation in

each signal region is obtained by multiplying the number of events observed in the corresponding control region by a transfer factor, defined as the ratio of the MC predicted yield in the signal region to that in the control region:

$$N_{\text{SR}} = \frac{N_{\text{SR}}^{\text{MC}}}{N_{\text{CR}}^{\text{MC}}} (N_{\text{CR}}^{\text{obs}} - N_{\text{CR}}^{\text{res}}) = T_f (N_{\text{CR}}^{\text{obs}} - N_{\text{CR}}^{\text{res}}) \quad (3)$$

where $N_{\text{CR}}^{\text{obs}}$ denotes the observed yield in the control region and $N_{\text{CR}}^{\text{res}}$ includes contributions from multi-jet production and, in the 0-lepton case, W and Z production. The advantage of this approach is that systematic uncertainties that are correlated between the numerator and the denominator of T_f largely cancel out, provided that the event kinematics in the corresponding signal and control region are similar.

Two control regions are defined for the 0-lepton channel, differing only in the number of b -tags required. These are used to determine the top background in the six signal regions. They are obtained by applying the same thresholds on the three jets and E_T^{miss} as for the SR0, but requiring exactly one signal electron or muon. The transverse mass must be in the range $40 \text{ GeV} < m_T < 100 \text{ GeV}$ and the effective mass m_{eff} should be larger than 600 GeV. The region CR0-1 is required to have at least one b -tag, and CR0-2 is required to have at least two b -tags. The definition of the control regions for the 0-lepton channel is summarised in the upper part of Table III. Figures 1 and 2 show the E_T^{miss} and m_{eff} distributions obtained in CR0-1 and CR0-2 respectively, for the 1-electron and 1-muon case.

The formula used to obtain the top background prediction in each of the six signal regions is:

$$N_{\text{SR0-}\alpha j} = T_f^{\alpha j} (N_{\text{CR0-}j}^{\text{obs}} - N_{\text{CR0-}j}^{\text{non-top}}) \quad (4)$$

$$T_f^{\alpha j} = \frac{N_{\text{SR0-}\alpha j}^{\text{MC,top}}}{N_{\text{CR0-}j}^{\text{MC,top}}} \quad (5)$$

where $\alpha = A, B, C$, $j = 1, 2$ denote the six signal regions, $N_{\text{CR0-}j}^{\text{non-top}}$ includes the estimate for W, Z and multi-jet production in the control region j , and all numbers are the sum of the corresponding electron and muon channel yields.

The remaining SM contributions to the SR0 are mainly from W and Z production in association with heavy-flavour quarks. This corresponds to about 30% (10%) of the total background in the signal regions defined with one b -tag (two b -tags), and it is estimated from MC simulation.

For the 1-lepton channel signal regions, the total SM background (more than 90% of which consists of top quark production) is determined using a similar technique, but using one single transfer factor for top, W/Z and di-boson production processes. In this case, only one control region (CR1) is defined, requiring the same kinematic cuts applied in SR1-D, with the exception that the

Pre-selection	Signal Region name	Selection
no leptons, at least three jets, $p_T(j1) > 130 \text{ GeV}$, $p_T(j2, j3) > 50 \text{ GeV}$, $E_T^{\text{miss}} > 130 \text{ GeV}$, $E_T^{\text{miss}}/m_{\text{eff}} > 0.25$, $\Delta\phi_{\text{min}} > 0.4$	SR0-A1	at least one b -tag, $m_{\text{eff}} > 500 \text{ GeV}$
	SR0-B1	at least one b -tag, $m_{\text{eff}} > 700 \text{ GeV}$
	SR0-C1	at least one b -tag, $m_{\text{eff}} > 900 \text{ GeV}$
	SR0-A2	at least two b -tags, $m_{\text{eff}} > 500 \text{ GeV}$
	SR0-B2	at least two b -tags, $m_{\text{eff}} > 700 \text{ GeV}$
	SR0-C2	at least two b -tags, $m_{\text{eff}} > 900 \text{ GeV}$
one lepton, at least four jets $p_T(j1) > 60 \text{ GeV}$, $p_T(j2, j3, j4) > 50 \text{ GeV}$, $E_T^{\text{miss}} > 80 \text{ GeV}$, $m_T > 100 \text{ GeV}$, at least one b -tag	SR1-D SR1-E	$m_{\text{eff}} > 700 \text{ GeV}$ $m_{\text{eff}} > 700 \text{ GeV}$, $E_T^{\text{miss}} > 200 \text{ GeV}$

TABLE II: Signal regions definition for the 0-lepton and 1-lepton channels. The first column summarises the common pre-selection applied, while the last column specifies the selection defining the different signal regions.

Pre-selection	Control region name	Selection
one lepton, at least three jets $p_T(j1) > 130 \text{ GeV}$, $p_T(j2, j3) > 50 \text{ GeV}$, $E_T^{\text{miss}} > 130 \text{ GeV}$, $40 \text{ GeV} < m_T < 100 \text{ GeV}$, $m_{\text{eff}} > 600 \text{ GeV}$	CR0-1	at least one b -tag
	CR0-2	at least two b -tags
one lepton, at least four jets $p_T(j1) > 60 \text{ GeV}$, $p_T(j2, j3, j4) > 50 \text{ GeV}$, $E_T^{\text{miss}} > 80 \text{ GeV}$, $40 \text{ GeV} < m_T < 100 \text{ GeV}$, $m_{\text{eff}} > 500 \text{ GeV}$	CR1	at least one b -tag

TABLE III: Control regions definition for the 0-lepton and 1-lepton channels. The first column summarises the common pre-selection applied, while the last column specifies the selection defining the control regions.

Control Region	top	W/Z	multi-jet/ di-boson	SM	data (2.05 fb^{-1})
CR0-1 (1 e)	187	48	1	235 ± 45	217
CR0-1 (1 μ)	146	22	1	169 ± 45	177
CR0-2 (1 e)	53	2	0.1	55 ± 20	64
CR0-2 (1 μ)	42	3	0.1	45 ± 17	62
CR1 (1 e)	414	40	3.6	460 ± 100	465
CR1 (1 μ)	377	25	5.2	410 ± 110	420

TABLE IV: Expected background composition and comparison of the predicted total SM event yield to the measured event yield for 2.05 fb^{-1} for each of the control regions defined in the text. The column “Top” includes contributions from the single top, $t\bar{t}$, $t\bar{t}b\bar{b}$ and $t\bar{t} + W/Z$ production processes. The quoted uncertainty on the SM prediction includes only experimental systematic uncertainties (among which jet energy scale and b -tagging uncertainties are dominant).

transverse mass should be in the range $40 \text{ GeV} < m_T < 100 \text{ GeV}$ and that $m_{\text{eff}} > 500 \text{ GeV}$. The last row of Table III summarises the event selection for the 1-lepton control region. Figure 3 shows the E_T^{miss} and m_{eff} distributions in CR1.

Multi-jet background estimation: The small contribution of multi-jet background in the SR0 signal region is estimated with the use of a jet response smearing technique [61]. Multi-jet events with possibly large E_T^{miss} are obtained by smearing jet energies in low E_T^{miss} “seed”

events according to jet response functions obtained with the MC simulation. The Gaussian core of the response function is tuned to data by considering the jet balance in di-jet events, while its non-Gaussian tail is adapted to reproduce the response in three-jet events where the E_T^{miss} can be unambiguously associated to a single jet.

The number of multi-jet events in the CR0, CR1 control regions and SR1 signal regions is estimated using a matrix method similar to the one described in Ref. [62]. The probability of misidentifying a tight lepton is estimated by computing the probability that pre-selected leptons are identified as signal leptons in low- E_T^{miss} control regions dominated by multi-jet events.

Total Background: The number of expected events for 2.05 fb^{-1} of integrated luminosity as predicted by the MC and by the data-driven multi-jet estimate for all control regions is compared to that obtained in data in Table IV. The uncertainty quoted on the Standard Model prediction includes experimental systematic uncertainties (jet energy scale and resolution, b -tagging efficiency, lepton identification and energy scale, and luminosity determination).

Further selection regions are used to validate the MC prediction in different kinematic regimes (in particular for small and large values of m_T at low value of m_{eff} , for both the 0-lepton and 1-lepton channels). In all cases, a good agreement between the data and MC predictions is found.

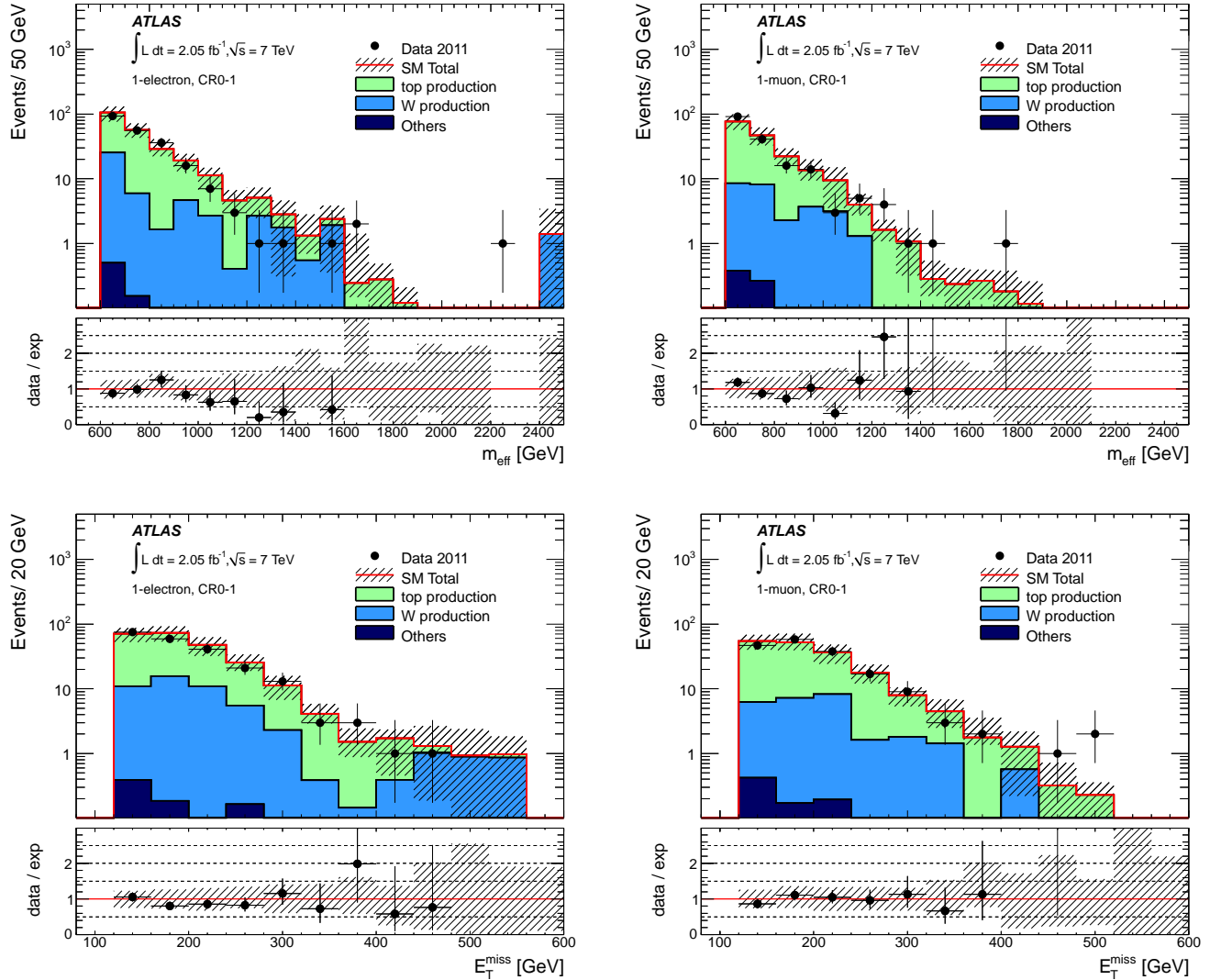


FIG. 1: Distribution of the effective mass (top) and E_T^{miss} (bottom) in the CR0-1 control region for the 1-electron (left) and 1-muon (right) channels. The colour labelled “Others” includes contributions from Z , di-boson and multi-jet production processes. The hatched band shows the systematic uncertainty, which includes both experimental uncertainties (among which JES and b -tagging uncertainties are dominant) and theoretical uncertainties on the background normalisation and shape. The small insets show the ratio between the observed distribution and that predicted for the Standard Model background. Although the distributions are presented separately for e and μ , the background estimation uses the sum of the e and μ yields in the CR0.

VII. SYSTEMATIC UNCERTAINTIES ON BACKGROUND ESTIMATION

Various systematic uncertainties affecting the background rates in the signal regions have been considered. Their treatment is discussed in the following paragraphs, and their impact on the absolute predicted event yield in the control and signal regions is evaluated. Such uncertainties are used either directly (W, Z for the 0-lepton channel) in the evaluation of the predicted background in the signal regions, or to compute the T_f . In the latter case, the uncertainties on the absolute predicted event

yield in the control regions and signal regions are propagated using Eq. 3 to obtain the signal region uncertainties.

Experimental systematic uncertainties arise from several sources:

Jet energy scale and resolution uncertainty:

The uncertainty on the jet energy scale (JES), derived using single particle response and test beam data, varies as a function of the jet p_T and pseudorapidity and it is about 2% at $p_T = 50$ GeV in the central detector region. Additional systematic uncertainties arise from the dependence of the jet response on the number of expected in-

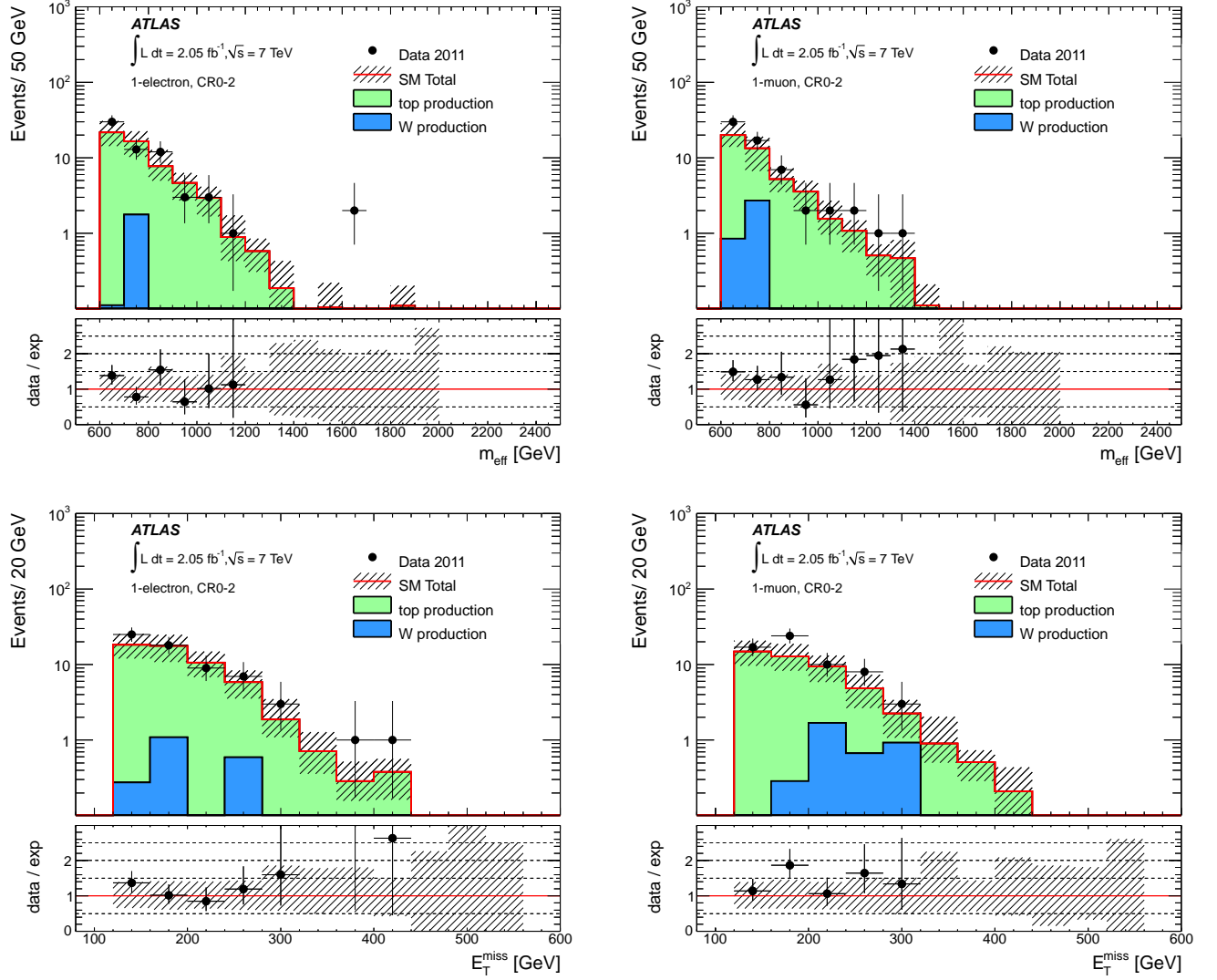


FIG. 2: Distribution of the effective mass (top) and E_T^{miss} (bottom) in the CR0-2 control region for the 1-electron (left) and 1-muon (right) channels. The hatched band shows the systematic uncertainty, which includes both experimental uncertainties (among which JES and b -tagging uncertainties are dominant) and theoretical uncertainties on the background normalisation and shape. The small insets show the ratio between the observed distribution and that predicted for the Standard Model background. Although the distributions are presented separately for e and μ , the background estimation uses the sum of the e and μ yields in the CR0.

teractions per bunch crossing and on the jet flavour. The total jet energy scale uncertainty at $p_T = 50$ GeV in the central detector region is about 5% [55]. The jet energy scale uncertainty is propagated to obtain an uncertainty on the event yield by varying it by $\pm 1\sigma$ in the MC simulation. Uncertainties related to the jet energy resolution (JER) are obtained with an in-situ measurement of the jet response asymmetry in di-jet events [63]. Their impact on the event yield is estimated by applying an additional smearing to the jet transverse momenta. The JES and JER relative uncertainties on the event yield amount to a total of 20-40% (depending on the signal region) and are completely dominated by the JES uncertainty.

b -tagging efficiency and mis-tagging uncertainties: The uncertainty associated with the tagging procedure used to identify b -jets is evaluated by varying the b -tagging efficiency and mis-tagging rates within the uncertainties evaluated on the central values measured in-situ [56]. The resulting relative uncertainty on the event yield is about 20% (35%) in the one b -tag (two b -tags) signal region.

Further experimental uncertainties: Other systematic uncertainties arise from the imperfect knowledge of the lepton identification efficiency and energy scale, the rate of lepton misidentification and from the luminosity determination. Their contribution to the

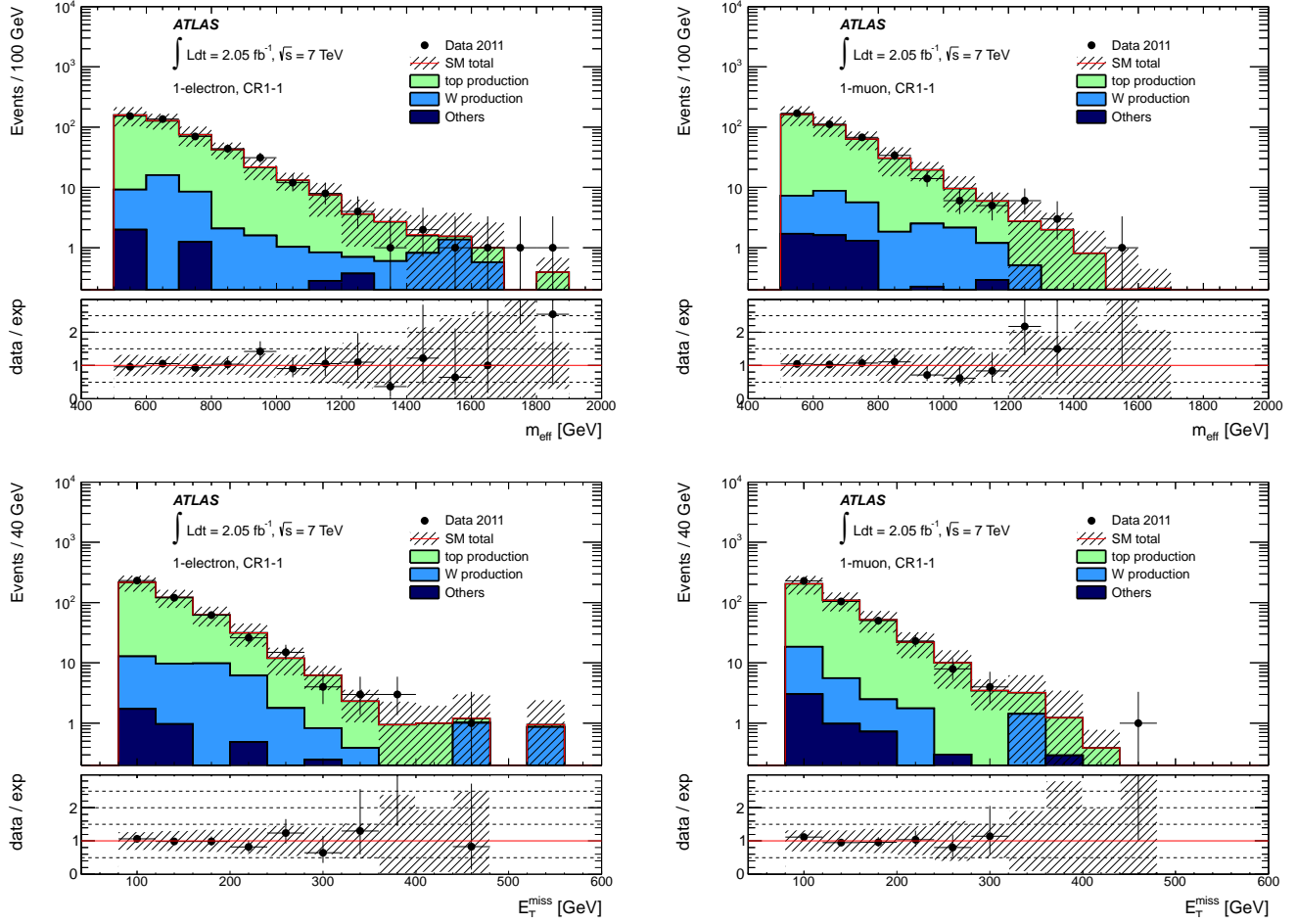


FIG. 3: Distribution of the effective mass (top) and E_T^{miss} (bottom) in the CR1 control region for the 1-electron (left) and 1-muon (right) channels. The colour labelled “Others” includes contributions from Z , di-boson and multi-jet production processes. The hatched band shows the systematic uncertainty, which includes both experimental uncertainties (among which JES and b -tagging uncertainties are dominant) and theoretical uncertainties on the background normalisation and shape. The small insets show the ratio between the observed distribution and that predicted for the Standard Model background.

final uncertainty is found to be negligibly small.

All the experimental systematic uncertainties are included, together with process-specific uncertainties, in the evaluation of the background uncertainty:

Multi-jet background: The systematic uncertainty on the estimation of the multi-jet background in the SR0 is determined by taking into account statistical uncertainties and possible biases in the selection of the seed events, as well as uncertainties in the tuning of the tail of the jet response function in the three-jet events. The relative uncertainty varies between 50% and 70% depending on the SR0 considered.

The estimated multi-jet background in the SR1 is affected by systematic uncertainties related to the determination of the lepton misidentification rate and to the subtraction of non-multi-jet contributions to the event yield in the multi-jet enhanced region. The estimated relative

uncertainty is 90% in SR1-D and 100% and SR1-E.

W and Z production processes: Systematic uncertainties on W and Z production are evaluated by varying the relative cross sections of the samples generated with the ALPGEN MC with different numbers of outgoing partons [64], resulting in an uncertainty of about 30%. Additional uncertainties of about 70% on the production cross section of W and Z bosons in association with b -quarks are considered. They are derived from direct measurements [23, 65], and extrapolated using the MC simulation to include differences in the phase space regions probed by this analysis. Uncertainties related to the parton density function choice have been evaluated and found to be small compared to the large uncertainty already considered.

Top production processes: Theoretical uncertainties on the shape of $t\bar{t}$ and single top kinematic distributions are evaluated by comparing different LO

SR	JES/ JER	<i>b</i> -tag	lepton ID	theory	others	total
SR0-A1	4	3	2	11	10	15
SR0-B1	3	3	2	20	10	22
SR0-C1	3	4	2	35	11	37
SR0-A2	3	3	2	15	11	19
SR0-B2	3	4	2	20	10	22
SR0-C2	3	2	2	30	12	32
SR1-D	6	1	1	34	7	35
SR1-E	7	1	1	53	10	55

TABLE V: Relative systematic uncertainties (in percent) associated with the background estimated by using transfer factors for all the signal regions considered. The column “others” includes statistical uncertainties on the event yield in the control regions, and, in the case of the 0-lepton channel, systematic uncertainties on the non-top production contributions subtracted from the control regions. The column “theory” contains theoretical uncertainties on the top production process addressed as discussed in the text.

and NLO generators (**ALPGEN** or **POWHEG**, the latter using both **PYTHIA** and **HERWIG** as parton shower), and using different parton shower tunes, still consistent with data from previous experiments [64]. An additional uncertainty of 100% is considered for $t\bar{t}$ production in association with $b\bar{b}$ or W/Z .

The T_f , used for the top and total SM background determination in the SR0 and SR1, respectively, are computed using MC predictions. Their values span from 1.8 to 0.05 depending on the signal region considered. Their associated uncertainty arises from both experimental (JES and JER, *b*-tagging efficiency and fake rate, lepton identification and energy scale) and event-generator level uncertainties. The use of control regions with similar kinematical properties to those of the signal regions strongly suppresses experimental uncertainties. Theoretical uncertainties typically dominate the total uncertainty on the T_f , which varies between 15% and 35%.

A summary of the systematic uncertainties for the background estimates with the use of transfer factors is shown in Table V.

VIII. RESULTS

The m_{eff} and $E_{\text{T}}^{\text{miss}}$ distributions are shown in Figure 4 for SR0-A1 and SR0-A2, and in Figure 5 for SR1-D. Tables VI and VII show the Standard Model background predictions and the observed number of events corresponding to 2.05 fb^{-1} in all signal regions. The top background in the 0-lepton signal regions is estimated making use of the transfer factors, and its uncertainty corresponds to the total systematic uncertainty of Table V. In parentheses, the MC prediction is reported for comparison. The W/Z background and uncertainty in

the SR0 are estimated directly with the MC simulation. The multi-jet background contribution in the SR0, obtained with a data-driven estimate, is summed together with that of di-boson background. The SM background uncertainty in the SR1 corresponds to the total systematic uncertainty of Table V, plus a small contribution arising from the data-driven estimate of the multi-jet background.

SR	Top	W/Z	multi-jet/ di-boson	Total	Data
SR0-A1	705 ± 110 (725)	248 ± 150	53 ± 21	1000 ± 180	1112
SR0-B1	119 ± 26 (122)	67 ± 42	7.3 ± 4.7	190 ± 50	197
SR0-C1	22 ± 8 (22)	16 ± 11	1.5 ± 1	39 ± 14	34
SR0-A2	272 ± 52 (212)	23 ± 15	21 ± 12	316 ± 54	299
SR0-B2	47 ± 10 (37)	4.5 ± 3	2.8 ± 1.7	54 ± 11	43
SR0-C2	8.5 ± 3 (6.6)	0.8 ± 1	0.5 ± 0.4	9.8 ± 3.2	8

TABLE VI: Summary of the expected and observed event yields corresponding to 2.05 fb^{-1} in the six 0-lepton channel signal regions. The errors on the top contribution correspond to the total errors of Table V. The errors quoted for all background processes include all the systematic uncertainties discussed in the text. The numbers in parentheses in the “Top” column are the yields predicted by the MC simulation.

SR	SM background	Data
SR1-D (e)	39 ± 12 (39)	43
SR1-D (μ)	38 ± 14 (37)	38
SR1-E (e)	8.1 ± 3.4 (7.9)	11
SR1-E (μ)	6.3 ± 4.2 (6.1)	6

TABLE VII: Summary of the expected and observed event yields corresponding to 2.05 fb^{-1} in the two 1-lepton channel signal regions. The Standard Model estimation is derived with the data-driven method discussed in the text. The numbers in parentheses in the “SM background” column are the sum of the yield predicted by the MC and the data-driven estimate for the multi-jet background.

The results are consistent with the Standard Model predictions, and they are therefore translated into 95% confidence-level (CL) upper limits on contributions from new physics using the CL_s prescription [66]. The likelihood function used is written as $L(n|s, b, \theta) = P_s \times C_{\text{Syst}}$; where n represents the number of observed events in data, s is the SUSY signal under consideration, b is the background, and θ represents the systematic uncertainties. The P_s function is a Poisson-probability distribution for event counts in the defined signal region and C_{Syst} repre-

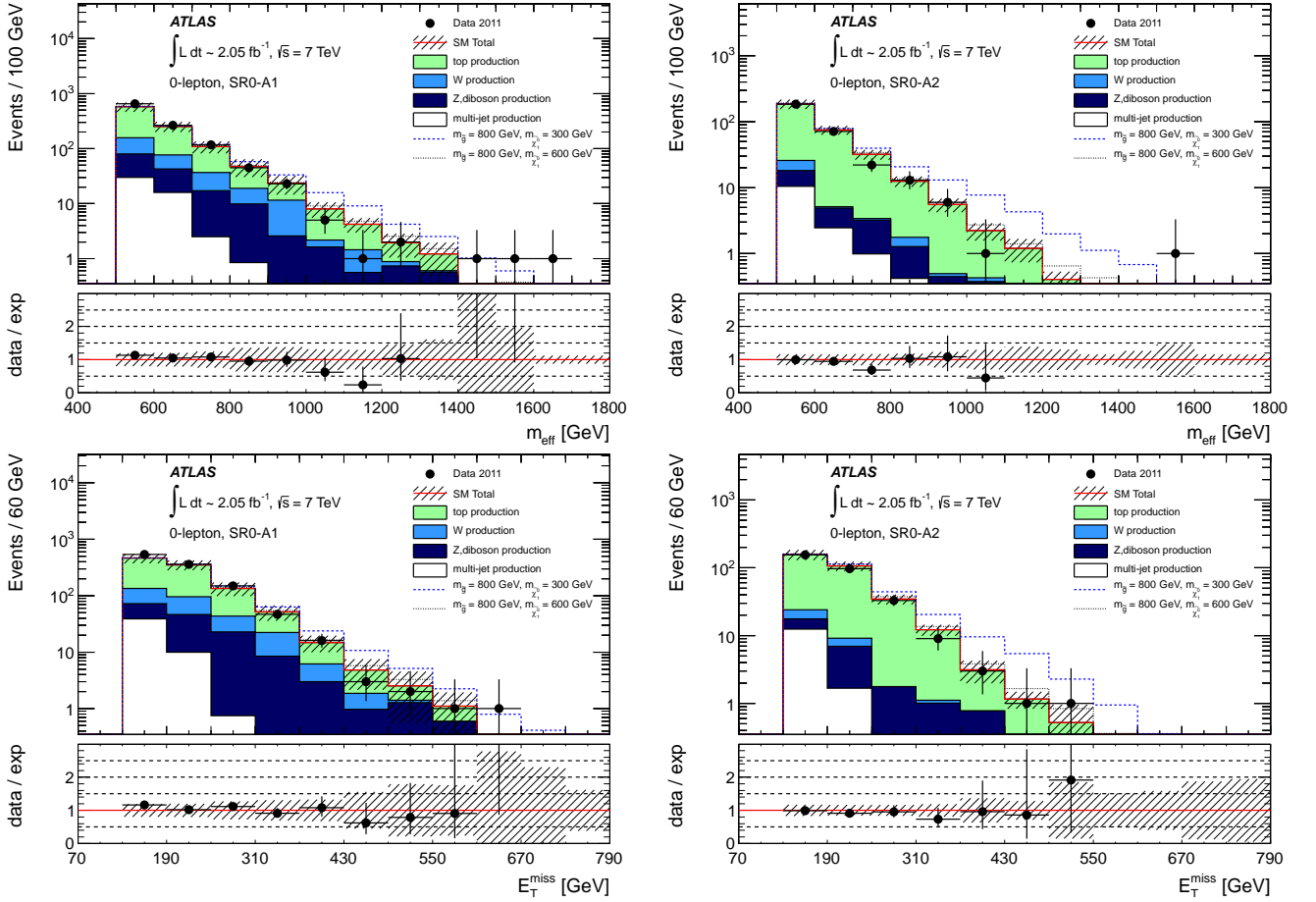


FIG. 4: Distribution of the effective mass (top) and E_T^{miss} (bottom) in SR0-A1 (left) and SR0-A2 (right). The hatched band shows the systematic uncertainty, which includes both experimental uncertainties (among which JES and b -tagging uncertainties are dominant) and theoretical uncertainties on the background normalisation and shape. The small insets show the ratio between the observed distribution and that predicted for the Standard Model background.

sents the constraints on systematic uncertainties, which are treated as nuisance parameters with a Gaussian probability density function and correlated when appropriate.

Upper limits at 95% CL on the number of signal events in the signal regions are obtained independently of new physics models and assuming no signal contamination in the control regions for the 0-lepton and 1-lepton final states. Results for observed and expected upper limits on the number of non-SM events in the signal regions are shown in Table VIII, as well as upper limits on the visible cross section, σ_{vis} , defined as cross section times experimental acceptance and efficiency.

IX. INTERPRETATION IN SIMPLIFIED SUSY MODELS

The interpretation of the results in terms of 95% CL exclusion limits are given for several SUSY scenarios. The exclusion limit contours are derived by subtracting possible signal contributions from the data yield in the con-

SR	95% CL upper limit	
	N events obs. (exp.)	$\sigma_{\text{vis}}(\text{fb})$ obs. (exp.)
SR0-A1	580 (520)	283 (254)
SR0-B1	133 (133)	65 (65)
SR0-C1	31.6 (34.6)	15.4 (16.9)
SR0-A2	124 (134)	61 (66)
SR0-B2	29.6 (31.0)	14.4 (15.0)
SR0-C2	8.9 (10.3)	4.3 (5.0)
SR1-D	45.5 (42.1)	22.2 (20.5)
SR1-E	17.5 (15.3)	8.5 (7.5)

TABLE VIII: Observed and expected 95% CL upper limits on the non-SM contributions to all signal regions. Limits are given on the number of signal events and in terms of visible cross sections. No assumptions are made on the possible presence of non-SM signal in the control regions. The systematic uncertainties on the SM background estimation are included.

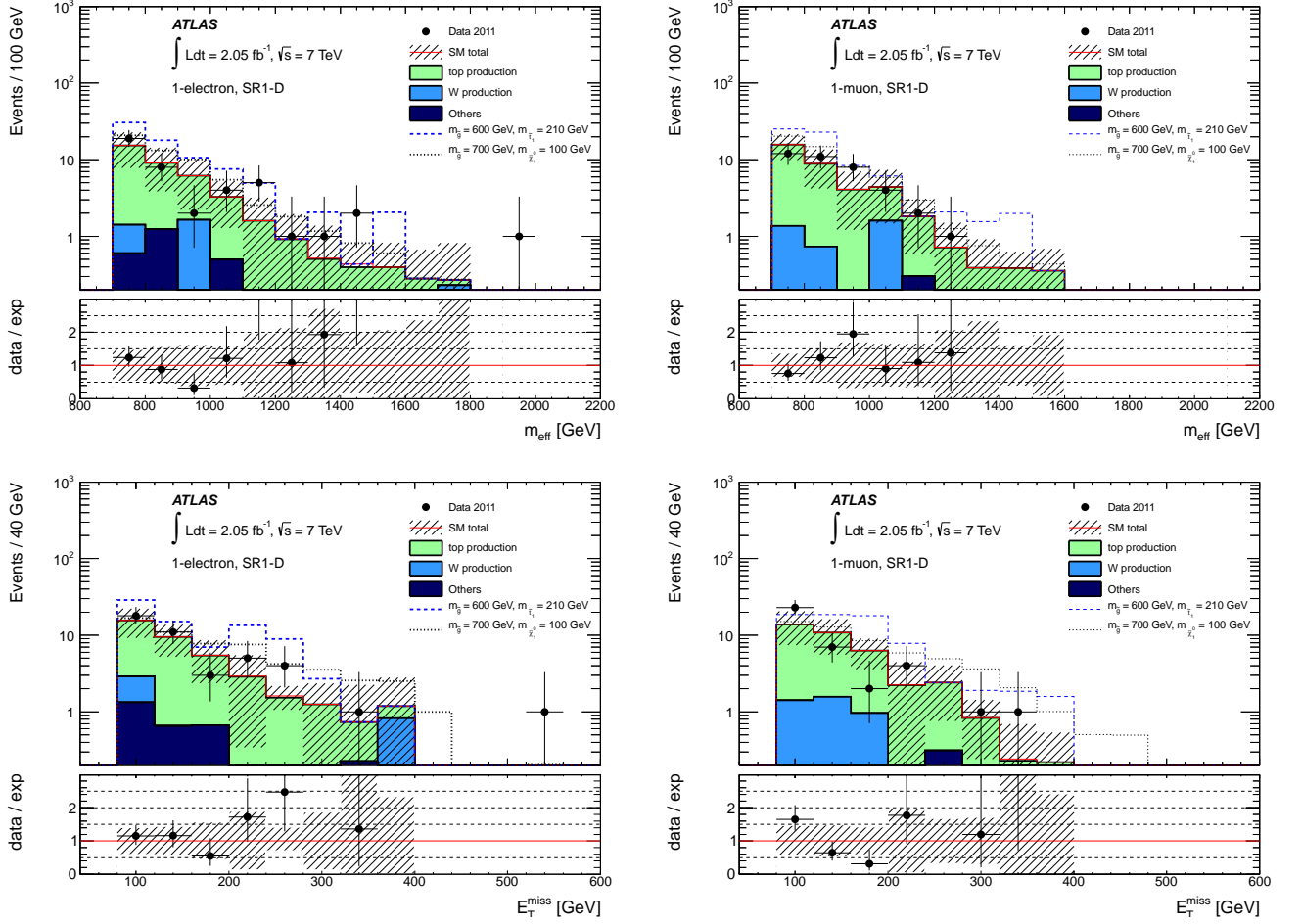


FIG. 5: Distribution of the effective mass (top) and E_T^{miss} (bottom) for the 1-electron (left) and 1-muon (right) channel in SR1-D. The color labelled ‘‘Others’’ includes contributions from Z , di-boson and multi-jet production processes. The hatched band shows the systematic uncertainty, which includes both experimental uncertainties (among which JES and b -tagging uncertainties are dominant) and theoretical uncertainties on the background normalisation and shape. The small insets show the ratio between the observed distribution and that predicted for the Standard Model background.

trol regions employed to estimate the SM background. The signal contamination is not negligible only for SUSY models leading to leptonic final states and accounts for less than 5% of the SM predictions around the expected exclusion limit contours.

Simplified models are characterised by well-defined SUSY particle production and decay modes yielding the final states under study. In the scenarios considered here scalar bottoms and tops are the only squarks to appear in the gluino decay cascade, leading to final states with large b -jet multiplicity. The models listed below are addressed (in parenthesis the channel which is used for the interpretation of the result is given):

Gluino-sbottom models (0-lepton): MSSM scenarios where the \tilde{b}_1 is the lightest squark, all other squarks are heavier than the gluino, and $m_{\tilde{g}} > m_{\tilde{b}_1} > m_{\tilde{\chi}_1^0}$, such that the branching ratio for $\tilde{g} \rightarrow \tilde{b}_1 b$ decays is

100%. Sbottoms are produced via $\tilde{g}\tilde{g}$ or by direct pair production $\tilde{b}_1\tilde{b}_1$ and are assumed to decay exclusively via $\tilde{b}_1 \rightarrow b\tilde{\chi}_1^0$, where $m_{\tilde{\chi}_1^0}$ is set to 60 GeV. Exclusion limits are presented in the $(m_{\tilde{g}}, m_{\tilde{b}_1})$ plane.

Gbb models (0-lepton): Simplified scenarios, where \tilde{b}_1 is the lightest squark but $m_{\tilde{g}} < m_{\tilde{b}_1}$. Pair production of gluinos is the only process taken into account since the mass of all other sparticles apart from the $\tilde{\chi}_1^0$ is set above the TeV scale. A three-body decay via off-shell sbottom is assumed for gluino, such that $\tilde{b}_1^{(*)} \rightarrow b\tilde{\chi}_1^0$ ($\text{BR}=100\%$ for $\tilde{g} \rightarrow b\bar{b}\tilde{\chi}_1^0$). Exclusion limits are presented in the $(m_{\tilde{g}}, m_{\tilde{\chi}_1^0})$ plane.

Gluino-stop models (1-lepton): MSSM scenarios where the \tilde{t}_1 is the lightest squark, all other squarks are heavier than the gluino, and $m_{\tilde{g}} > m_{\tilde{t}_1} + m_t$, such that the branching ratio for $\tilde{g} \rightarrow \tilde{t}_1 t$ decays is 100%. Stops

are produced via $\tilde{g}\tilde{g}$ and $\tilde{t}_1\tilde{t}_1$ and are assumed to decay exclusively via $\tilde{t}_1 \rightarrow b\tilde{\chi}_1^\pm$. The neutralino mass is set to 60 GeV, the chargino mass to 120 GeV and the latter is assumed to decay through a virtual W boson ($\text{BR}(\tilde{\chi}_1^\pm \rightarrow \tilde{\chi}_1^0 l^\pm \nu) = 11\%$). If $m_{\tilde{t}_1} > m_{\tilde{\chi}_1^0} + m_t$, the decay $\tilde{t}_1 \rightarrow t\tilde{\chi}_1^0$ is also kinematically allowed, with BR depending on the MSSM parameters settings. However, this mode is not considered for this interpretation, leading to conservative results, and is adopted in the Gtt scenario, described below. Exclusion limits are presented in the $(m_{\tilde{g}}, m_{\tilde{t}_1})$ plane.

Gtt models (1-lepton): Simplified scenarios, where \tilde{t}_1 is the lightest squark but $m_{\tilde{g}} < m_{\tilde{t}_1}$. Pair production of gluinos is the only process taken into account since the mass of all other sparticles apart from the $\tilde{\chi}_1^0$ is set above the TeV scale. A three-body decay via off-shell stop is assumed for the gluino, such that $\tilde{t}_1^{(*)} \rightarrow t\tilde{\chi}_1^0$ ($\text{BR}=100\%$ for $\tilde{g} \rightarrow t\bar{t}\tilde{\chi}_1^0$). Exclusion limits are presented in the $(m_{\tilde{g}}, m_{\tilde{\chi}_1^0})$ plane.

Gtb models (1-lepton): Simplified scenarios, where \tilde{b}_1 and \tilde{t}_1 are the lightest squarks but $m_{\tilde{g}} < m_{\tilde{b}_1, \tilde{t}_1}$. As for the models above, pair production of gluinos is the only process taken into account, with gluinos decaying via virtual stops or sbottoms with a BR of 100% assumed for $\tilde{t}_1 \rightarrow b + \tilde{\chi}_1^\pm$ and $\tilde{b}_1 \rightarrow t + \tilde{\chi}_1^\pm$, respectively. The mass difference between charginos and neutralinos is set to 2 GeV, such that the products of $\tilde{\chi}_1^\pm \rightarrow \tilde{\chi}_1^0 + ff'$ are invisible to the event selection, and gluino decays result in three-body final states ($b\bar{t}\tilde{\chi}_1^0$ or $t\bar{b}\tilde{\chi}_1^0$). Exclusion limits are presented in the $(m_{\tilde{g}}, m_{\tilde{\chi}_1^0})$ plane.

The 0-lepton analysis is mostly sensitive to the SUSY scenarios where sbottom production dominates, whilst the 1-lepton analysis results are employed to set exclusion limits in models characterised by on-shell or off-shell stop production, where top-enriched final states are expected. Since several signal regions are defined for each analysis, the SR with the best expected sensitivity at each point in parameter space is adopted as the nominal result across the different planes.

The efficiency times acceptance of the selection strongly depends on the parameters of the model and the signal region considered. It varies between 5% and 50% in the proximity of the expected limit for the gluino-sbottom model. For the Gbb models, the efficiency times acceptance is highly dependent on the difference in mass between the gluino and the neutralino. It is about 1% for a mass difference of about 200 GeV, and it increases up to 45% for larger mass splitting. In the Gtb , gluino-stop and Gtt models, the efficiency times acceptance varies typically between 1 and 20% in the proximity of the expected limit.

Systematic uncertainties on the signal include experimental (JES, JER, b -tagging) and theoretical uncertainties. Experimental uncertainties are considered fully correlated with those obtained for the background, and they

typically amount to 10-30% depending on the signal region and model considered. Theoretical uncertainties on the expected SUSY signal are estimated by varying the factorisation and renormalisation scales in PROSPINO between half and twice their default values and by considering the PDF uncertainties provided by CTEQ6. Uncertainties are calculated for individual production processes and are typically 20-35% in the vicinity of the expected limit.

Figure 6 shows the observed and expected exclusion regions in the $(m_{\tilde{g}}, m_{\tilde{b}_1})$ plane for the gluino-sbottom model. The selection SR0-C2 provides the best sensitivity in most cases. If $m_{\tilde{g}} - m_{\tilde{b}_1} < 100$ GeV, signal regions with one b -tag are preferred, due to the lower number of expected b -jets above p_T thresholds. Gluino masses below 920 GeV are excluded for sbottom masses up to about 800 GeV. The exclusion is less stringent in the region with low $m_{\tilde{g}} - m_{\tilde{b}_1}$, where low E_T^{miss} is expected. This search extends the previous ATLAS exclusion limit in the same scenario by about 200 GeV, and it is complementary to direct searches for sbottom pair production published by the ATLAS collaboration [23] using the same data-set. The limits do not strongly depend on the neutralino mass assumption as long as $m_{\tilde{g}} - m_{\tilde{\chi}_0}$ is larger than 300 GeV, due to the harsh kinematic cuts.

The interpretation of the results in the Gbb models, defined in the $(m_{\tilde{g}}, m_{\tilde{\chi}_1^0})$ plane at sbottom mass larger than 1 TeV, can be considered complementary to the previous one, defined in $m_{\tilde{g}}, m_{\tilde{b}_1}$ at fixed $\tilde{\chi}_1^0$ mass. Figure 7 shows the expected and observed exclusion limit contours and the maximum 95% upper cross section limit for each model. Gluino masses below 900 GeV are excluded for neutralino masses up to about 300 GeV.

Figures 8 to 10 report the interpretations of the 1-lepton analysis results in different scenarios. As for the 0-lepton results, the selection yielding the best expected limit for a given parameter point is used.

Figure 8 shows upper limits in the $(m_{\tilde{g}}, m_{\tilde{t}_1})$ plane for the gluino-stop model. Gluino masses below 620 GeV are excluded at 95% CL for stop masses up to 440 GeV. The observed and expected upper limits at 95% CL extracted in the $(m_{\tilde{g}}, m_{\tilde{\chi}_1^0})$ plane for the Gtt models are shown in Figure 9. The upper cross section limits at 95% CL are also reported for each MSSM scenario. In this case, gluino masses below 750 GeV are excluded at 95% CL for $m_{\tilde{\chi}_1^0} = 50$ GeV while neutralino masses below 160 GeV are excluded at 95% CL for $m_{\tilde{g}} = 700$ GeV.

Figure 10 shows upper limits at 95% CL for the Gtb models. Only scenarios with chargino masses above the experimental limits from LEP experiments are considered, and gluino masses below 720 GeV are excluded at 95% CL for $m_{\tilde{\chi}_1^0} = 100$ GeV while neutralino masses below 200 GeV are excluded at 95% CL for $m_{\tilde{g}} = 600$ GeV. The contribution of the 0-lepton channel signal regions to the significance has been also evaluated for this scenario and found to be lower than that of the 1-lepton channel.

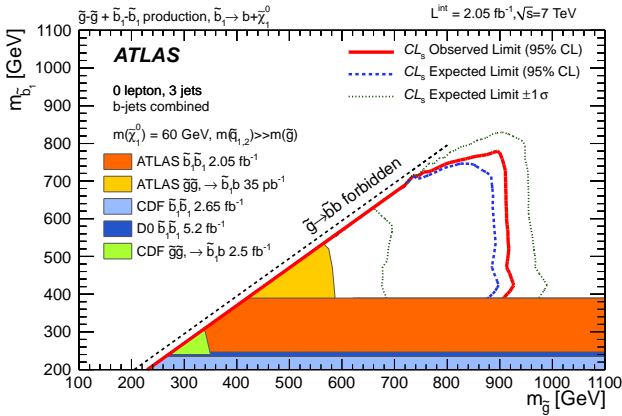


FIG. 6: Observed and expected 95% CL exclusion limits in the $(m_{\tilde{g}}, m_{\tilde{b}_1})$ plane (gluino-sbottom models). For each scenario, the signal region providing the best expected limit is chosen. The neutralino mass is assumed to be 60 GeV and the NLO cross sections are calculated using PROSPINO. The result is compared to previous results from ATLAS [21] and CDF [67] searches which assume the same gluino-sbottom decays hypotheses. Exclusion limits from the CDF [68], D0 [69] and ATLAS [23] experiments on direct sbottom pair production are also shown.

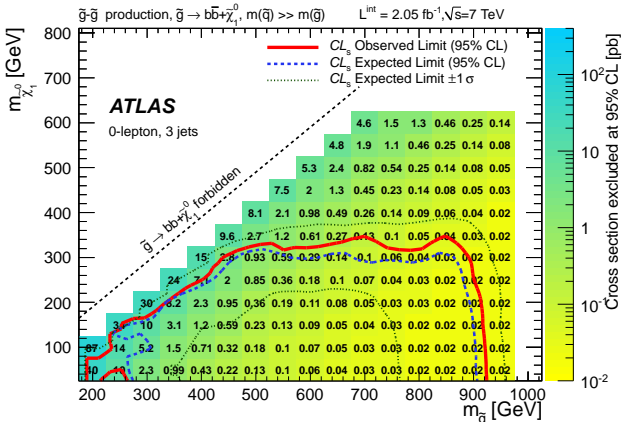


FIG. 7: Observed and expected 95% CL exclusion limits in the $(m_{\tilde{g}}, m_{\tilde{\chi}_1^0})$ plane (G_{bb} models). For each scenario, the signal region selection providing the best expected limit is chosen.

X. INTERPRETATION IN SO(10) MODELS

In addition to the simplified model interpretation, results are interpreted in the context of two SO(10) models [70] with $t - b - \tau$ Yukawa coupling unification : the D-term splitting model, DR3, and the Higgs splitting model, HS. For both models the SUSY particle mass spectrum is characterised by the low masses of the gluinos (300-600 GeV), charginos (100-180 GeV) and

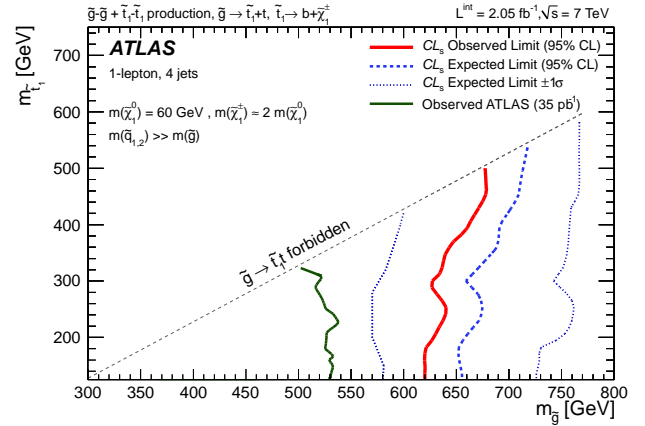


FIG. 8: The observed and expected 95% CL exclusion limits in the $(m_{\tilde{g}}, m_{\tilde{t}_1})$ plane (gluino-stop models) using the best expected limit between SR1-D and SR1-E for each signal point. The result is compared to previous results from ATLAS [21] searches which assume the same gluino-stop decays hypotheses.

neutralinos (50-90 GeV), whereas all scalar particles have masses beyond the TeV scale. Depending on the sparticle masses, chargino-neutralino or gluino-pair production dominates. At low gluino masses, the three-body gluino decays $\tilde{g} \rightarrow b\bar{b}\tilde{\chi}_1^0$ and $\tilde{g} \rightarrow b\bar{b}\tilde{\chi}_2^0$ dominate in the DR3 and the HS model, respectively. Final states with high b -jet multiplicities are then expected in both models with a harder E_T^{miss} spectrum in the DR3 scenario due to the direct gluino decay into $\tilde{\chi}_1^0$ and with a higher lepton content in the HS scenario due to the subsequent decay $\tilde{\chi}_2^0 \rightarrow \ell\bar{\ell}\tilde{\chi}_1^0$. For heavy gluinos, the gluino decay modes $\tilde{g} \rightarrow b\tilde{t}\tilde{t}^\pm$ and $\tilde{g} \rightarrow t\bar{t}\tilde{\chi}_1^0$ become more relevant, enhancing final states with leptons in both scenarios.

Results of both 0-lepton and 1-lepton analyses have been employed to extract exclusion limits at 95% CL on the gluino mass in the two SO(10) scenarios, DR3 and HS. The 0-lepton analysis has the best sensitivity at low gluino masses while the lepton-based selection is more sensitive to heavy gluinos. For each gluino mass, the signal region leading to the best expected significance is used to extract the 95% CL exclusion limits. Figure 11 shows the PROSPINO NLO cross section and the observed and expected upper limit at 95% CL for the DR3 (Figure 11(a)) and HS (Figure 11(b)) models as a function of the gluino mass. At the nominal NLO cross section, gluino masses below 650 GeV and 620 GeV are excluded at 95% CL for the DR3 and HS models respectively.

These limits on the gluino masses can be interpreted in terms of Yukawa coupling unification in the third generation. The degree of Yukawa unification is quantified by:

$$R = \max(f_t, f_b, f_\tau) / \min(f_t, f_b, f_\tau) \quad (6)$$

where f_t, f_b, f_τ are the t, b and τ Yukawa couplings evalu-

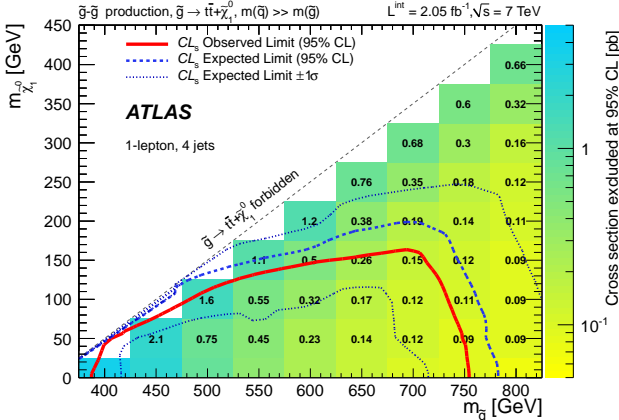


FIG. 9: The observed and expected 95% CL exclusion limits in the $(m_{\tilde{g}}, m_{\tilde{\chi}_1^0})$ plane (Gtt) using the best expected limit between SR1-D and SR1-E for each signal point.

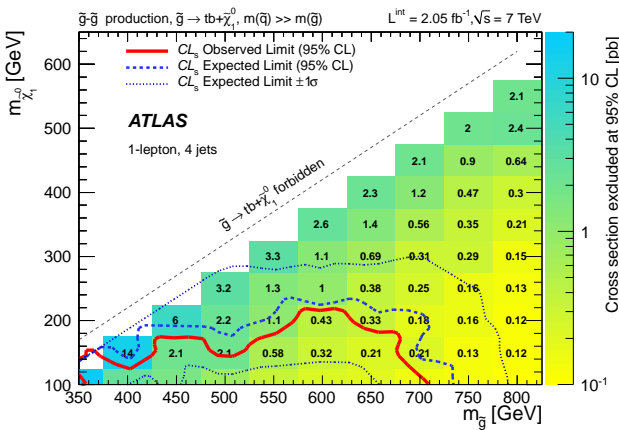


FIG. 10: The observed and expected 95% CL exclusion limits in the $(m_{\tilde{g}}, m_{\tilde{\chi}_1^0})$ plane (Gtb models) using the best expected limit between SR1-D and SR1-E for each signal point.

ated at the scale $Q = M_{\text{GUT}}$. In both DR3 and HS model lines, the degree of Yukawa unification increases together with the gluino mass and Yukawa coupling unification occurs at a few percent level only for $m_{\tilde{g}} \leq 500$ GeV. Consequently, the most favored range of gluino masses is excluded for the two SO(10) model lines considered as the degree of Yukawa unification should be further loosen up to pull the gluino mass to higher values. However, Yukawa coupling unification can still be realized at a few percent level for heavier gluino masses in different model lines [71].

XI. CONCLUSIONS

An updated search for supersymmetry in final states with missing transverse momentum and at least one or two b -jets in proton-proton collisions at 7 TeV is pre-

sented. The results are based on data corresponding to an integrated luminosity of 2.05 fb^{-1} collected by ATLAS at the Large Hadron Collider during 2011. The search is sensitive mainly to gluino-mediated production of sbottoms and stops, the supersymmetric partners of the third generation quarks, which, due to mixing effects, might be the lightest squarks. No excess above the expectations from Standard Model processes was found and the results are used to exclude parameter regions in various R -parity conserving SUSY models.

Glino masses up to 800–900 GeV are excluded at 95% CL in simplified models where the squark \tilde{b}_1 is produced either on- or off-shell and decays in 100% of the cases into $b\tilde{\chi}_1^0$. In scenarios where the squark \tilde{t}_1 is produced (on- or off-shell) via gluino decay, gluino masses up to 620–750 GeV (depending on the specific model considered) are excluded at 95% CL. In models where gluinos decay via an off-shell stop or sbottom ($b\tilde{t}\tilde{\chi}_1^0$ final states), gluino masses are excluded up to about 720 GeV for a neutralino mass of 100 GeV.

In specific models based on the gauge group SO(10), gluinos with masses below 650 GeV and 620 GeV are excluded for the DR3 and HS models, respectively. This analysis significantly extends the previous published limits on the same subject by the ATLAS and CMS collaborations.

Acknowledgements

We thank CERN for the very successful operation of the LHC, as well as the support staff from our institutions without whom ATLAS could not be operated efficiently.

We acknowledge the support of ANPCyT, Argentina; YerPhI, Armenia; ARC, Australia; BMWF, Austria; ANAS, Azerbaijan; SSTC, Belarus; CNPq and FAPESP, Brazil; NSERC, NRC and CFI, Canada; CERN; CONICYT, Chile; CAS, MOST and NSFC, China; COLCIENCIAS, Colombia; MSMT CR, MPO CR and VSC CR, Czech Republic; DNRF, DNSRC and Lundbeck Foundation, Denmark; EPLANET and ERC, European Union; IN2P3-CNRS, CEA-DSM/IRFU, France; GNAS, Georgia; BMBF, DFG, HGF, MPG and AvH Foundation, Germany; GSRT, Greece; ISF, MINERVA, GIF, DIP and Benoziyo Center, Israel; INFN, Italy; MEXT and JSPS, Japan; CNRST, Morocco; FOM and NWO, Netherlands; RCN, Norway; MNiSW, Poland; GRICES and FCT, Portugal; MERYS (MECTS), Romania; MES of Russia and ROSATOM, Russian Federation; JINR; MSTD, Serbia; MSSR, Slovakia; ARRS and MVZT, Slovenia; DST/NRF, South Africa; MICINN, Spain; SRC and Wallenberg Foundation, Sweden; SER, SNSF and Cantons of Bern and Geneva, Switzerland; NSC, Taiwan; TAEK, Turkey; STFC, the Royal Society and Leverhulme Trust, United Kingdom; DOE and NSF, United States of America.

The crucial computing support from all WLCG partners is acknowledged gratefully, in particular from

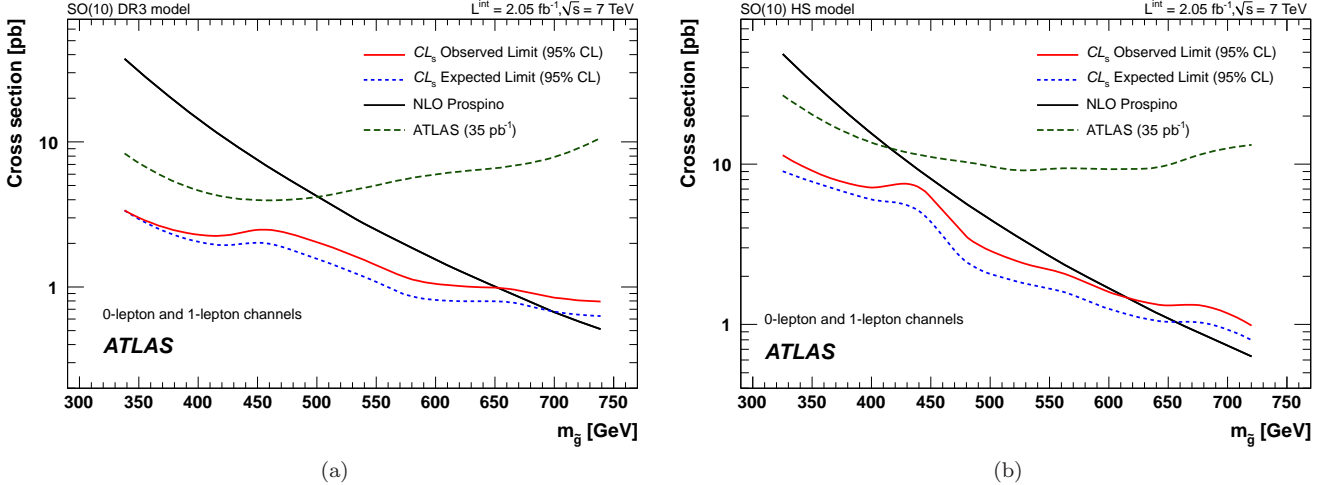


FIG. 11: Cross sections as a function of the gluino mass for DR3 (a) and HS (b) models. The observed and expected 95% CL exclusion limits are shown respectively in red and in blue. For each gluino mass, the signal region yielding the best expected limit is used. The NLO theoretical cross section from PROSPINO is shown in black. Previous limits obtained by ATLAS [21] with $\mathcal{L} = 35 \text{ pb}^{-1}$ are superimposed for reference.

CERN and the ATLAS Tier-1 facilities at TRIUMF (Canada), NDGF (Denmark, Norway, Sweden), CC-IN2P3 (France), KIT/GridKA (Germany), INFN-CNAF

(Italy), NL-T1 (Netherlands), PIC (Spain), ASGC (Taiwan), RAL (UK) and BNL (USA) and in the Tier-2 facilities worldwide.

-
- [1] H. Miyazawa, *Prog. Theor. Phys.* **36** (6), 1266 (1966).
- [2] P. Ramond, *Phys. Rev.* **D3**, 2415 (1971).
- [3] Y. Gofman and E. Likhtman, *JETP Lett.* **13**, 323 (1971).
- [4] A. Neveu and J. H. Schwarz, *Nucl. Phys.* **B31**, 86 (1971).
- [5] A. Neveu and J. H. Schwarz, *Phys. Rev.* **D4**, 1109 (1971).
- [6] J. Gervais and B. Sakita, *Nucl. Phys.* **B34**, 632 (1971).
- [7] D. Volkov and V. Akulov, *Phys. Lett.* **B46**, 109 (1973).
- [8] J. Wess and B. Zumino, *Phys. Lett.* **B49**, 52 (1974).
- [9] J. Wess and B. Zumino, *Nucl. Phys.* **B70**, 39 (1974).
- [10] S. Weinberg, *Phys. Rev.* **D13**, 974 (1976).
- [11] E. Gildener, *Phys. Rev.* **D14**, 1667 (1976).
- [12] S. Weinberg, *Phys. Rev.* **D19**, 1277 (1979).
- [13] L. Susskind, *Phys. Rev.* **D20**, 2619 (1979).
- [14] P. Fayet, *Phys. Lett.* **B64**, 159 (1976).
- [15] P. Fayet, *Phys. Lett.* **B69**, 489 (1977).
- [16] G. R. Farrar and P. Fayet, *Phys. Lett.* **B76**, 575 (1978).
- [17] P. Fayet, *Phys. Lett.* **B84**, 416 (1979).
- [18] S. Dimopoulos and H. Georgi, *Nucl. Phys.* **B193**, 150 (1981).
- [19] H. Fritzsch and P. Minkowski, *Annals of Physics* **93**, 193 (1975).
- [20] M. Gell-Mann, P. Ramond, and R. Slansky, *Rev. Mod. Phys.* **50**, 721 (1978).
- [21] ATLAS Collaboration, *Phys. Lett.* **B701**, 398 (2011).
- [22] CMS Collaboration, *JHEP* **07**, 113 (2011).
- [23] ATLAS Collaboration, arXiv:1112.3832 [hep-ex] (2012). Accepted by *Phys. Rev. Lett.*
- [24] ATLAS Collaboration, *JINST* **3**, S08003 (2008).
- [25] ATLAS uses a right-handed coordinate system, with the z axis along the beam line. The azimuthal angle ϕ is measured around the beam axis and the polar angle θ is the angle from the beam axis. The pseudorapidity is defined as $\eta = -\ln \tan(\theta/2)$. The distance ΔR in the $\eta - \phi$ space is defined as $\Delta R = \sqrt{(\Delta\eta)^2 + (\Delta\phi)^2}$.
- [26] S. Frixione and B. Webber, hep-ph/0601192 (2006).
- [27] P. M. Nadolsky *et al.*, *Phys. Rev.* **D78**, 013004 (2008).
- [28] S. Frixione *et al.*, *JHEP* **11**, 070 (2007).
- [29] B. Kersevan and E. Richter-Was, hep-ph/0405247 (2004).
- [30] M. Mangano *et al.*, *JHEP* **07**, 001 (2003).
- [31] J. Pumplin *et al.*, *JHEP* **07**, 012 (2002).
- [32] G. Corcella *et al.*, *JHEP* **01**, 010 (2001).
- [33] J. Butterworth, J. R. Forshaw, and M. Seymour, *Z. Phys.* **C72**, 637 (1996).
- [34] J. Alwall, M. Herquet, F. Maltoni, O. Mattelaer, and T. Stelzer, *JHEP* **06**, 128 (2011).
- [35] T. Sjöstrand, S. Mrenna, and P. Skands, *JHEP* **0605**, 026 (2006).
- [36] M. Bahr *et al.*, *Eur. Phys. J.* **C58**, 639 (2008).
- [37] W. Beenakker, M. Kramer, T. Plehn, M. Spira, and P. Zerwas, *Nucl. Phys.* **B515**, 3 (1998).
- [38] D. Stump *et al.*, *JHEP* **10**, 046 (2003).
- [39] ATLAS Collaboration, *ATL-PHYS-PUB-2010-014*. <http://cdsweb.cern.ch/record/1303025> (2010).
- [40] ATLAS Collaboration, *ATLAS-CONF-2010-031*. <http://cdsweb.cern.ch/record/1277665> (2010).
- [41] ATLAS Collaboration, *Eur. Phys. J.* **C70**, 823 (2010).
- [42] S. Agostinelli *et al.* (GEANT4), *Nucl. Instrum. Meth.* **A506**, 250 (2003).
- [43] J. Campbell and R. Ellis, *Phys. Rev.* **D60**, 113006 (1999).

- [44] J. M. Campbell, R. K. Ellis, and C. Williams, *JHEP* **07**, 018 (2011).
- [45] R. Hamberg, W. L. van Neerven, and T. Matsuura, *Nucl. Phys.* **B359**, 343 (1991), erratum-*ibid.* **B644**:403-404,2002.
- [46] K. Melnikov and F. Petriello, *Phys. Rev.* **D74**, 114017 (2006).
- [47] K. Melnikov and F. Petriello, *Phys. Rev. Lett.* **96**, 231803 (2006).
- [48] R. Bonciani, S. Catani, M. L. Mangano, and P. Nason, *Nucl. Phys.* **B529**, 424 (1998).
- [49] S. Moch and P. Uwer, *Phys. Rev.* **D78**, 034003 (2008).
- [50] M. Beneke, M. Czakon, P. Falgari, A. Mitov, and C. Schwinn, *Phys. Lett.* **B690**, 483 (2010).
- [51] ATLAS Collaboration, arXiv:1110.3174 [hep-ex] (2011). Accepted by *Eur. Phys. J. C*.
- [52] In case of multiple vertices, the primary vertex is taken to be the one for which the sum of the square of momenta of the associated tracks p_T^2 is the largest.
- [53] M. Cacciari, G. Salam, and G. Soyez, *JHEP* **04**, 063 (2008).
- [54] M. Cacciari and G. Salam, *Phys. Lett. B* **641**, 57 (2006).
- [55] ATLAS Collaboration, arXiv:1112.6426 [hep-ex] (2011). Submitted to *Eur. Phys. J. C*.
- [56] ATLAS Collaboration, [ATLAS-CONF-2011-102](http://cdsweb.cern.ch/record/1369219).
<http://cdsweb.cern.ch/record/1369219> (2011).
- [57] ATLAS Collaboration, *Eur. Phys. J.* **C72**, 1844 (2012).
- [58] ATLAS Collaboration, *Eur. Phys. J.* **C71**, 1630 (2011).
- [59] ATLAS Collaboration, [ATLAS-CONF-2011-116](http://cdsweb.cern.ch/record/1376384).
<http://cdsweb.cern.ch/record/1376384> (2011).
- [60] ATLAS Collaboration, [CERN-PH-EP-2012-061](http://cdsweb.cern.ch/record/1423602/).
<http://cdsweb.cern.ch/record/1423602/> (2012).
- [61] ATLAS Collaboration, arXiv:1109.6572 [hep-ex] (2011). Accepted by *Phys. Lett. B*.
- [62] ATLAS Collaboration, *JHEP* **12**, 060 (2010).
- [63] ATLAS Collaboration, [ATLAS-CONF-2010-054](http://cdsweb.cern.ch/record/1281311/).
<http://cdsweb.cern.ch/record/1281311/> (2010).
- [64] ATLAS Collaboration, *Eur. Phys. J.* **C71**, 1577 (2011).
- [65] ATLAS Collaboration, *Phys. Lett.* **B707**, 418 (2011).
- [66] G. Cowan, K. Cranmer, E. Gross, and O. Vitells, *Eur. Phys. J.* **C71**, 1554 (2011).
- [67] CDF Collaboration, T. Aaltonen *et al.*, *Phys. Rev. Lett.* **102**, 221801 (2009).
- [68] CDF Collaboration, T. Aaltonen *et al.*, *Phys. Rev. Lett.* **105**, 081802 (2010).
- [69] D0 Collaboration, V.M. Abazov *et al.*, *Phys. Lett.* **B693**, 95 (2010).
- [70] H. Baer, S. Kraml, A. Lessa, and S. Sekmen, *JHEP* **1002**, 055 (2010).
- [71] H. Baer, H. Raza, and Q. Shafi, arXiv:1201.5668 [hep-ph] (2012).

The ATLAS Collaboration

G. Aad⁴⁸, B. Abbott¹¹⁰, J. Abdallah¹¹, S. Abdel Khalek¹¹⁴, A.A. Abdelalim⁴⁹, A. Abdesselam¹¹⁷, O. Abdinov¹⁰, B. Abi¹¹¹, M. Abolins⁸⁷, O.S. AbouZeid¹⁵⁷, H. Abramowicz¹⁵², H. Abreu¹¹⁴, E. Acerbi^{88a,88b}, B.S. Acharya^{163a,163b}, L. Adamczyk³⁷, D.L. Adams²⁴, T.N. Addy⁵⁶, J. Adelman¹⁷⁴, M. Aderholz⁹⁸, S. Adomeit⁹⁷, P. Adragna⁷⁴, T. Adye¹²⁸, S. Aefsky²², J.A. Aguilar-Saavedra^{123b,a}, M. Aharrouche⁸⁰, S.P. Ahlen²¹, F. Ahles⁴⁸, A. Ahmad¹⁴⁷, M. Ahsan⁴⁰, G. Aielli^{132a,132b}, T. Akdogan^{18a}, T.P.A. Åkesson⁷⁸, G. Akimoto¹⁵⁴, A.V. Akimov⁹³, A. Akiyama⁶⁶, M.S. Alam¹, M.A. Alam⁷⁵, J. Albert¹⁶⁸, S. Albrand⁵⁵, M. Aleksa²⁹, I.N. Aleksandrov⁶⁴, F. Alessandria^{88a}, C. Alexa^{25a}, G. Alexander¹⁵², G. Alexandre⁴⁹, T. Alexopoulos⁹, M. Althroob²⁰, M. Aliev¹⁵, G. Alimonti^{88a}, J. Alison¹¹⁹, M. Aliyev¹⁰, B.M.M. Allbrooke¹⁷, P.P. Allport⁷², S.E. Allwood-Spiers⁵³, J. Almond⁸¹, A. Aloisio^{101a,101b}, R. Alon¹⁷⁰, A. Alonso⁷⁸, B. Alvarez Gonzalez⁸⁷, M.G. Alviggi^{101a,101b}, K. Amako⁶⁵, P. Amaral²⁹, C. Amelung²², V.V. Ammosov¹²⁷, A. Amorim^{123a,b}, G. Amorós¹⁶⁶, N. Amram¹⁵², C. Anastopoulos²⁹, L.S. Ancu¹⁶, N. Andari¹¹⁴, T. Andeen³⁴, C.F. Anders²⁰, G. Anders^{58a}, K.J. Anderson³⁰, A. Andreazza^{88a,88b}, V. Andrei^{58a}, M-L. Andrieux⁵⁵, X.S. Anduaga⁶⁹, A. Angerami³⁴, F. Anghinolfi²⁹, A. Anisenkov¹⁰⁶, N. Anjos^{123a}, A. Annovi⁴⁷, A. Antonaki⁸, M. Antonelli⁴⁷, A. Antonov⁹⁵, J. Antos^{143b}, F. Anulli^{131a}, S. Aoun⁸², L. Aperio Bella⁴, R. Apolle^{117,c}, G. Arabidze⁸⁷, I. Aracena¹⁴², Y. Arai⁶⁵, A.T.H. Arce⁴⁴, S. Arfaoui¹⁴⁷, J-F. Arguin¹⁴, E. Arik^{18a,*}, M. Arik^{18a}, A.J. Armbruster⁸⁶, O. Arnaez⁸⁰, V. Arnal⁷⁹, C. Arnault¹¹⁴, A. Artamonov⁹⁴, G. Artoni^{131a,131b}, D. Arutinov²⁰, S. Asai¹⁵⁴, R. Asfandiyarov¹⁷¹, S. Ask²⁷, B. Åsman^{145a,145b}, L. Asquith⁵, K. Assamagan²⁴, A. Astbury¹⁶⁸, A. Astvatsaturov⁵², B. Aubert⁴, E. Auge¹¹⁴, K. Augsten¹²⁶, M. Aurousseau^{144a}, G. Avolio¹⁶², R. Avramidou⁹, D. Axen¹⁶⁷, C. Ay⁵⁴, G. Azuelos^{92,d}, Y. Azuma¹⁵⁴, M.A. Baak²⁹, G. Baccaglioni^{88a}, C. Bacci^{133a,133b}, A.M. Bach¹⁴, H. Bachacou¹³⁵, K. Bachas²⁹, M. Backes⁴⁹, M. Backhaus²⁰, E. Badescu^{25a}, P. Bagnaia^{131a,131b}, S. Bahinipati², Y. Bai^{32a}, D.C. Bailey¹⁵⁷, T. Bain¹⁵⁷, J.T. Baines¹²⁸, O.K. Baker¹⁷⁴, M.D. Baker²⁴, S. Baker⁷⁶, E. Banas³⁸, P. Banerjee⁹², Sw. Banerjee¹⁷¹, D. Banfi²⁹, A. Bangert¹⁴⁹, V. Bansal¹⁶⁸, H.S. Bansil¹⁷, L. Barak¹⁷⁰, S.P. Baranov⁹³, A. Barashkou⁶⁴, A. Barbaro Galtieri¹⁴, T. Barber⁴⁸, E.L. Barberio⁸⁵, D. Barberis^{50a,50b}, M. Barbero²⁰, D.Y. Bardin⁶⁴, T. Barilliari⁹⁸, M. Barisonzi¹⁷³, T. Barklow¹⁴², N. Barlow²⁷, B.M. Barnett¹²⁸, R.M. Barnett¹⁴, A. Baroncelli^{133a}, G. Barone⁴⁹, A.J. Barr¹¹⁷, F. Barreiro⁷⁹, J. Barreiro Guimarães da Costa⁵⁷, P. Barrillon¹¹⁴, R. Bartoldus¹⁴², A.E. Barton⁷⁰, V. Bartsch¹⁴⁸, R.L. Bates⁵³, L. Batkova^{143a}, J.R. Batley²⁷, A. Battaglia¹⁶, M. Battistin²⁹, F. Bauer¹³⁵, H.S. Bawa^{142,e}, S. Beale⁹⁷, T. Beau⁷⁷, P.H. Beauchemin¹⁶⁰, R. Becccherle^{50a}, P. Bechtle²⁰, H.P. Beck¹⁶, S. Becker⁹⁷, M. Beckingham¹³⁷, K.H. Becks¹⁷³, A.J. Beddall^{18c}, A. Beddall^{18c}, S. Bedikian¹⁷⁴, V.A. Bednyakov⁶⁴, C.P. Bee⁸², M. Begel²⁴, S. Behar Harpz¹⁵¹, P.K. Behera⁶², M. Beimforde⁹⁸, C. Belanger-Champagne⁸⁴, P.J. Bell⁴⁹, W.H. Bell⁴⁹, G. Bella¹⁵², L. Bellagamba^{19a}, F. Bellina²⁹, M. Bellomo²⁹, A. Belloni⁵⁷, O. Beloborodova^{106,f}, K. Belotskiy⁹⁵, O. Beltramello²⁹, O. Benary¹⁵², D. Benchekroun^{134a}, M. Bendel⁸⁰, N. Benekos¹⁶⁴, Y. Benhammou¹⁵², E. Benhar Noccioli⁴⁹, J.A. Benitez Garcia^{158b}, D.P. Benjamin⁴⁴, M. Benoit¹¹⁴, J.R. Bensinger²², K. Benslama¹²⁹, S. Bentvelsen¹⁰⁴, D. Berge²⁹, E. Bergeaas Kuutmann⁴¹, N. Berger⁴, F. Berghaus¹⁶⁸, E. Berglund¹⁰⁴, J. Beringer¹⁴, P. Bernat⁷⁶, R. Bernhard⁴⁸, C. Bernius²⁴, T. Berry⁷⁵, C. Bertella⁸², A. Bertin^{19a,19b}, F. Bertinelli²⁹, F. Bertolucci^{121a,121b}, M.I. Besana^{88a,88b}, N. Besson¹³⁵, S. Bethke⁹⁸, W. Bhimji⁴⁵, R.M. Bianchi²⁹, M. Bianco^{71a,71b}, O. Biebel⁹⁷, S.P. Bieniek⁷⁶, K. Bierwagen⁵⁴, J. Biesiada¹⁴, M. Biglietti^{133a}, H. Bilokon⁴⁷, M. Bindi^{19a,19b}, S. Binet¹¹⁴, A. Bingul^{18c}, C. Bini^{131a,131b}, C. Biscarat¹⁷⁶, U. Bitenc⁴⁸, K.M. Black²¹, R.E. Blair⁵, J.-B. Blanchard¹³⁵, G. Blanchot²⁹, T. Blazek^{143a}, C. Blocker²², J. Blocki³⁸, A. Blondel⁴⁹, W. Blum⁸⁰, U. Blumenschein⁵⁴, G.J. Bobbink¹⁰⁴, V.B. Bobrovnikov¹⁰⁶, S.S. Bocchetta⁷⁸, A. Bocci⁴⁴, C.R. Boddy¹¹⁷, M. Boehler⁴¹, J. Boek¹⁷³, N. Boelaert³⁵, J.A. Bogaerts²⁹, A. Bogdanchikov¹⁰⁶, A. Bogouch^{89,*}, C. Bohm^{145a}, J. Bohm¹²⁴, V. Boisvert⁷⁵, T. Bold³⁷, V. Boldea^{25a}, N.M. Bolnet¹³⁵, M. Bomben⁷⁷, M. Bona⁷⁴, V.G. Bondarenko⁹⁵, M. Bondioli¹⁶², M. Boonekamp¹³⁵, C.N. Booth¹³⁸, S. Bordoni⁷⁷, C. Borer¹⁶, A. Borisov¹²⁷, G. Borissov⁷⁰, I. Borjanovic^{12a}, M. Borri⁸¹, S. Borroni⁸⁶, V. Bortolotto^{133a,133b}, K. Bos¹⁰⁴, D. Boscherini^{19a}, M. Bosman¹¹, H. Boterenbrood¹⁰⁴, D. Botterill¹²⁸, J. Bouchami⁹², J. Boudreau¹²², E.V. Bouhova-Thacker⁷⁰, D. Boumediene³³, C. Bourdarios¹¹⁴, N. Bousson⁸², A. Boveia³⁰, J. Boyd²⁹, I.R. Boyko⁶⁴, N.I. Bozhko¹²⁷, I. Bozovic-Jelisavcic^{12b}, J. Bracinik¹⁷, A. Braem²⁹, P. Branchini^{133a}, G.W. Brandenburg⁵⁷, A. Brandt⁷, G. Brandt¹¹⁷, O. Brandt⁵⁴, U. Bratzler¹⁵⁵, B. Brau⁸³, J.E. Brau¹¹³, H.M. Braun¹⁷³, B. Brelier¹⁵⁷, J. Bremer²⁹, K. Brendlinger¹¹⁹, R. Brenner¹⁶⁵, S. Bressler¹⁷⁰, D. Britton⁵³, F.M. Brochu²⁷, I. Brock²⁰, R. Brock⁸⁷, T.J. Brodbeck⁷⁰, E. Brodet¹⁵², F. Broggi^{88a}, C. Bromberg⁸⁷, J. Bronner⁹⁸, G. Brooijmans³⁴, W.K. Brooks^{31b}, G. Brown⁸¹, H. Brown⁷, P.A. Bruckman de Renstrom³⁸, D. Bruncko^{143b}, R. Bruneliere⁴⁸, S. Brunet⁶⁰, A. Brunii^{19a}, G. Bruni^{19a}, M. Bruschi^{19a}, T. Buanes¹³, Q. Buat⁵⁵, F. Bucci⁴⁹, J. Buchanan¹¹⁷, N.J. Buchanan², P. Buchholz¹⁴⁰, R.M. Buckingham¹¹⁷, A.G. Buckley⁴⁵, S.I. Buda^{25a}, I.A. Budagov⁶⁴, B. Budick¹⁰⁷, V. Büscher⁸⁰, L. Bugge¹¹⁶, O. Bulekov⁹⁵, M. Bunse⁴², T. Buran¹¹⁶, H. Burckhart²⁹, S. Burdin⁷², T. Burgess¹³, S. Burke¹²⁸, E. Busato³³, P. Bussey⁵³, C.P. Buszello¹⁶⁵, F. Butin²⁹, B. Butler¹⁴², J.M. Butler²¹, C.M. Buttar⁵³, J.M. Butterworth⁷⁶, W. Buttlinger²⁷, S. Cabrera Urbán¹⁶⁶, D. Caforio^{19a,19b}, O. Cakir^{3a}, P. Calafiura¹⁴, G. Calderini⁷⁷, P. Calfayan⁹⁷, R. Calkins¹⁰⁵, L.P. Caloba^{23a}, R. Caloi^{131a,131b}, D. Calvet³³, S. Calvet³³, R. Camacho Toro³³, P. Camarri^{132a,132b}, M. Cambiagh^{118a,118b}, D. Cameron¹¹⁶,

L.M. Caminada¹⁴, S. Campana²⁹, M. Campanelli⁷⁶, V. Canale^{101a,101b}, F. Canelli^{30,g}, A. Canepa^{158a}, J. Cantero⁷⁹, L. Capasso^{101a,101b}, M.D.M. Capeans Garrido²⁹, I. Caprini^{25a}, M. Caprini^{25a}, D. Capriotti⁹⁸, M. Capua^{36a,36b}, R. Caputo⁸⁰, R. Cardarelli^{132a}, T. Carli²⁹, G. Carlino^{101a}, L. Carminati^{88a,88b}, B. Caron⁸⁴, S. Caron¹⁰³, E. Carquin^{31b}, G.D. Carrillo Montoya¹⁷¹, A.A. Carter⁷⁴, J.R. Carter²⁷, J. Carvalho^{123a,h}, D. Casadei¹⁰⁷, M.P. Casado¹¹, M. Cascella^{121a,121b}, C. Caso^{50a,50b,*}, A.M. Castaneda Hernandez¹⁷¹, E. Castaneda-Miranda¹⁷¹, V. Castillo Gimenez¹⁶⁶, N.F. Castro^{123a}, G. Cataldi^{71a}, A. Catinaccio²⁹, J.R. Catmore²⁹, A. Cattai²⁹, G. Cattani^{132a,132b}, S. Caughron⁸⁷, D. Cauz^{163a,163c}, P. Cavalleri⁷⁷, D. Cavalli^{88a}, M. Cavalli-Sforza¹¹, V. Cavasinni^{121a,121b}, F. Ceradini^{133a,133b}, A.S. Cerqueira^{23b}, A. Cerri²⁹, L. Cerrito⁷⁴, F. Cerutti⁴⁷, S.A. Cetin^{18b}, F. Cevenini^{101a,101b}, A. Chafaq^{134a}, D. Chakraborty¹⁰⁵, K. Chan², B. Chapleau⁸⁴, J.D. Chapman²⁷, J.W. Chapman⁸⁶, E. Chareyre⁷⁷, D.G. Charlton¹⁷, V. Chavda⁸¹, C.A. Chavez Barajas²⁹, S. Cheatham⁸⁴, S. Chekanov⁵, S.V. Chekulaev^{158a}, G.A. Chelkov⁶⁴, M.A. Chelstowska¹⁰³, C. Chen⁶³, H. Chen²⁴, S. Chen^{32c}, T. Chen^{32c}, X. Chen¹⁷¹, S. Cheng^{32a}, A. Cheplakov⁶⁴, V.F. Chepurnov⁶⁴, R. Cherkaoui El Moursli^{134e}, V. Chernyatin²⁴, E. Cheu⁶, S.L. Cheung¹⁵⁷, L. Chevalier¹³⁵, G. Chieffari^{101a,101b}, L. Chikovani^{51a}, J.T. Childers²⁹, A. Chilingarov⁷⁰, G. Chiodini^{71a}, A.S. Chisholm¹⁷, R.T. Chislett⁷⁶, M.V. Chizhov⁶⁴, G. Choudalakis³⁰, S. Chouridou¹³⁶, I.A. Christidi⁷⁶, A. Christov⁴⁸, D. Chromek-Burckhart²⁹, M.L. Chu¹⁵⁰, J. Chudoba¹²⁴, G. Ciapetti^{131a,131b}, A.K. Ciftci^{3a}, R. Ciftci^{3a}, D. Cinca³³, V. Cindro⁷³, M.D. Ciobotaru¹⁶², C. Ciocca^{19a}, A. Ciocio¹⁴, M. Cirilli⁸⁶, M. Citterio^{88a}, M. Ciubancan^{25a}, A. Clark⁴⁹, P.J. Clark⁴⁵, W. Cleland¹²², J.C. Clemens⁸², B. Clement⁵⁵, C. Clement^{145a,145b}, R.W. Clift¹²⁸, Y. Coadou⁸², M. Cobal^{163a,163c}, A. Coccaro¹⁷¹, J. Cochran⁶³, P. Coe¹¹⁷, J.G. Cogan¹⁴², J. Coggeshall¹⁶⁴, E. Cogneras¹⁷⁶, J. Colas⁴, A.P. Colijn¹⁰⁴, N.J. Collins¹⁷, C. Collins-Tooth⁵³, J. Collot⁵⁵, G. Colon⁸³, P. Conde Muiño^{123a}, E. Coniavitis¹¹⁷, M.C. Conidi¹¹, M. Consonni¹⁰³, S.M. Consonni^{88a,88b}, V. Consorti⁴⁸, S. Constantinescu^{25a}, C. Conta^{118a,118b}, G. Conti⁵⁷, F. Conventi^{101a,i}, J. Cook²⁹, M. Cooke¹⁴, B.D. Cooper⁷⁶, A.M. Cooper-Sarkar¹¹⁷, K. Copic¹⁴, T. Cornelissen¹⁷³, M. Corradi^{19a}, F. Corriveau^{84,j}, A. Cortes-Gonzalez¹⁶⁴, G. Cortiana⁹⁸, G. Costa^{88a}, M.J. Costa¹⁶⁶, D. Costanzo¹³⁸, T. Costin³⁰, D. Côté²⁹, R. Coura Torres^{23a}, L. Courneyea¹⁶⁸, G. Cowan⁷⁵, C. Cowden²⁷, B.E. Cox⁸¹, K. Cranmer¹⁰⁷, F. Crescioli^{121a,121b}, M. Cristinziani²⁰, G. Crosetti^{36a,36b}, R. Crupi^{71a,71b}, S. Crépé-Renaudin⁵⁵, C.-M. Cuciuc^{25a}, C. Cuenda Almenar¹⁷⁴, T. Cuhadar Donszelmann¹³⁸, M. Curatolo⁴⁷, C.J. Curtis¹⁷, C. Cuthbert¹⁴⁹, P. Cwetanski⁶⁰, H. Czirr¹⁴⁰, P. Czodrowski⁴³, Z. Czyczula¹⁷⁴, S. D'Auria⁵³, M. D'Onofrio⁷², A. D'Orazio^{131a,131b}, P.V.M. Da Silva^{23a}, C. Da Via⁸¹, W. Dabrowski³⁷, A. Dafinca¹¹⁷, T. Dai⁸⁶, C. Dallapiccola⁸³, M. Dam³⁵, M. Dameri^{50a,50b}, D.S. Damiani¹³⁶, H.O. Danielsson²⁹, D. Dannheim⁹⁸, V. Dao⁴⁹, G. Darbo^{50a}, G.L. Darlea^{25b}, W. Davey²⁰, T. Davidek¹²⁵, N. Davidson⁸⁵, R. Davidson⁷⁰, E. Davies^{117,c}, M. Davies⁹², A.R. Davison⁷⁶, Y. Davygora^{58a}, E. Dawe¹⁴¹, I. Dawson¹³⁸, J.W. Dawson^{5,*}, R.K. Daya-Ishmukhametova²², K. De⁷, R. de Asmundis^{101a}, S. De Castro^{19a,19b}, P.E. De Castro Faria Salgado²⁴, S. De Cecco⁷⁷, J. de Graat⁹⁷, N. De Groot¹⁰³, P. de Jong¹⁰⁴, C. De La Taille¹¹⁴, H. De la Torre⁷⁹, B. De Lotto^{163a,163c}, L. de Mora⁷⁰, L. De Nooij¹⁰⁴, D. De Pedis^{131a}, A. De Salvo^{131a}, U. De Sanctis^{163a,163c}, A. De Santo¹⁴⁸, J.B. De Vivie De Regie¹¹⁴, G. De Zorzi^{131a,131b}, S. Dean⁷⁶, W.J. Dearnaley⁷⁰, R. Debbe²⁴, C. Debenedetti⁴⁵, B. Dechenaux⁵⁵, D.V. Dedovich⁶⁴, J. Degenhardt¹¹⁰, M. Dehchar¹¹⁷, C. Del Papa^{163a,163c}, J. Del Peso⁷⁹, T. Del Prete^{121a,121b}, T. Delemontex⁵⁵, M. Deliyergiyev⁷³, A. Dell'Acqua²⁹, L. Dell'Asta²¹, M. Della Pietra^{101a,i}, D. della Volpe^{101a,101b}, M. Delmastro⁴, N. Delruelle²⁹, P.A. Delsart⁵⁵, C. Deluca¹⁴⁷, S. Demers¹⁷⁴, M. Demichev⁶⁴, B. Demirkoz^{11,k}, J. Deng¹⁶², S.P. Denisov¹²⁷, D. Derendarz³⁸, J.E. Derkaoui^{134d}, F. Derue⁷⁷, P. Dervan⁷², K. Desch²⁰, E. Devetak¹⁴⁷, P.O. Deviveiros¹⁰⁴, A. Dewhurst¹²⁸, B. DeWilde¹⁴⁷, S. Dhaliwal¹⁵⁷, R. Dhullipudi^{24,l}, A. Di Ciaccio^{132a,132b}, L. Di Ciaccio⁴, A. Di Girolamo²⁹, B. Di Girolamo²⁹, S. Di Luise^{133a,133b}, A. Di Mattia¹⁷¹, B. Di Micco²⁹, R. Di Nardo⁴⁷, A. Di Simone^{132a,132b}, R. Di Sipio^{19a,19b}, M.A. Diaz^{31a}, F. Diblen^{18c}, E.B. Diehl⁸⁶, J. Dietrich⁴¹, T.A. Dietzsches^{58a}, S. Diglio⁸⁵, K. Dindar Yagci³⁹, J. Dingfelder²⁰, C. Dionisi^{131a,131b}, P. Dita^{25a}, S. Dita^{25a}, F. Dittus²⁹, F. Djama⁸², T. Djobava^{51b}, M.A.B. do Vale^{23c}, A. Do Valle Wemans^{123a}, T.K.O. Doan⁴, M. Dobbs⁸⁴, R. Dobinson^{29,*}, D. Dobos²⁹, E. Dobson^{29,m}, J. Dodd³⁴, C. Doglioni⁴⁹, T. Doherty⁵³, Y. Doi^{65,*}, J. Dolejsi¹²⁵, I. Dolenc⁷³, Z. Dolezal¹²⁵, B.A. Dolgoshein^{95,*}, T. Dohmae¹⁵⁴, M. Donadelli^{23d}, M. Donega¹¹⁹, J. Donini³³, J. Dopke²⁹, A. Doria^{101a}, A. Dos Anjos¹⁷¹, M. Dosil¹¹, A. Dotti^{121a,121b}, M.T. Dova⁶⁹, A.D. Doxiadis¹⁰⁴, A.T. Doyle⁵³, Z. Drasal¹²⁵, J. Drees¹⁷³, N. Dressnandt¹¹⁹, H. Drevermann²⁹, C. Driouichi³⁵, M. Dris⁹, J. Dubbert⁹⁸, S. Dube¹⁴, E. Duchovni¹⁷⁰, G. Duckeck⁹⁷, A. Dudarev²⁹, F. Dudziak⁶³, M. Dührssen²⁹, I.P. Duerdorff⁸¹, L. Duflot¹¹⁴, M-A. Dufour⁸⁴, M. Dunford²⁹, H. Duran Yildiz^{3a}, R. Duxfield¹³⁸, M. Dwuznik³⁷, F. Dydak²⁹, M. Düren⁵², W.L. Ebenstein⁴⁴, J. Ebke⁹⁷, S. Eckweiler⁸⁰, K. Edmonds⁸⁰, C.A. Edwards⁷⁵, N.C. Edwards⁵³, W. Ehrenfeld⁴¹, T. Ehrlich⁹⁸, T. Eifert¹⁴², G. Eigen¹³, K. Einsweiler¹⁴, E. Eisenhandler⁷⁴, T. Ekelof¹⁶⁵, M. El Kacimi^{134c}, M. Ellert¹⁶⁵, S. Elles⁴, F. Ellinghaus⁸⁰, K. Ellis⁷⁴, N. Ellis²⁹, J. Elmsheuser⁹⁷, M. Elsing²⁹, D. Emeliyanov¹²⁸, R. Engelmann¹⁴⁷, A. Engl⁹⁷, B. Epp⁶¹, A. Eppig⁸⁶, J. Erdmann⁵⁴, A. Ereditato¹⁶, D. Eriksson^{145a}, J. Ernst¹, M. Ernst²⁴, J. Ernwein¹³⁵, D. Errede¹⁶⁴, S. Errede¹⁶⁴, E. Ertel⁸⁰, M. Escalier¹¹⁴, C. Escobar¹²², X. Espinal Curull¹¹, B. Esposito⁴⁷, F. Etienne⁸², A.I. Etienvre¹³⁵, E. Etzion¹⁵², D. Evangelakou⁵⁴, H. Evans⁶⁰, L. Fabbri^{19a,19b}, C. Fabre²⁹, R.M. Fakhrutdinov¹²⁷, S. Falciano^{131a}, Y. Fang¹⁷¹, M. Fanti^{88a,88b}, A. Farbin⁷, A. Farilla^{133a}, J. Farley¹⁴⁷, T. Farooque¹⁵⁷, S. Farrell¹⁶², S.M. Farrington¹¹⁷, P. Farthouat²⁹,

- P. Fassnacht²⁹, D. Fassouliotis⁸, B. Fatholahzadeh¹⁵⁷, A. Favareto^{88a,88b}, L. Fayard¹¹⁴, S. Fazio^{36a,36b}, R. Febbraro³³, P. Federic^{143a}, O.L. Fedin¹²⁰, W. Fedorko⁸⁷, M. Fehling-Kaschek⁴⁸, L. Feligioni⁸², D. Fellmann⁵, C. Feng^{32d}, E.J. Feng³⁰, A.B. Fenyuk¹²⁷, J. Ferencei^{143b}, J. Ferland⁹², W. Fernando¹⁰⁸, S. Ferrag⁵³, J. Ferrando⁵³, V. Ferrara⁴¹, A. Ferrari¹⁶⁵, P. Ferrari¹⁰⁴, R. Ferrari^{118a}, D.E. Ferreira de Lima⁵³, A. Ferrer¹⁶⁶, M.L. Ferrer⁴⁷, D. Ferrere⁴⁹, C. Ferretti⁸⁶, A. Ferretto Parodi^{50a,50b}, M. Fiascaris³⁰, F. Fiedler⁸⁰, A. Filipčič⁷³, A. Filippas⁹, F. Filthaut¹⁰³, M. Fincke-Keeler¹⁶⁸, M.C.N. Fiolhais^{123a,h}, L. Fiorini¹⁶⁶, A. Firat³⁹, G. Fischer⁴¹, P. Fischer²⁰, M.J. Fisher¹⁰⁸, M. Flechl⁴⁸, I. Fleck¹⁴⁰, J. Fleckner⁸⁰, P. Fleischmann¹⁷², S. Fleischmann¹⁷³, T. Flick¹⁷³, A. Floderus⁷⁸, L.R. Flores Castillo¹⁷¹, M.J. Flowerdew⁹⁸, M. Fokitis⁹, T. Fonseca Martin¹⁶, D.A. Forbush¹³⁷, A. Formica¹³⁵, A. Forti⁸¹, D. Fortin^{158a}, J.M. Foster⁸¹, D. Fournier¹¹⁴, A. Foussat²⁹, A.J. Fowler⁴⁴, K. Fowler¹³⁶, H. Fox⁷⁰, P. Francavilla¹¹, S. Franchino^{118a,118b}, D. Francis²⁹, T. Frank¹⁷⁰, M. Franklin⁵⁷, S. Franz²⁹, M. Fraternali^{118a,118b}, S. Fratina¹¹⁹, S.T. French²⁷, F. Friedrich⁴³, R. Froeschl²⁹, D. Froidevaux²⁹, J.A. Frost²⁷, C. Fukunaga¹⁵⁵, E. Fullana Torregrosa²⁹, J. Fuster¹⁶⁶, C. Gabaldon²⁹, O. Gabizon¹⁷⁰, T. Gadfort²⁴, S. Gadomski⁴⁹, G. Gagliardi^{50a,50b}, P. Gagnon⁶⁰, C. Galea⁹⁷, E.J. Gallas¹¹⁷, V. Gallo¹⁶, B.J. Gallop¹²⁸, P. Gallus¹²⁴, K.K. Gan¹⁰⁸, Y.S. Gao^{142,e}, V.A. Gapienko¹²⁷, A. Gaponenko¹⁴, F. Garberson¹⁷⁴, M. Garcia-Sciveres¹⁴, C. García¹⁶⁶, J.E. García Navarro¹⁶⁶, R.W. Gardner³⁰, N. Garelli²⁹, H. Garitaonandia¹⁰⁴, V. Garonne²⁹, J. Garvey¹⁷, C. Gatti⁴⁷, G. Gaudio^{118a}, B. Gaur¹⁴⁰, L. Gauthier¹³⁵, P. Gauzzi^{131a,131b}, I.L. Gavrilenko⁹³, C. Gay¹⁶⁷, G. Gaycken²⁰, J-C. Gayde²⁹, E.N. Gazis⁹, P. Ge^{32d}, C.N.P. Gee¹²⁸, D.A.A. Geerts¹⁰⁴, Ch. Geich-Gimbel²⁰, K. Gellerstedt^{145a,145b}, C. Gemme^{50a}, A. Gemmell⁵³, M.H. Genest⁵⁵, S. Gentile^{131a,131b}, M. George⁵⁴, S. George⁷⁵, P. Gerlach¹⁷³, A. Gershon¹⁵², C. Geweniger^{58a}, H. Ghazlane^{134b}, N. Ghodbane³³, B. Giacobbe^{19a}, S. Giagu^{131a,131b}, V. Giakoumopoulou⁸, V. Giangiobbe¹¹, F. Gianotti²⁹, B. Gibbard²⁴, A. Gibson¹⁵⁷, S.M. Gibson²⁹, L.M. Gilbert¹¹⁷, V. Gilewsky⁹⁰, D. Gillberg²⁸, A.R. Gillman¹²⁸, D.M. Gingrich^{2,d}, J. Ginzburg¹⁵², N. Giokaris⁸, M.P. Giordani^{163c}, R. Giordano^{101a,101b}, F.M. Giorgi¹⁵, P. Giovannini⁹⁸, P.F. Giraud¹³⁵, D. Giugni^{88a}, M. Giunta⁹², P. Giusti^{19a}, B.K. Gjelsten¹¹⁶, L.K. Gladilin⁹⁶, C. Glasman⁷⁹, J. Glatzer⁴⁸, A. Glazov⁴¹, K.W. Glitza¹⁷³, G.L. Glonti⁶⁴, J.R. Goddard⁷⁴, J. Godfrey¹⁴¹, J. Godlewski²⁹, M. Goebel⁴¹, T. Göpfert⁴³, C. Goeringer⁸⁰, C. Gössling⁴², T. Göttfert⁹⁸, S. Goldfarb⁸⁶, T. Golling¹⁷⁴, A. Gomes^{123a,b}, L.S. Gomez Fajardo⁴¹, R. Gonçalo⁷⁵, J. Goncalves Pinto Firmino Da Costa⁴¹, L. Gonella²⁰, A. Gonidec²⁹, S. Gonzalez¹⁷¹, S. González de la Hoz¹⁶⁶, G. Gonzalez Parra¹¹, M.L. Gonzalez Silva²⁶, S. Gonzalez-Sevilla⁴⁹, J.J. Goodson¹⁴⁷, L. Goossens²⁹, P.A. Gorbounov⁹⁴, H.A. Gordon²⁴, I. Gorelov¹⁰², G. Gorfine¹⁷³, B. Gorini²⁹, E. Gorini^{71a,71b}, A. Gorišek⁷³, E. Gornicki³⁸, V.N. Goryachev¹²⁷, B. Gosdzik⁴¹, A.T. Goshaw⁵, M. Gosselink¹⁰⁴, M.I. Gostkin⁶⁴, I. Gough Eschrich¹⁶², M. Gouighri^{134a}, D. Goujdami^{134c}, M.P. Goulette⁴⁹, A.G. Goussiou¹³⁷, C. Goy⁴, S. Gozpinar²², I. Grabowska-Bold³⁷, P. Grafström²⁹, K-J. Grahn⁴¹, F. Grancagnolo^{71a}, S. Grancagnolo¹⁵, V. Grassi¹⁴⁷, V. Gratchev¹²⁰, N. Grau³⁴, H.M. Gray²⁹, J.A. Gray¹⁴⁷, E. Graziani^{133a}, O.G. Grebenyuk¹²⁰, T. Greenshaw⁷², Z.D. Greenwood^{24,l}, K. Gregersen³⁵, I.M. Gregor⁴¹, P. Grenier¹⁴², J. Griffiths¹³⁷, N. Grigalashvili⁶⁴, A.A. Grillo¹³⁶, S. Grinstein¹¹, Y.V. Grishkevich⁹⁶, J.-F. Grivaz¹¹⁴, M. Groh⁹⁸, E. Gross¹⁷⁰, J. Grosse-Knetter⁵⁴, J. Groth-Jensen¹⁷⁰, K. Grybel¹⁴⁰, V.J. Guarino⁵, D. Guest¹⁷⁴, C. Guicheney³³, A. Guida^{71a,71b}, S. Guindon⁵⁴, H. Guler^{84,n}, J. Gunther¹²⁴, B. Guo¹⁵⁷, J. Guo³⁴, A. Gupta³⁰, Y. Gusakov⁶⁴, V.N. Gushchin¹²⁷, P. Gutierrez¹¹⁰, N. Guttman¹⁵², O. Gutzwiler¹⁷¹, C. Guyot¹³⁵, C. Gwenlan¹¹⁷, C.B. Gwilliam⁷², A. Haas¹⁴², S. Haas²⁹, C. Haber¹⁴, H.K. Hadavand³⁹, D.R. Hadley¹⁷, P. Haefner⁹⁸, F. Hahn²⁹, S. Haider²⁹, Z. Hajduk³⁸, H. Hakobyan¹⁷⁵, D. Hall¹¹⁷, J. Haller⁵⁴, K. Hamacher¹⁷³, P. Hamal¹¹², M. Hamer⁵⁴, A. Hamilton^{144b,o}, S. Hamilton¹⁶⁰, H. Han^{32a}, L. Han^{32b}, K. Hanagaki¹¹⁵, K. Hanawa¹⁵⁹, M. Hance¹⁴, C. Handel⁸⁰, P. Hanke^{58a}, J.R. Hansen³⁵, J.B. Hansen³⁵, J.D. Hansen³⁵, P.H. Hansen³⁵, P. Hansson¹⁴², K. Hara¹⁵⁹, G.A. Hare¹³⁶, T. Harenberg¹⁷³, S. Harkusha⁸⁹, D. Harper⁸⁶, R.D. Harrington⁴⁵, O.M. Harris¹³⁷, K. Harrison¹⁷, J. Hartert⁴⁸, F. Hartjes¹⁰⁴, T. Haruyama⁶⁵, A. Harvey⁵⁶, S. Hasegawa¹⁰⁰, Y. Hasegawa¹³⁹, S. Hassani¹³⁵, M. Hatch²⁹, D. Hauff⁹⁸, S. Haug¹⁶, M. Hauschild²⁹, R. Hauser⁸⁷, M. Havranek²⁰, B.M. Hawes¹¹⁷, C.M. Hawkes¹⁷, R.J. Hawkings²⁹, A.D. Hawkins⁷⁸, D. Hawkins¹⁶², T. Hayakawa⁶⁶, T. Hayashi¹⁵⁹, D. Hayden⁷⁵, H.S. Hayward⁷², S.J. Haywood¹²⁸, E. Hazen²¹, M. He^{32d}, S.J. Head¹⁷, V. Hedberg⁷⁸, L. Heelan⁷, S. Heim⁸⁷, B. Heinemann¹⁴, S. Heisterkamp³⁵, L. Helary⁴, C. Heller⁹⁷, M. Heller²⁹, S. Hellman^{145a,145b}, D. Hellmich²⁰, C. Helsens¹¹, R.C.W. Henderson⁷⁰, M. Henke^{58a}, A. Henrichs⁵⁴, A.M. Henriques Correia²⁹, S. Henrot-Versille¹¹⁴, F. Henry-Couannier⁸², C. Hensel⁵⁴, T. Henß¹⁷³, C.M. Hernandez⁷, Y. Hernández Jiménez¹⁶⁶, R. Herrberg¹⁵, A.D. Hershenhorn¹⁵¹, G. Herten⁴⁸, R. Hertenberger⁹⁷, L. Hervas²⁹, G.G. Hesketh⁷⁶, N.P. Hessey¹⁰⁴, E. Higón-Rodriguez¹⁶⁶, D. Hill^{5,*}, J.C. Hill²⁷, N. Hill⁵, K.H. Hiller⁴¹, S. Hillert²⁰, S.J. Hillier¹⁷, I. Hinchliffe¹⁴, E. Hines¹¹⁹, M. Hirose¹¹⁵, F. Hirsch⁴², D. Hirschbuehl¹⁷³, J. Hobbs¹⁴⁷, N. Hod¹⁵², M.C. Hodgkinson¹³⁸, P. Hodgson¹³⁸, A. Hoecker²⁹, M.R. Hoferkamp¹⁰², J. Hoffman³⁹, D. Hoffmann⁸², M. Hohlfeld⁸⁰, M. Holder¹⁴⁰, S.O. Holmgren^{145a}, T. Holy¹²⁶, J.L. Holzbauer⁸⁷, Y. Homma⁶⁶, T.M. Hong¹¹⁹, L. Hooft van Huysduynen¹⁰⁷, T. Horazdovsky¹²⁶, C. Horn¹⁴², S. Horner⁴⁸, J-Y. Hostachy⁵⁵, S. Hou¹⁵⁰, M.A. Houlden⁷², A. Hoummada^{134a}, J. Howarth⁸¹, D.F. Howell¹¹⁷, I. Hristova¹⁵, J. Hrivnac¹¹⁴, I. Hruska¹²⁴, T. Hrynová⁴, P.J. Hsu⁸⁰, S.-C. Hsu¹⁴, G.S. Huang¹¹⁰, Z. Hubacek¹²⁶, F. Hubaut⁸², F. Huegging²⁰, A. Huettmann⁴¹, T.B. Huffman¹¹⁷, E.W. Hughes³⁴, G. Hughes⁷⁰, R.E. Hughes-Jones⁸¹, M. Huhtinen²⁹, P. Hurst⁵⁷, M. Hurwitz¹⁴, U. Husemann⁴¹, N. Huseynov^{64,p}, J. Huston⁸⁷, J. Huth⁵⁷, G. Iacobucci⁴⁹,

- G. Iakovidis⁹, M. Ibbotson⁸¹, I. Ibragimov¹⁴⁰, R. Ichimiya⁶⁶, L. Iconomidou-Fayard¹¹⁴, J. Idarraga¹¹⁴, P. Iengo^{101a}, O. Igonkina¹⁰⁴, Y. Ikegami⁶⁵, M. Ikeno⁶⁵, Y. Ilchenko³⁹, D. Iliadis¹⁵³, N. Ilic¹⁵⁷, M. Imori¹⁵⁴, T. Ince²⁰, J. Inigo-Golfin²⁹, P. Ioannou⁸, M. Iodice^{133a}, V. Ippolito^{131a,131b}, A. Irles Quiles¹⁶⁶, C. Isaksson¹⁶⁵, A. Ishikawa⁶⁶, M. Ishino⁶⁷, R. Ishmukhametov³⁹, C. Issever¹¹⁷, S. Istin^{18a}, A.V. Ivashin¹²⁷, W. Iwanski³⁸, H. Iwasaki⁶⁵, J.M. Izen⁴⁰, V. Izzo^{101a}, B. Jackson¹¹⁹, J.N. Jackson⁷², P. Jackson¹⁴², M.R. Jaekel²⁹, V. Jain⁶⁰, K. Jakobs⁴⁸, S. Jakobsen³⁵, J. Jakubek¹²⁶, D.K. Jana¹¹⁰, E. Jansen²⁹, H. Jansen²⁹, A. Jantsch⁹⁸, M. Janus⁴⁸, G. Jarlskog⁷⁸, L. Jeanty⁵⁷, K. Jelen³⁷, I. Jen-La Plante³⁰, P. Jenni²⁹, A. Jeremie⁴, P. Jež³⁵, S. Jézéquel⁴, M.K. Jha^{19a}, H. Ji¹⁷¹, W. Ji⁸⁰, J. Jia¹⁴⁷, Y. Jiang^{32b}, M. Jimenez Belenguer⁴¹, G. Jin^{32b}, S. Jin^{32a}, O. Jimmouchi¹⁵⁶, M.D. Joergensen³⁵, D. Joffe³⁹, L.G. Johansen¹³, M. Johansen^{145a,145b}, K.E. Johansson^{145a}, P. Johansson¹³⁸, S. Johnert⁴¹, K.A. Johns⁶, K. Jon-And^{145a,145b}, G. Jones¹¹⁷, R.W.L. Jones⁷⁰, T.W. Jones⁷⁶, T.J. Jones⁷², O. Jonsson²⁹, C. Joram²⁹, P.M. Jorge^{123a}, J. Joseph¹⁴, K.D. Joshi⁸¹, J. Jovicevic¹⁴⁶, T. Jovin^{12b}, X. Ju¹⁷¹, C.A. Jung⁴², R.M. Jungst²⁹, V. Juraneck¹²⁴, P. Jussel⁶¹, A. Juste Rozas¹¹, V.V. Kabachenko¹²⁷, S. Kabana¹⁶, M. Kaci¹⁶⁶, A. Kaczmarska³⁸, P. Kadlecik³⁵, M. Kado¹¹⁴, H. Kagan¹⁰⁸, M. Kagan⁵⁷, S. Kaiser⁹⁸, E. Kajomovitz¹⁵¹, S. Kalinin¹⁷³, L.V. Kalinovskaya⁶⁴, S. Kama³⁹, N. Kanaya¹⁵⁴, M. Kaneda²⁹, S. Kaneti²⁷, T. Kanno¹⁵⁶, V.A. Kantserov⁹⁵, J. Kanzaki⁶⁵, B. Kaplan¹⁷⁴, A. Kapliy³⁰, J. Kaplon²⁹, D. Kar⁴³, M. Karagounis²⁰, M. Karagoz¹¹⁷, M. Karnevskiy⁴¹, V. Kartvelishvili⁷⁰, A.N. Karyukhin¹²⁷, L. Kashif¹⁷¹, G. Kasieczka^{58b}, R.D. Kass¹⁰⁸, A. Kastanas¹³, M. Kataoka⁴, Y. Kataoka¹⁵⁴, E. Katsoufis⁹, J. Katzy⁴¹, V. Kaushik⁶, K. Kawagoe⁶⁶, T. Kawamoto¹⁵⁴, G. Kawamura⁸⁰, M.S. Kayl¹⁰⁴, V.A. Kazanin¹⁰⁶, M.Y. Kazarinov⁶⁴, R. Keeler¹⁶⁸, R. Kehoe³⁹, M. Keil⁵⁴, G.D. Kekelidze⁶⁴, J.S. Keller¹³⁷, J. Kennedy⁹⁷, M. Kenyon⁵³, O. Kepka¹²⁴, N. Kerschen²⁹, B.P. Kerševan⁷³, S. Kersten¹⁷³, K. Kessoku¹⁵⁴, J. Keung¹⁵⁷, F. Khalil-zada¹⁰, H. Khandanyan¹⁶⁴, A. Khanov¹¹¹, D. Kharchenko⁶⁴, A. Khodinov⁹⁵, A.G. Kholodenko¹²⁷, A. Khomich^{58a}, T.J. Khoo²⁷, G. Khoriauli²⁰, A. Khoroshilov¹⁷³, N. Khovanskiy⁶⁴, V. Khovanskiy⁹⁴, E. Khramov⁶⁴, J. Khubua^{51b}, H. Kim^{145a,145b}, M.S. Kim², S.H. Kim¹⁵⁹, N. Kimura¹⁶⁹, O. Kind¹⁵, B.T. King⁷², M. King⁶⁶, R.S.B. King¹¹⁷, J. Kirk¹²⁸, L.E. Kirsch²², A.E. Kiryunin⁹⁸, T. Kishimoto⁶⁶, D. Kisielewska³⁷, T. Kittelmann¹²², A.M. Kiver¹²⁷, E. Kladiva^{143b}, M. Klein⁷², U. Klein⁷², K. Kleinknecht⁸⁰, M. Klemetti⁸⁴, A. Klier¹⁷⁰, P. Klimek^{145a,145b}, A. Klimentov²⁴, R. Klingenberg⁴², J.A. Klinger⁸¹, E.B. Klinkby³⁵, T. Klioutchnikova²⁹, P.F. Klok¹⁰³, S. Klous¹⁰⁴, E.-E. Kluge^{58a}, T. Kluge⁷², P. Kluit¹⁰⁴, S. Kluth⁹⁸, N.S. Knecht¹⁵⁷, E. Kneringer⁶¹, J. Knobloch²⁹, E.B.F.G. Knoops⁸², A. Knue⁵⁴, B.R. Ko⁴⁴, T. Kobayashi¹⁵⁴, M. Kobel⁴³, M. Kocian¹⁴², P. Kodys¹²⁵, K. Köneke²⁹, A.C. König¹⁰³, S. Koenig⁸⁰, L. Köpke⁸⁰, F. Koetsveld¹⁰³, P. Koevesarki²⁰, T. Koffas²⁸, E. Koffeman¹⁰⁴, L.A. Kogan¹¹⁷, F. Kohn⁵⁴, Z. Kohout¹²⁶, T. Kohriki⁶⁵, T. Koi¹⁴², T. Kokott²⁰, G.M. Kolachev¹⁰⁶, H. Kolanoski¹⁵, V. Kolesnikov⁶⁴, I. Koletsou^{88a}, J. Koll⁸⁷, M. Kollefrath⁴⁸, S.D. Kolya⁸¹, A.A. Komar⁹³, Y. Komori¹⁵⁴, T. Kondo⁶⁵, T. Kono^{41,q}, A.I. Kononov⁴⁸, R. Konoplich^{107,r}, N. Konstantinidis⁷⁶, A. Kootz¹⁷³, S. Koperny³⁷, K. Korcyl³⁸, K. Kordas¹⁵³, V. Koreshev¹²⁷, A. Korn¹¹⁷, A. Korol¹⁰⁶, I. Korolkov¹¹, E.V. Korolkova¹³⁸, V.A. Korotkov¹²⁷, O. Kortner⁹⁸, S. Kortner⁹⁸, V.V. Kostyukhin²⁰, M.J. Kotamäki²⁹, S. Kotov⁹⁸, V.M. Kotov⁶⁴, A. Kotwal⁴⁴, C. Kourkoumelis⁸, V. Kouskoura¹⁵³, A. Koutsman^{158a}, R. Kowalewski¹⁶⁸, T.Z. Kowalski³⁷, W. Kozanecki¹³⁵, A.S. Kozhin¹²⁷, V. Kral¹²⁶, V.A. Kramarenko⁹⁶, G. Kramberger⁷³, M.W. Krasny⁷⁷, A. Krasznahorkay¹⁰⁷, J. Kraus⁸⁷, J.K. Kraus²⁰, A. Kreisel¹⁵², F. Krejci¹²⁶, J. Kretzschmar⁷², N. Kriege⁵⁴, P. Krieger¹⁵⁷, K. Kroeninger⁵⁴, H. Kroha⁹⁸, J. Kroll¹¹⁹, J. Kroseberg²⁰, J. Krstic^{12a}, U. Kruchonak⁶⁴, H. Krüger²⁰, T. Krucker¹⁶, N. Krumnack⁶³, Z.V. Krumshteyn⁶⁴, A. Kruth²⁰, T. Kubota⁸⁵, S. Kuday^{3a}, S. Kuehn⁴⁸, A. Kugel^{58c}, T. Kuhl⁴¹, D. Kuhn⁶¹, V. Kukhtin⁶⁴, Y. Kulchitsky⁸⁹, S. Kuleshov^{31b}, C. Kummer⁹⁷, M. Kuna⁷⁷, N. Kundu¹¹⁷, J. Kunkle¹¹⁹, A. Kupco¹²⁴, H. Kurashige⁶⁶, M. Kurata¹⁵⁹, Y.A. Kurochkin⁸⁹, V. Kus¹²⁴, E.S. Kuwertz¹⁴⁶, M. Kuze¹⁵⁶, J. Kvita¹⁴¹, R. Kwee¹⁵, A. La Rosa⁴⁹, L. La Rotonda^{36a,36b}, L. Labarga⁷⁹, J. Labbe⁴, S. Lablak^{134a}, C. Lacasta¹⁶⁶, F. Lacava^{131a,131b}, H. Lacker¹⁵, D. Lacour⁷⁷, V.R. Lacuesta¹⁶⁶, E. Ladygin⁶⁴, R. Lafaye⁴, B. Laforge⁷⁷, T. Lagouri⁷⁹, S. Lai⁴⁸, E. Laisne⁵⁵, M. Lamanna²⁹, L. Lambourne⁷⁶, C.L. Lampen⁶, W. Lampl⁶, E. Lancon¹³⁵, U. Landgraf⁴⁸, M.P.J. Landon⁷⁴, J.L. Lane⁸¹, C. Lange⁴¹, A.J. Lankford¹⁶², F. Lanni²⁴, K. Lantzsch¹⁷³, S. Laplace⁷⁷, C. Lapoire²⁰, J.F. Laporte¹³⁵, T. Lari^{88a}, A.V. Larionov¹²⁷, A. Larner¹¹⁷, C. Lasseur²⁹, M. Lassnig²⁹, P. Laurelli⁴⁷, V. Lavorini^{36a,36b}, W. Lavrijsen¹⁴, P. Laycock⁷², A.B. Lazarev⁶⁴, O. Le Dortz⁷⁷, E. Le Guirriec⁸², C. Le Maner¹⁵⁷, E. Le Menedeu¹¹, C. Lebel⁹², T. LeCompte⁵, F. Ledroit-Guillon⁵⁵, H. Lee¹⁰⁴, J.S.H. Lee¹¹⁵, S.C. Lee¹⁵⁰, L. Lee¹⁷⁴, M. Lefebvre¹⁶⁸, M. Legendre¹³⁵, A. Leger⁴⁹, B.C. LeGeyt¹¹⁹, F. Legger⁹⁷, C. Leggett¹⁴, M. Lehmacher²⁰, G. Lehmann Miotto²⁹, X. Lei⁶, M.A.L. Leite^{23d}, R. Leitner¹²⁵, D. Lellouch¹⁷⁰, M. Leltchouk³⁴, B. Lemmer⁵⁴, V. Lendermann^{58a}, K.J.C. Leney^{144b}, T. Lenz¹⁰⁴, G. Lenzen¹⁷³, B. Lenzi²⁹, K. Leonhardt⁴³, S. Leontsinis⁹, C. Leroy⁹², J-R. Lessard¹⁶⁸, J. Lesser^{145a}, C.G. Lester²⁷, A. Leung Fook Cheong¹⁷¹, J. Levéque⁴, D. Levin⁸⁶, L.J. Levinson¹⁷⁰, M.S. Levitski¹²⁷, A. Lewis¹¹⁷, G.H. Lewis¹⁰⁷, A.M. Leyko²⁰, M. Leyton¹⁵, B. Li⁸², H. Li^{171,s}, S. Li^{32b,t}, X. Li⁸⁶, Z. Liang^{117,u}, H. Liao³³, B. Liberti^{132a}, P. Lichard²⁹, M. Lichtnecker⁹⁷, K. Lie¹⁶⁴, W. Liebig¹³, C. Limbach²⁰, A. Limosani⁸⁵, M. Limper⁶², S.C. Lin^{150,v}, F. Linde¹⁰⁴, J.T. Linnemann⁸⁷, E. Lipeles¹¹⁹, L. Lipinsky¹²⁴, A. Lipniacka¹³, T.M. Liss¹⁶⁴, D. Lissauer²⁴, A. Lister⁴⁹, A.M. Litke¹³⁶, C. Liu²⁸, D. Liu¹⁵⁰, H. Liu⁸⁶, J.B. Liu⁸⁶, M. Liu^{32b}, Y. Liu^{32b}, M. Livan^{118a,118b}, S.S.A. Livermore¹¹⁷, A. Lleres⁵⁵, J. Llorente Merino⁷⁹, S.L. Lloyd⁷⁴, E. Lobodzinska⁴¹, P. Loch⁶, W.S. Lockman¹³⁶, T. Laddenkoetter²⁰, F.K. Loebinger⁸¹, A. Loginov¹⁷⁴, C.W. Loh¹⁶⁷, T. Lohse¹⁵, K. Lohwasser⁴⁸, M. Lokajicek¹²⁴,

- J. Loken¹¹⁷, V.P. Lombardo⁴, R.E. Long⁷⁰, L. Lopes^{123a}, D. Lopez Mateos⁵⁷, J. Lorenz⁹⁷, N. Lorenzo Martinez¹¹⁴, M. Losada¹⁶¹, P. Loscutoff¹⁴, F. Lo Sterzo^{131a,131b}, M.J. Losty^{158a}, X. Lou⁴⁰, A. Lounis¹¹⁴, K.F. Loureiro¹⁶¹, J. Love²¹, P.A. Love⁷⁰, A.J. Lowe^{142,e}, F. Lu^{32a}, H.J. Lubatti¹³⁷, C. Luci^{131a,131b}, A. Lucotte⁵⁵, A. Ludwig⁴³, D. Ludwig⁴¹, I. Ludwig⁴⁸, J. Ludwig⁴⁸, F. Luehring⁶⁰, G. Luijckx¹⁰⁴, W. Lukas⁶¹, D. Lumb⁴⁸, L. Luminari^{131a}, E. Lund¹¹⁶, B. Lund-Jensen¹⁴⁶, B. Lundberg⁷⁸, J. Lundberg^{145a,145b}, J. Lundquist³⁵, M. Lungwitz⁸⁰, G. Lutz⁹⁸, D. Lynn²⁴, J. Lys¹⁴, E. Lytken⁷⁸, H. Ma²⁴, L.L. Ma¹⁷¹, J.A. Macana Goia⁹², G. Maccarrone⁴⁷, A. Macchiolo⁹⁸, B. Maček⁷³, J. Machado Miguens^{123a}, R. Mackeprang³⁵, R.J. Madaras¹⁴, W.F. Mader⁴³, R. Maenner^{58c}, T. Maeno²⁴, P. Mättig¹⁷³, S. Mättig⁴¹, L. Magnoni²⁹, E. Magradze⁵⁴, Y. Mahalalel¹⁵², K. Mahboubi⁴⁸, S. Mahmoud⁷², G. Mahout¹⁷, C. Maiani^{131a,131b}, C. Maidantchik^{23a}, A. Maio^{123a,b}, S. Majewski²⁴, Y. Makida⁶⁵, N. Makovec¹¹⁴, P. Mal¹³⁵, B. Malaescu²⁹, Pa. Malecki³⁸, P. Malecki³⁸, V.P. Maleev¹²⁰, F. Malek⁵⁵, U. Mallik⁶², D. Malon⁵, C. Malone¹⁴², S. Maltezos⁹, V. Malyshev¹⁰⁶, S. Malyukov²⁹, R. Mameghani⁹⁷, J. Mamuzic^{12b}, A. Manabe⁶⁵, L. Mandelli^{88a}, I. Mandić⁷³, R. Mandrysch¹⁵, J. Maneira^{123a}, P.S. Mangeard⁸⁷, L. Manhaes de Andrade Filho^{23a}, I.D. Manjavidze⁶⁴, A. Mann⁵⁴, P.M. Manning¹³⁶, A. Manousakis-Katsikakis⁸, B. Mansoulie¹³⁵, A. Manz⁹⁸, A. Mapelli²⁹, L. Mapelli²⁹, L. March⁷⁹, J.F. Marchand²⁸, F. Marchese^{132a,132b}, G. Marchiori⁷⁷, M. Marcisovsky¹²⁴, C.P. Marino¹⁶⁸, F. Marroquim^{23a}, R. Marshall⁸¹, Z. Marshall²⁹, F.K. Martens¹⁵⁷, S. Marti-Garcia¹⁶⁶, A.J. Martin¹⁷⁴, B. Martin²⁹, B. Martin⁸⁷, F.F. Martin¹¹⁹, J.P. Martin⁹², Ph. Martin⁵⁵, T.A. Martin¹⁷, V.J. Martin⁴⁵, B. Martin dit Latour⁴⁹, S. Martin-Haugh¹⁴⁸, M. Martinez¹¹, V. Martinez Outschoorn⁵⁷, A.C. Martyniuk¹⁶⁸, M. Marx⁸¹, F. Marzano^{131a}, A. Marzin¹¹⁰, L. Masetti⁸⁰, T. Mashimo¹⁵⁴, R. Mashinistov⁹³, J. Masik⁸¹, A.L. Maslennikov¹⁰⁶, I. Massa^{19a,19b}, G. Massaro¹⁰⁴, N. Massol⁴, P. Mastrandrea^{131a,131b}, A. Mastroberardino^{36a,36b}, T. Masubuchi¹⁵⁴, P. Matricon¹¹⁴, H. Matsumoto¹⁵⁴, H. Matsunaga¹⁵⁴, T. Matsushita⁶⁶, C. Mattravers^{117,c}, J.M. Maugain²⁹, J. Maurer⁸², S.J. Maxfield⁷², D.A. Maximov^{106,f}, E.N. May⁵, A. Mayne¹³⁸, R. Mazini¹⁵⁰, M. Mazur²⁰, M. Mazzanti^{88a}, S.P. Mc Kee⁸⁶, A. McCarn¹⁶⁴, R.L. McCarthy¹⁴⁷, T.G. McCarthy²⁸, N.A. McCubbin¹²⁸, K.W. McFarlane⁵⁶, J.A. McFayden¹³⁸, H. McGlone⁵³, G. Mchedlidze^{51b}, R.A. McLaren²⁹, T. McLaughlan¹⁷, S.J. McMahon¹²⁸, R.A. McPherson^{168,j}, A. Meade⁸³, J. Mechnick¹⁰⁴, M. Mechtel¹⁷³, M. Medinnis⁴¹, R. Meera-Lebbai¹¹⁰, T. Meguro¹¹⁵, R. Mehdiyev⁹², S. Mehlhase³⁵, A. Mehta⁷², K. Meier^{58a}, B. Meirose⁷⁸, C. Melachrinos³⁰, B.R. Mellado Garcia¹⁷¹, L. Mendoza Navas¹⁶¹, Z. Meng^{150,s}, A. Mengarelli^{19a,19b}, S. Menke⁹⁸, C. Menot²⁹, E. Meoni¹¹, K.M. Mercurio⁵⁷, P. Mermod⁴⁹, L. Merola^{101a,101b}, C. Meroni^{88a}, F.S. Merritt³⁰, H. Merritt¹⁰⁸, A. Messina²⁹, J. Metcalfe¹⁰², A.S. Mete⁶³, C. Meyer⁸⁰, C. Meyer³⁰, J-P. Meyer¹³⁵, J. Meyer¹⁷², J. Meyer⁵⁴, T.C. Meyer²⁹, W.T. Meyer⁶³, J. Miao^{32d}, S. Michal²⁹, L. Micu^{25a}, R.P. Middleton¹²⁸, S. Migas⁷², L. Mijović⁴¹, G. Mikenberg¹⁷⁰, M. Mikestikova¹²⁴, M. Mikuž⁷³, D.W. Miller³⁰, R.J. Miller⁸⁷, W.J. Mills¹⁶⁷, C. Mills⁵⁷, A. Milov¹⁷⁰, D.A. Milstead^{145a,145b}, D. Milstein¹⁷⁰, A.A. Minaenko¹²⁷, M. Miñano Moya¹⁶⁶, I.A. Minashvili⁶⁴, A.I. Mincer¹⁰⁷, B. Mindur³⁷, M. Mineev⁶⁴, Y. Ming¹⁷¹, L.M. Mir¹¹, G. Mirabelli^{131a}, L. Miralles Verge¹¹, A. Misiejuk⁷⁵, J. Mitrevski¹³⁶, G.Y. Mitrofanov¹²⁷, V.A. Mitsou¹⁶⁶, S. Mitsui⁶⁵, P.S. Miyagawa¹³⁸, K. Miyazaki⁶⁶, J.U. Mjörnmark⁷⁸, T. Moa^{145a,145b}, P. Mockett¹³⁷, S. Moed⁵⁷, V. Moeller²⁷, K. Möning⁴¹, N. Möser²⁰, S. Mohapatra¹⁴⁷, W. Mohr⁴⁸, S. Mohrdieck-Möck⁹⁸, R. Moles-Valls¹⁶⁶, J. Molina-Perez²⁹, J. Monk⁷⁶, E. Monnier⁸², S. Montesano^{88a,88b}, F. Monticelli⁶⁹, S. Monzani^{19a,19b}, R.W. Moore², G.F. Moorhead⁸⁵, C. Mora Herrera⁴⁹, A. Moraes⁵³, N. Morange¹³⁵, J. Morel⁵⁴, G. Morello^{36a,36b}, D. Moreno⁸⁰, M. Moreno Llácer¹⁶⁶, P. Morettini^{50a}, M. Morgenstern⁴³, M. Morii⁵⁷, J. Morin⁷⁴, A.K. Morley²⁹, G. Mornacchi²⁹, S.V. Morozov⁹⁵, J.D. Morris⁷⁴, L. Morvaj¹⁰⁰, H.G. Moser⁹⁸, M. Mosidze^{51b}, J. Moss¹⁰⁸, R. Mount¹⁴², E. Mountricha^{9,w}, S.V. Mouraviev⁹³, E.J.W. Moyse⁸³, M. Mudrimic^{12b}, F. Mueller^{58a}, J. Mueller¹²², K. Mueller²⁰, T.A. Müller⁹⁷, T. Mueller⁸⁰, D. Muenstermann²⁹, A. Muir¹⁶⁷, Y. Munwes¹⁵², W.J. Murray¹²⁸, I. Mussche¹⁰⁴, E. Musto^{101a,101b}, A.G. Myagkov¹²⁷, M. Myska¹²⁴, J. Nadal¹¹, K. Nagai¹⁵⁹, K. Nagano⁶⁵, A. Nagarkar¹⁰⁸, Y. Nagasaka⁵⁹, M. Nagel⁹⁸, A.M. Nairz²⁹, Y. Nakahama²⁹, K. Nakamura¹⁵⁴, T. Nakamura¹⁵⁴, I. Nakano¹⁰⁹, G. Nanava²⁰, A. Napier¹⁶⁰, R. Narayan^{58b}, M. Nash^{76,c}, N.R. Nation²¹, T. Nattermann²⁰, T. Naumann⁴¹, G. Navarro¹⁶¹, H.A. Neal⁸⁶, E. Nebot⁷⁹, P.Yu. Nechaeva⁹³, T.J. Neep⁸¹, A. Negri^{118a,118b}, G. Negri²⁹, S. Nektarijevic⁴⁹, A. Nelson¹⁶², T.K. Nelson¹⁴², S. Nemecek¹²⁴, P. Nemethy¹⁰⁷, A.A. Nepomuceno^{23a}, M. Nessi^{29,x}, M.S. Neubauer¹⁶⁴, A. Neusiedl⁸⁰, R.M. Neves¹⁰⁷, P. Nevski²⁴, P.R. Newman¹⁷, V. Nguyen Thi Hong¹³⁵, R.B. Nickerson¹¹⁷, R. Nicolaïdou¹³⁵, L. Nicolas¹³⁸, B. Nicquevert²⁹, F. Niedercorn¹¹⁴, J. Nielsen¹³⁶, T. Niinikoski²⁹, N. Nikiforou³⁴, A. Nikiforov¹⁵, V. Nikolaenko¹²⁷, K. Nikolaev⁶⁴, I. Nikolic-Audit⁷⁷, K. Nikolics⁴⁹, K. Nikolopoulos²⁴, H. Nilsen⁴⁸, P. Nilsson⁷, Y. Ninomiya¹⁵⁴, A. Nisati^{131a}, T. Nishiyama⁶⁶, R. Nisius⁹⁸, L. Nodulman⁵, M. Nomachi¹¹⁵, I. Nomidis¹⁵³, M. Nordberg²⁹, P.R. Norton¹²⁸, J. Novakova¹²⁵, M. Nozaki⁶⁵, L. Nozka¹¹², I.M. Nugent^{158a}, A.-E. Nuncio-Quiroz²⁰, G. Nunes Hanninger⁸⁵, T. Nunnemann⁹⁷, E. Nurse⁷⁶, B.J. O'Brien⁴⁵, S.W. O'Neale^{17,*}, D.C. O'Neil¹⁴¹, V. O'Shea⁵³, L.B. Oakes⁹⁷, F.G. Oakham^{28,d}, H. Oberlack⁹⁸, J. Ocariz⁷⁷, A. Ochi⁶⁶, S. Oda¹⁵⁴, S. Odaka⁶⁵, J. Odier⁸², H. Ogren⁶⁰, A. Oh⁸¹, S.H. Oh⁴⁴, C.C. Ohm^{145a,145b}, T. Ohshima¹⁰⁰, H. Ohshita¹³⁹, S. Okada⁶⁶, H. Okawa¹⁶², Y. Okumura¹⁰⁰, T. Okuyama¹⁵⁴, A. Olariu^{25a}, M. Olcese^{50a}, A.G. Olchevski⁶⁴, S.A. Olivares Pino^{31a}, M. Oliveira^{123a,h}, D. Oliveira Damazio²⁴, E. Oliver Garcia¹⁶⁶, D. Olivito¹¹⁹, A. Olszewski³⁸, J. Olszowska³⁸, C. Omachi⁶⁶, A. Onofre^{123a,y}, P.U.E. Onyisi³⁰, C.J. Oram^{158a}, M.J. Oreglia³⁰, Y. Oren¹⁵²,

- D. Orestano^{133a,133b}, N. Orlando^{71a,71b}, I. Orlov¹⁰⁶, C. Oropeza Barrera⁵³, R.S. Orr¹⁵⁷, B. Osculati^{50a,50b}, R. Ospanov¹¹⁹, C. Osuna¹¹, G. Otero y Garzon²⁶, J.P. Ottersbach¹⁰⁴, M. Ouchrif^{134d}, E.A. Ouellette¹⁶⁸, F. Ould-Saada¹¹⁶, A. Ouraou¹³⁵, Q. Ouyang^{32a}, A. Ovcharova¹⁴, M. Owen⁸¹, S. Owen¹³⁸, V.E. Ozcan^{18a}, N. Ozturk⁷, A. Pacheco Pages¹¹, C. Padilla Aranda¹¹, S. Pagan Griso¹⁴, E. Paganis¹³⁸, F. Paige²⁴, P. Pais⁸³, K. Pajchel¹¹⁶, G. Palacino^{158b}, C.P. Paleari⁶, S. Palestini²⁹, D. Pallin³³, A. Palma^{123a}, J.D. Palmer¹⁷, Y.B. Pan¹⁷¹, E. Panagiotopoulou⁹, B. Panes^{31a}, N. Panikashvili⁸⁶, S. Panitkin²⁴, D. Pantea^{25a}, M. Panuskova¹²⁴, V. Paolone¹²², A. Papadelis^{145a}, Th.D. Papadopoulos⁹, A. Paramonov⁵, D. Paredes Hernandez³³, W. Park^{24,z}, M.A. Parker²⁷, F. Parodi^{50a,50b}, J.A. Parsons³⁴, U. Parzefall⁴⁸, S. Pashapour⁵⁴, E. Pasqualucci^{131a}, S. Passaggio^{50a}, A. Passeri^{133a}, F. Pastore^{133a,133b}, Fr. Pastore⁷⁵, G. Pásztor^{49,aa}, S. Pataraia¹⁷³, N. Patel¹⁴⁹, J.R. Pater⁸¹, S. Patricelli^{101a,101b}, T. Pauly²⁹, M. Pecsy^{143a}, M.I. Pedraza Morales¹⁷¹, S.V. Peleganchuk¹⁰⁶, H. Peng^{32b}, B. Penning³⁰, A. Penson³⁴, J. Penwell⁶⁰, M. Perantoni^{23a}, K. Perez^{34,ab}, T. Perez Cavalcanti⁴¹, E. Perez Codina^{158a}, M.T. Pérez García-Estañ¹⁶⁶, V. Perez Reale³⁴, L. Perini^{88a,88b}, H. Pernegger²⁹, R. Perrino^{71a}, P. Perrodo⁴, S. Perseme^{3a}, V.D. Peshekhonov⁶⁴, K. Peters²⁹, B.A. Petersen²⁹, J. Petersen²⁹, T.C. Petersen³⁵, E. Petit⁴, A. Petridis¹⁵³, C. Petridou¹⁵³, E. Petrolo^{131a}, F. Petrucci^{133a,133b}, D. Petschull⁴¹, M. Pettenu¹⁴¹, R. Pezoa^{31b}, A. Phan⁸⁵, P.W. Phillips¹²⁸, G. Piacquadio²⁹, A. Picazio⁴⁹, E. Piccaro⁷⁴, M. Piccinini^{19a,19b}, S.M. Piec⁴¹, R. Piegaia²⁶, D.T. Pignotti¹⁰⁸, J.E. Pilcher³⁰, A.D. Pilkington⁸¹, J. Pina^{123a,b}, M. Pinamonti^{163a,163c}, A. Pinder¹¹⁷, J.L. Pinfold², J. Ping^{32c}, B. Pinto^{123a}, O. Pirotte²⁹, C. Pizio^{88a,88b}, M. Plamondon¹⁶⁸, M.-A. Pleier²⁴, A.V. Pleskach¹²⁷, E. Plotnikova⁶⁴, A. Poblaguev²⁴, S. Poddar^{58a}, F. Podlaski³³, L. Poggioli¹¹⁴, T. Poghosyan²⁰, M. Pohl⁴⁹, F. Polci⁵⁵, G. Polesello^{118a}, A. Policicchio^{36a,36b}, A. Polini^{19a}, J. Poll⁷⁴, V. Polychronakos²⁴, D.M. Pomarede¹³⁵, D. Pomeroy²², K. Pommès²⁹, L. Pontecorvo^{131a}, B.G. Pope⁸⁷, G.A. Popeneciu^{25a}, D.S. Popovic^{12a}, A. Poppleton²⁹, X. Portell Bueso²⁹, C. Posch²¹, G.E. Pospelov⁹⁸, S. Pospisil¹²⁶, I.N. Potrap⁹⁸, C.J. Potter¹⁴⁸, C.T. Potter¹¹³, G. Pouillard²⁹, J. Poveda¹⁷¹, V. Pozdnyakov⁶⁴, R. Prabhu⁷⁶, P. Pralavorio⁸², A. Pranko¹⁴, S. Prasad²⁹, R. Pravahan⁷, S. Prell⁶³, K. Pretzl¹⁶, L. Pribyl²⁹, D. Price⁶⁰, J. Price⁷², L.E. Price⁵, M.J. Price²⁹, D. Prieur¹²², M. Primavera^{71a}, K. Prokofiev¹⁰⁷, F. Prokoshin^{31b}, S. Protopopescu²⁴, J. Proudfoot⁵, X. Prudent⁴³, M. Przybycien³⁷, H. Przysiecki⁴, S. Psoroulas²⁰, E. Ptacek¹¹³, E. Pueschel⁸³, J. Purdham⁸⁶, M. Purohit^{24,z}, P. Puzo¹¹⁴, Y. Pylypchenko⁶², J. Qian⁸⁶, Z. Qian⁸², Z. Qin⁴¹, A. Quadt⁵⁴, D.R. Quarrie¹⁴, W.B. Quayle¹⁷¹, F. Quinonez^{31a}, M. Raas¹⁰³, V. Radescu⁴¹, B. Radics²⁰, P. Radloff¹¹³, T. Rador^{18a}, F. Ragusa^{88a,88b}, G. Rahal¹⁷⁶, A.M. Rahimi¹⁰⁸, D. Rahm²⁴, S. Rajagopalan²⁴, M. Rammensee⁴⁸, M. Rammes¹⁴⁰, A.S. Randle-Conde³⁹, K. Randrianarivony²⁸, P.N. Ratoff⁷⁰, F. Rauscher⁹⁷, T.C. Rave⁴⁸, M. Raymond²⁹, A.L. Read¹¹⁶, D.M. Rebuzzi^{118a,118b}, A. Redelbach¹⁷², G. Redlinger²⁴, R. Reece¹¹⁹, K. Reeves⁴⁰, A. Reichold¹⁰⁴, E. Reinherz-Aronis¹⁵², A. Reinsch¹¹³, I. Reisinger⁴², C. Rembser²⁹, Z.L. Ren¹⁵⁰, A. Renaud¹¹⁴, M. Rescigno^{131a}, S. Resconi^{88a}, B. Resende¹³⁵, P. Reznicek⁹⁷, R. Rezvani¹⁵⁷, A. Richards⁷⁶, R. Richter⁹⁸, E. Richter-Was^{4,ac}, M. Ridel⁷⁷, M. Rijpstra¹⁰⁴, M. Rijssenbeek¹⁴⁷, A. Rimoldi^{118a,118b}, L. Rinaldi^{19a}, R.R. Rios³⁹, I. Riu¹¹, G. Rivoltella^{88a,88b}, F. Rizatdinova¹¹¹, E. Rizvi⁷⁴, S.H. Robertson^{84,j}, A. Robichaud-Veronneau¹¹⁷, D. Robinson²⁷, J.E.M. Robinson⁷⁶, A. Robson⁵³, J.G. Rocha de Lima¹⁰⁵, C. Roda^{121a,121b}, D. Roda Dos Santos²⁹, D. Rodriguez¹⁶¹, A. Roe⁵⁴, S. Roe²⁹, O. Røhne¹¹⁶, V. Rojo¹, S. Rolli¹⁶⁰, A. Romaniouk⁹⁵, M. Romano^{19a,19b}, V.M. Romanov⁶⁴, G. Romeo²⁶, E. Romero Adam¹⁶⁶, L. Roos⁷⁷, E. Ros¹⁶⁶, S. Rosati^{131a}, K. Rosbach⁴⁹, A. Rose¹⁴⁸, M. Rose⁷⁵, G.A. Rosenbaum¹⁵⁷, E.I. Rosenberg⁶³, P.L. Rosendahl¹³, O. Rosenthal¹⁴⁰, L. Rosselet⁴⁹, V. Rossetti¹¹, E. Rossi^{131a,131b}, L.P. Rossi^{50a}, M. Rotaru^{25a}, I. Roth¹⁷⁰, J. Rothberg¹³⁷, D. Rousseau¹¹⁴, C.R. Royon¹³⁵, A. Rozanov⁸², Y. Rozen¹⁵¹, X. Ruan^{32a,ad}, F. Rubbo¹¹, I. Rubinskiy⁴¹, B. Ruckert⁹⁷, N. Ruckstuhl¹⁰⁴, V.I. Rud⁹⁶, C. Rudolph⁴³, G. Rudolph⁶¹, F. Rühr⁶, F. Ruggieri^{133a,133b}, A. Ruiz-Martinez⁶³, V. Rumiantsev^{90,*}, L. Rumiantsev⁶⁴, K. Runge⁴⁸, Z. Rurikova⁴⁸, N.A. Rusakovich⁶⁴, J.P. Rutherford⁶, C. Ruwiedel¹⁴, P. Ruzicka¹²⁴, Y.F. Ryabov¹²⁰, V. Ryadovikov¹²⁷, P. Ryan⁸⁷, M. Rybar¹²⁵, G. Rybkin¹¹⁴, N.C. Ryder¹¹⁷, S. Rzaeva¹⁰, A.F. Saavedra¹⁴⁹, I. Sadeh¹⁵², H.F-W. Sadrozinski¹³⁶, R. Sadykov⁶⁴, F. Safai Tehrani^{131a}, H. Sakamoto¹⁵⁴, G. Salamanna⁷⁴, A. Salamon^{132a}, M. Saleem¹¹⁰, D. Salek²⁹, D. Salihagic⁹⁸, A. Salnikov¹⁴², J. Salt¹⁶⁶, B.M. Salvachua Ferrando⁵, D. Salvatore^{36a,36b}, F. Salvatore¹⁴⁸, A. Salvucci¹⁰³, A. Salzburger²⁹, D. Sampsonidis¹⁵³, B.H. Samset¹¹⁶, A. Sanchez^{101a,101b}, V. Sanchez Martinez¹⁶⁶, H. Sandaker¹³, H.G. Sander⁸⁰, M.P. Sanders⁹⁷, M. Sandhoff¹⁷³, T. Sandoval²⁷, C. Sandoval¹⁶¹, R. Sandstroem⁹⁸, S. Sandvoss¹⁷³, D.P.C. Sankey¹²⁸, A. Sansoni⁴⁷, C. Santamarina Rios⁸⁴, C. Santoni³³, R. Santonico^{132a,132b}, H. Santos^{123a}, J.G. Saraiva^{123a}, T. Sarangi¹⁷¹, E. Sarkisyan-Grinbaum⁷, F. Sarri^{121a,121b}, G. Sartisohn¹⁷³, O. Sasaki⁶⁵, N. Sasao⁶⁷, I. Satsounkevitch⁸⁹, G. Sauvage⁴, E. Sauvan⁴, J.B. Sauvan¹¹⁴, P. Savard^{157,d}, V. Savinov¹²², D.O. Savu²⁹, L. Sawyer^{24,l}, D.H. Saxon⁵³, J. Saxon¹¹⁹, L.P. Says³³, C. Sbarra^{19a}, A. Sbrizzi^{19a,19b}, O. Scallon⁹², D.A. Scannicchio¹⁶², M. Scarcella¹⁴⁹, J. Schaarschmidt¹¹⁴, P. Schacht⁹⁸, D. Schaefer¹¹⁹, U. Schäfer⁸⁰, S. Schaepe²⁰, S. Schaetzl^{58b}, A.C. Schaffer¹¹⁴, D. Schaille⁹⁷, R.D. Schamberger¹⁴⁷, A.G. Schamov¹⁰⁶, V. Scharf^{58a}, V.A. Schegelsky¹²⁰, D. Scheirich⁸⁶, M. Schernau¹⁶², M.I. Scherzer³⁴, C. Schiavi^{50a,50b}, J. Schieck⁹⁷, M. Schioppa^{36a,36b}, S. Schlenker²⁹, J.L. Schlereth⁵, E. Schmidt⁴⁸, K. Schmieden²⁰, C. Schmitt⁸⁰, S. Schmitt^{58b}, M. Schmitz²⁰, A. Schöning^{58b}, M. Schott²⁹, D. Schouten^{158a}, J. Schovancova¹²⁴, M. Schram⁸⁴, C. Schroeder⁸⁰, N. Schroer^{58c}, G. Schuler²⁹, M.J. Schultens²⁰, J. Schultes¹⁷³, H.-C. Schultz-Coulon^{58a}, H. Schulz¹⁵, J.W. Schumacher²⁰, M. Schumacher⁴⁸, B.A. Schumm¹³⁶, Ph. Schune¹³⁵, C. Schwanenberger⁸¹, A. Schwartzman¹⁴²,

- Ph. Schwemling⁷⁷, R. Schwienhorst⁸⁷, R. Schwierz⁴³, J. Schwindling¹³⁵, T. Schwindt²⁰, M. Schwoerer⁴, G. Sciolla²², W.G. Scott¹²⁸, J. Searcy¹¹³, G. Sedov⁴¹, E. Sedykh¹²⁰, E. Segura¹¹, S.C. Seidel¹⁰², A. Seiden¹³⁶, F. Seifert⁴³, J.M. Seixas^{23a}, G. Sekhniaidze^{101a}, S.J. Sekula³⁹, K.E. Selbach⁴⁵, D.M. Seliverstov¹²⁰, B. Sellden^{145a}, G. Sellers⁷², M. Seman^{143b}, N. Semprini-Cesari^{19a,19b}, C. Serfon⁹⁷, L. Serin¹¹⁴, L. Serkin⁵⁴, R. Seuster⁹⁸, H. Severini¹¹⁰, M.E. Sevior⁸⁵, A. Sfyrla²⁹, E. Shabalina⁵⁴, M. Shamim¹¹³, L.Y. Shan^{32a}, J.T. Shank²¹, Q.T. Shao⁸⁵, M. Shapiro¹⁴, P.B. Shatalov⁹⁴, L. Shaver⁶, K. Shaw^{163a,163c}, D. Sherman¹⁷⁴, P. Sherwood⁷⁶, A. Shibata¹⁰⁷, H. Shichi¹⁰⁰, S. Shimizu²⁹, M. Shimojima⁹⁹, T. Shin⁵⁶, M. Shiyakova⁶⁴, A. Shmeleva⁹³, M.J. Shochet³⁰, D. Short¹¹⁷, S. Shrestha⁶³, E. Shulga⁹⁵, M.A. Shupe⁶, P. Sicho¹²⁴, A. Sidoti^{131a}, F. Siegert⁴⁸, Dj. Sijacki^{12a}, O. Silbert¹⁷⁰, J. Silva^{123a}, Y. Silver¹⁵², D. Silverstein¹⁴², S.B. Silverstein^{145a}, V. Simak¹²⁶, O. Simard¹³⁵, Lj. Simic^{12a}, S. Simion¹¹⁴, B. Simmons⁷⁶, R. Simonello^{88a,88b}, M. Simonyan³⁵, P. Sinervo¹⁵⁷, N.B. Sinev¹¹³, V. Sipica¹⁴⁰, G. Siragusa¹⁷², A. Sircar²⁴, A.N. Sisakyan⁶⁴, S.Yu. Sivoklokov⁹⁶, J. Sjölin^{145a,145b}, T.B. Sjursen¹³, L.A. Skinnari¹⁴, H.P. Skottowe⁵⁷, K. Skovpen¹⁰⁶, P. Skubic¹¹⁰, N. Skvorodnev²², M. Slater¹⁷, T. Slavicek¹²⁶, K. Sliwa¹⁶⁰, J. Sloper²⁹, V. Smakhtin¹⁷⁰, B.H. Smart⁴⁵, S.Yu. Smirnov⁹⁵, Y. Smirnov⁹⁵, L.N. Smirnova⁹⁶, O. Smirnova⁷⁸, B.C. Smith⁵⁷, D. Smith¹⁴², K.M. Smith⁵³, M. Smizanska⁷⁰, K. Smolek¹²⁶, A.A. Snesarev⁹³, S.W. Snow⁸¹, J. Snow¹¹⁰, J. Snuverink¹⁰⁴, S. Snyder²⁴, M. Soares^{123a}, R. Sobie^{168,j}, J. Sodomka¹²⁶, A. Soffer¹⁵², C.A. Solans¹⁶⁶, M. Solar¹²⁶, J. Solc¹²⁶, E. Soldatov⁹⁵, U. Soldevila¹⁶⁶, E. Sofifaroli Camillocci^{131a,131b}, A.A. Solodkov¹²⁷, O.V. Solovyanov¹²⁷, N. Soni², V. Sopko¹²⁶, B. Sopko¹²⁶, M. Sosebee⁷, R. Soualah^{163a,163c}, A. Soukharev¹⁰⁶, S. Spagnolo^{71a,71b}, F. Spanò⁷⁵, R. Spighi^{19a}, G. Spigo²⁹, F. Spila^{131a,131b}, R. Spiwoks²⁹, M. Spousta¹²⁵, T. Spreitzer¹⁵⁷, B. Spurlock⁷, R.D. St. Denis⁵³, J. Stahlman¹¹⁹, R. Stamen^{58a}, E. Stanecka³⁸, R.W. Stanek⁵, C. Stanescu^{133a}, M. Stanescu-Bellu⁴¹, S. Stapnes¹¹⁶, E.A. Starchenko¹²⁷, J. Stark⁵⁵, P. Staroba¹²⁴, P. Starovoitov⁹⁰, A. Staude⁹⁷, P. Stavina^{143a}, G. Steele⁵³, P. Steinbach⁴³, P. Steinberg²⁴, I. Stekl¹²⁶, B. Stelzer¹⁴¹, H.J. Stelzer⁸⁷, O. Stelzer-Chilton^{158a}, H. Stenzel⁵², S. Stern⁹⁸, K. Stevenson⁷⁴, G.A. Stewart²⁹, J.A. Stillings²⁰, M.C. Stockton⁸⁴, K. Stoerig⁴⁸, G. Stoicea^{25a}, S. Stonjek⁹⁸, P. Strachota¹²⁵, A.R. Stradling⁷, A. Straessner⁴³, J. Strandberg¹⁴⁶, S. Strandberg^{145a,145b}, A. Strandlie¹¹⁶, M. Strang¹⁰⁸, E. Strauss¹⁴², M. Strauss¹¹⁰, P. Strizenec^{143b}, R. Ströhmer¹⁷², D.M. Strom¹¹³, J.A. Strong^{75,*}, R. Stroynowski³⁹, J. Strube¹²⁸, B. Stugu¹³, I. Stumer^{24,*}, J. Stupak¹⁴⁷, P. Sturm¹⁷³, N.A. Styles⁴¹, D.A. Soh^{150,u}, D. Su¹⁴², HS. Subramania², A. Succurro¹¹, Y. Sugaya¹¹⁵, T. Sugimoto¹⁰⁰, C. Suhr¹⁰⁵, K. Suita⁶⁶, M. Suk¹²⁵, V.V. Sulin⁹³, S. Sultansoy^{3d}, T. Sumida⁶⁷, X. Sun⁵⁵, J.E. Sundermann⁴⁸, K. Suruliz¹³⁸, S. Sushkov¹¹, G. Susinno^{36a,36b}, M.R. Sutton¹⁴⁸, Y. Suzuki⁶⁵, Y. Suzuki⁶⁶, M. Svatos¹²⁴, Yu.M. Sviridov¹²⁷, S. Swedish¹⁶⁷, I. Sykora^{143a}, T. Sykora¹²⁵, B. Szeless²⁹, J. Sánchez¹⁶⁶, D. Ta¹⁰⁴, K. Tackmann⁴¹, A. Taffard¹⁶², R. Tafirout^{158a}, N. Taiblum¹⁵², Y. Takahashi¹⁰⁰, H. Takai²⁴, R. Takashima⁶⁸, H. Takeda⁶⁶, T. Takeshita¹³⁹, Y. Takubo⁶⁵, M. Talby⁸², A. Talyshев^{106,f}, M.C. Tamsett²⁴, J. Tanaka¹⁵⁴, R. Tanaka¹¹⁴, S. Tanaka¹³⁰, S. Tanaka⁶⁵, Y. Tanaka⁹⁹, A.J. Tanasijczuk¹⁴¹, K. Tani⁶⁶, N. Tannoury⁸², G.P. Tappern²⁹, S. Tapprogge⁸⁰, D. Tardif¹⁵⁷, S. Tarem¹⁵¹, F. Tarrade²⁸, G.F. Tartarelli^{88a}, P. Tas¹²⁵, M. Tasevsky¹²⁴, E. Tassi^{36a,36b}, M. Tatarkhanov¹⁴, Y. Tayalati^{134d}, C. Taylor⁷⁶, F.E. Taylor⁹¹, G.N. Taylor⁸⁵, W. Taylor^{158b}, M. Teinturier¹¹⁴, M. Teixeira Dias Castanheira⁷⁴, P. Teixeira-Dias⁷⁵, K.K. Temming⁴⁸, H. Ten Kate²⁹, P.K. Teng¹⁵⁰, S. Terada⁶⁵, K. Terashi¹⁵⁴, J. Terron⁷⁹, M. Testa⁴⁷, R.J. Teuscher^{157,j}, J. Thadome¹⁷³, J. Therhaag²⁰, T. Theveneaux-Pelzer⁷⁷, M. Thioye¹⁷⁴, S. Thoma⁴⁸, J.P. Thomas¹⁷, E.N. Thompson³⁴, P.D. Thompson¹⁷, P.D. Thompson¹⁵⁷, A.S. Thompson⁵³, L.A. Thomsen³⁵, E. Thomson¹¹⁹, M. Thomson²⁷, R.P. Thun⁸⁶, F. Tian³⁴, M.J. Tibbetts¹⁴, T. Tic¹²⁴, V.O. Tikhomirov⁹³, Y.A. Tikhonov^{106,f}, S. Timoshenko⁹⁵, P. Tipton¹⁷⁴, F.J. Tique Aires Viegas²⁹, S. Tisserant⁸², B. Toczek³⁷, T. Todorov⁴, S. Todorova-Nova¹⁶⁰, B. Toggerson¹⁶², J. Tojo⁶⁵, S. Tokár^{143a}, K. Tokunaga⁶⁶, K. Tokushuku⁶⁵, K. Tollefson⁸⁷, M. Tomoto¹⁰⁰, L. Tompkins³⁰, K. Toms¹⁰², G. Tong^{32a}, A. Tonoyan¹³, C. Topfel¹⁶, N.D. Topilin⁶⁴, I. Torchiani²⁹, E. Torrence¹¹³, H. Torres⁷⁷, E. Torró Pastor¹⁶⁶, J. Toth^{82,aa}, F. Touchard⁸², D.R. Tovey¹³⁸, T. Trefzger¹⁷², L. Tremblet²⁹, A. Tricoli²⁹, I.M. Trigger^{158a}, S. Trincaz-Duvold⁷⁷, T.N. Trinh⁷⁷, M.F. Tripiana⁶⁹, W. Trischuk¹⁵⁷, A. Trivedi^{24,z}, B. Trocmé⁵⁵, C. Troncon^{88a}, M. Trottier-McDonald¹⁴¹, M. Trzebinski³⁸, A. Trzupek³⁸, C. Tsarouchas²⁹, J.C-L. Tseng¹¹⁷, M. Tsiakiris¹⁰⁴, P.V. Tsiareshka⁸⁹, D. Tsionou^{4,ae}, G. Tsipolitis⁹, V. Tsiskaridze⁴⁸, E.G. Tskhadadze^{51a}, I.I. Tsukerman⁹⁴, V. Tsulaia¹⁴, J.-W. Tsung²⁰, S. Tsuno⁶⁵, D. Tsybychev¹⁴⁷, A. Tua¹³⁸, A. Tudorache^{25a}, V. Tudorache^{25a}, J.M. Tuggle³⁰, M. Turala³⁸, D. Turecek¹²⁶, I. Turk Cakir^{3e}, E. Turlay¹⁰⁴, R. Turra^{88a,88b}, P.M. Tuts³⁴, A. Tykhonov⁷³, M. Tylmad^{145a,145b}, M. Tyndel¹²⁸, G. Tzanakos⁸, K. Uchida²⁰, I. Ueda¹⁵⁴, R. Ueno²⁸, M. Ugland¹³, M. Uhlenbrock²⁰, M. Uhrmacher⁵⁴, F. Ukegawa¹⁵⁹, G. Unal²⁹, D.G. Underwood⁵, A. Undrus²⁴, G. Unel¹⁶², Y. Unno⁶⁵, D. Urbaniec³⁴, G. Usai⁷, M. Uslenghi^{118a,118b}, L. Vacavant⁸², V. Vacek¹²⁶, B. Vachon⁸⁴, S. Vahsen¹⁴, J. Valenta¹²⁴, P. Valente^{131a}, S. Valentini^{19a,19b}, S. Valkar¹²⁵, E. Valladolid Gallego¹⁶⁶, S. Vallecorsa¹⁵¹, J.A. Valls Ferrer¹⁶⁶, H. van der Graaf¹⁰⁴, E. van der Kraaij¹⁰⁴, R. Van Der Leeuw¹⁰⁴, E. van der Poel¹⁰⁴, D. van der Ster²⁹, N. van Eldik⁸³, P. van Gemmeren⁵, Z. van Kesteren¹⁰⁴, I. van Vulpen¹⁰⁴, M. Vanadia⁹⁸, W. Vandelli²⁹, G. Vandoni²⁹, A. Vaniachine⁵, P. Vankov⁴¹, F. Vannucci⁷⁷, F. Varela Rodriguez²⁹, R. Vari^{131a}, E.W. Varnes⁶, T. Varol⁸³, D. Varouchas¹⁴, A. Vartapetian⁷, K.E. Varvell¹⁴⁹, V.I. Vassilakopoulos⁵⁶, F. Vazeille³³, T. Vazquez Schroeder⁵⁴, G. Vegni^{88a,88b}, J.J. Veillet¹¹⁴, C. Vellidis⁸, F. Veloso^{123a}, R. Veness²⁹, S. Veneziano^{131a}, A. Ventura^{71a,71b},

D. Ventura¹³⁷, M. Venturi⁴⁸, N. Venturi¹⁵⁷, V. Vercesi^{118a}, M. Verducci¹³⁷, W. Verkerke¹⁰⁴, J.C. Vermeulen¹⁰⁴, A. Vest⁴³, M.C. Vetterli^{141,d}, I. Vichou¹⁶⁴, T. Vickey^{144b,af}, O.E. Vickey Boeriu^{144b}, G.H.A. Viehauser¹¹⁷, S. Viel¹⁶⁷, M. Villa^{19a,19b}, M. Villaplana Perez¹⁶⁶, E. Vilucchi⁴⁷, M.G. Vinchter²⁸, E. Vinek²⁹, V.B. Vinogradov⁶⁴, M. Virchaux^{135,*}, J. Virzi¹⁴, O. Vitells¹⁷⁰, M. Viti⁴¹, I. Vivarelli⁴⁸, F. Vives Vaque², S. Vlachos⁹, D. Vladouli⁹⁷, M. Vlasak¹²⁶, N. Vlasov²⁰, A. Vogel²⁰, P. Vokac¹²⁶, G. Volpi⁴⁷, M. Volpi⁸⁵, G. Volpini^{88a}, H. von der Schmitt⁹⁸, J. von Loeben⁹⁸, H. von Radziewski⁴⁸, E. von Toerne²⁰, V. Vorobel¹²⁵, A.P. Vorobiev¹²⁷, V. Vorwerk¹¹, M. Vos¹⁶⁶, R. Voss²⁹, T.T. Voss¹⁷³, J.H. Vossebeld⁷², N. Vranjes¹³⁵, M. Vranjes Milosavljevic¹⁰⁴, V. Vrba¹²⁴, M. Vreeswijk¹⁰⁴, T. Vu Anh⁴⁸, R. Vuillermet²⁹, I. Vukotic¹¹⁴, W. Wagner¹⁷³, P. Wagner¹¹⁹, H. Wahlen¹⁷³, J. Wakabayashi¹⁰⁰, S. Walch⁸⁶, J. Walder⁷⁰, R. Walker⁹⁷, W. Walkowiak¹⁴⁰, R. Wall¹⁷⁴, P. Waller⁷², C. Wang⁴⁴, H. Wang¹⁷¹, H. Wang^{32b,ag}, J. Wang¹⁵⁰, J. Wang⁵⁵, J.C. Wang¹³⁷, R. Wang¹⁰², S.M. Wang¹⁵⁰, T. Wang²⁰, A. Warburton⁸⁴, C.P. Ward²⁷, M. Warsinsky⁴⁸, C. Wasicki⁴¹, P.M. Watkins¹⁷, A.T. Watson¹⁷, I.J. Watson¹⁴⁹, M.F. Watson¹⁷, G. Watts¹³⁷, S. Watts⁸¹, A.T. Waugh¹⁴⁹, B.M. Waugh⁷⁶, M. Weber¹²⁸, M.S. Weber¹⁶, P. Weber⁵⁴, A.R. Weidberg¹¹⁷, P. Weigell⁹⁸, J. Weingarten⁵⁴, C. Weiser⁴⁸, H. Wellenstein²², P.S. Wells²⁹, T. Wenaus²⁴, D. Wendland¹⁵, S. Wendler¹²², Z. Weng^{150,u}, T. Wengler²⁹, S. Wenig²⁹, N. Wermes²⁰, M. Werner⁴⁸, P. Werner²⁹, M. Werth¹⁶², M. Wessels^{58a}, J. Wetter¹⁶⁰, C. Weydert⁵⁵, K. Whalen²⁸, S.J. Wheeler-Ellis¹⁶², S.P. Whitaker²¹, A. White⁷, M.J. White⁸⁵, S.R. Whitehead¹¹⁷, D. Whiteson¹⁶², D. Whittington⁶⁰, F. Wicek¹¹⁴, D. Wicke¹⁷³, F.J. Wickens¹²⁸, W. Wiedenmann¹⁷¹, M. Wieler¹²⁸, P. Wienemann²⁰, C. Wiglesworth⁷⁴, L.A.M. Wiik-Fuchs⁴⁸, P.A. Wijeratne⁷⁶, A. Wildauer¹⁶⁶, M.A. Wildt^{41,q}, I. Wilhelm¹²⁵, H.G. Wilkens²⁹, J.Z. Will⁹⁷, E. Williams³⁴, H.H. Williams¹¹⁹, W. Willis³⁴, S. Willocq⁸³, J.A. Wilson¹⁷, M.G. Wilson¹⁴², A. Wilson⁸⁶, I. Wingerter-Seez⁴, S. Winkelmann⁴⁸, F. Winklmeier²⁹, M. Wittgen¹⁴², M.W. Wolter³⁸, H. Wolters^{123a,h}, W.C. Wong⁴⁰, G. Wooden⁸⁶, B.K. Wosiek³⁸, J. Wotschack²⁹, M.J. Woudstra⁸³, K.W. Wozniak³⁸, K. Wraight⁵³, C. Wright⁵³, M. Wright⁵³, B. Wrona⁷², S.L. Wu¹⁷¹, X. Wu⁴⁹, Y. Wu^{32b,ah}, E. Wulf³⁴, R. Wunstorf⁴², B.M. Wynne⁴⁵, S. Xella³⁵, M. Xiao¹³⁵, S. Xie⁴⁸, Y. Xie^{32a}, C. Xu^{32b,w}, D. Xu¹³⁸, G. Xu^{32a}, B. Yabsley¹⁴⁹, S. Yacoob^{144b}, M. Yamada⁶⁵, H. Yamaguchi¹⁵⁴, A. Yamamoto⁶⁵, K. Yamamoto⁶³, S. Yamamoto¹⁵⁴, T. Yamamura¹⁵⁴, T. Yamanaka¹⁵⁴, J. Yamaoka⁴⁴, T. Yamazaki¹⁵⁴, Y. Yamazaki⁶⁶, Z. Yan²¹, H. Yang⁸⁶, U.K. Yang⁸¹, Y. Yang⁶⁰, Y. Yang^{32a}, Z. Yang^{145a,145b}, S. Yanush⁹⁰, Y. Yao¹⁴, Y. Yasu⁶⁵, G.V. Ybeles Smit¹²⁹, J. Ye³⁹, S. Ye²⁴, M. Yilmaz^{3c}, R. Yoosoofmiya¹²², K. Yorita¹⁶⁹, R. Yoshida⁵, C. Young¹⁴², S. Youssef²¹, D. Yu²⁴, J. Yu⁷, J. Yu¹¹¹, L. Yuan^{32a,ai}, A. Yurkewicz¹⁰⁵, B. Zabinski³⁸, V.G. Zaets¹²⁷, R. Zaidan⁶², A.M. Zaitsev¹²⁷, Z. Zajacova²⁹, L. Zanello^{131a,131b}, A. Zaytsev¹⁰⁶, C. Zeitnitz¹⁷³, M. Zeller¹⁷⁴, M. Zeman¹²⁴, A. Zemla³⁸, C. Zendler²⁰, O. Zenin¹²⁷, T. Ženiš^{143a}, Z. Zinonos^{121a,121b}, S. Zenz¹⁴, D. Zerwas¹¹⁴, G. Zevi della Porta⁵⁷, Z. Zhan^{32d}, D. Zhang^{32b,ag}, H. Zhang⁸⁷, J. Zhang⁵, X. Zhang^{32d}, Z. Zhang¹¹⁴, L. Zhao¹⁰⁷, T. Zhao¹³⁷, Z. Zhao^{32b}, A. Zhemchugov⁶⁴, S. Zheng^{32a}, J. Zhong¹¹⁷, B. Zhou⁸⁶, N. Zhou¹⁶², Y. Zhou¹⁵⁰, C.G. Zhu^{32d}, H. Zhu⁴¹, J. Zhu⁸⁶, Y. Zhu^{32b}, X. Zhuang⁹⁷, V. Zhuravlov⁹⁸, D. Ziemska⁶⁰, R. Zimmermann²⁰, S. Zimmermann²⁰, S. Zimmermann⁴⁸, M. Ziolkowski¹⁴⁰, R. Zitoun⁴, L. Živković³⁴, V.V. Zmouchko^{127,*}, G. Zobernig¹⁷¹, A. Zoccoli^{19a,19b}, A. Zsenei²⁹, M. zur Nedden¹⁵, V. Zutshi¹⁰⁵, L. Zwalski²⁹.

¹ University at Albany, Albany NY, United States of America² Department of Physics, University of Alberta, Edmonton AB, Canada³ ^(a)Department of Physics, Ankara University, Ankara; ^(b)Department of Physics, Dumlupinar University, Kutahya;^(c)Department of Physics, Gazi University, Ankara; ^(d)Division of Physics, TOBB University of Economics and Technology, Ankara; ^(e)Turkish Atomic Energy Authority, Ankara, Turkey⁴ LAPP, CNRS/IN2P3 and Université de Savoie, Annecy-le-Vieux, France⁵ High Energy Physics Division, Argonne National Laboratory, Argonne IL, United States of America⁶ Department of Physics, University of Arizona, Tucson AZ, United States of America⁷ Department of Physics, The University of Texas at Arlington, Arlington TX, United States of America⁸ Physics Department, University of Athens, Athens, Greece⁹ Physics Department, National Technical University of Athens, Zografou, Greece¹⁰ Institute of Physics, Azerbaijan Academy of Sciences, Baku, Azerbaijan¹¹ Institut de Física d'Altes Energies and Departament de Física de la Universitat Autònoma de Barcelona and ICREA, Barcelona, Spain¹² ^(a)Institute of Physics, University of Belgrade, Belgrade; ^(b)Vinca Institute of Nuclear Sciences, University of Belgrade, Belgrade, Serbia¹³ Department for Physics and Technology, University of Bergen, Bergen, Norway¹⁴ Physics Division, Lawrence Berkeley National Laboratory and University of California, Berkeley CA, United States of America¹⁵ Department of Physics, Humboldt University, Berlin, Germany¹⁶ Albert Einstein Center for Fundamental Physics and Laboratory for High Energy Physics, University of Bern, Bern, Switzerland¹⁷ School of Physics and Astronomy, University of Birmingham, Birmingham, United Kingdom

- ¹⁸ ^(a)Department of Physics, Bogazici University, Istanbul; ^(b)Division of Physics, Dogus University, Istanbul;
^(c)Department of Physics Engineering, Gaziantep University, Gaziantep; ^(d)Department of Physics, Istanbul Technical University, Istanbul, Turkey
- ¹⁹ ^(a)INFN Sezione di Bologna; ^(b)Dipartimento di Fisica, Università di Bologna, Bologna, Italy
- ²⁰ Physikalisches Institut, University of Bonn, Bonn, Germany
- ²¹ Department of Physics, Boston University, Boston MA, United States of America
- ²² Department of Physics, Brandeis University, Waltham MA, United States of America
- ²³ ^(a)Universidade Federal do Rio De Janeiro COPPE/EE/IF, Rio de Janeiro; ^(b)Federal University of Juiz de Fora (UFJF), Juiz de Fora; ^(c)Federal University of Sao Joao del Rei (UFSJ), Sao Joao del Rei; ^(d)Instituto de Fisica, Universidade de Sao Paulo, Sao Paulo, Brazil
- ²⁴ Physics Department, Brookhaven National Laboratory, Upton NY, United States of America
- ²⁵ ^(a)National Institute of Physics and Nuclear Engineering, Bucharest; ^(b)University Politehnica Bucharest, Bucharest; ^(c)West University in Timisoara, Timisoara, Romania
- ²⁶ Departamento de Física, Universidad de Buenos Aires, Buenos Aires, Argentina
- ²⁷ Cavendish Laboratory, University of Cambridge, Cambridge, United Kingdom
- ²⁸ Department of Physics, Carleton University, Ottawa ON, Canada
- ²⁹ CERN, Geneva, Switzerland
- ³⁰ Enrico Fermi Institute, University of Chicago, Chicago IL, United States of America
- ³¹ ^(a)Departamento de Fisica, Pontificia Universidad Católica de Chile, Santiago; ^(b)Departamento de Física, Universidad Técnica Federico Santa María, Valparaíso, Chile
- ³² ^(a)Institute of High Energy Physics, Chinese Academy of Sciences, Beijing; ^(b)Department of Modern Physics, University of Science and Technology of China, Anhui; ^(c)Department of Physics, Nanjing University, Jiangsu; ^(d)School of Physics, Shandong University, Shandong, China
- ³³ Laboratoire de Physique Corpusculaire, Clermont Université and Université Blaise Pascal and CNRS/IN2P3, Aubiere Cedex, France
- ³⁴ Nevis Laboratory, Columbia University, Irvington NY, United States of America
- ³⁵ Niels Bohr Institute, University of Copenhagen, Kobenhavn, Denmark
- ³⁶ ^(a)INFN Gruppo Collegato di Cosenza; ^(b)Dipartimento di Fisica, Università della Calabria, Arcavata di Rende, Italy
- ³⁷ AGH University of Science and Technology, Faculty of Physics and Applied Computer Science, Krakow, Poland
- ³⁸ The Henryk Niewodniczanski Institute of Nuclear Physics, Polish Academy of Sciences, Krakow, Poland
- ³⁹ Physics Department, Southern Methodist University, Dallas TX, United States of America
- ⁴⁰ Physics Department, University of Texas at Dallas, Richardson TX, United States of America
- ⁴¹ DESY, Hamburg and Zeuthen, Germany
- ⁴² Institut für Experimentelle Physik IV, Technische Universität Dortmund, Dortmund, Germany
- ⁴³ Institut für Kern- und Teilchenphysik, Technical University Dresden, Dresden, Germany
- ⁴⁴ Department of Physics, Duke University, Durham NC, United States of America
- ⁴⁵ SUPA - School of Physics and Astronomy, University of Edinburgh, Edinburgh, United Kingdom
- ⁴⁶ Fachhochschule Wiener Neustadt, Johannes Gutenbergstrasse 3 2700 Wiener Neustadt, Austria
- ⁴⁷ INFN Laboratori Nazionali di Frascati, Frascati, Italy
- ⁴⁸ Fakultät für Mathematik und Physik, Albert-Ludwigs-Universität, Freiburg i.Br., Germany
- ⁴⁹ Section de Physique, Université de Genève, Geneva, Switzerland
- ⁵⁰ ^(a)INFN Sezione di Genova; ^(b)Dipartimento di Fisica, Università di Genova, Genova, Italy
- ⁵¹ ^(a)E.Andronikashvili Institute of Physics, Tbilisi State University, Tbilisi; ^(b)High Energy Physics Institute, Tbilisi State University, Tbilisi, Georgia
- ⁵² II Physikalisches Institut, Justus-Liebig-Universität Giessen, Giessen, Germany
- ⁵³ SUPA - School of Physics and Astronomy, University of Glasgow, Glasgow, United Kingdom
- ⁵⁴ II Physikalisches Institut, Georg-August-Universität, Göttingen, Germany
- ⁵⁵ Laboratoire de Physique Subatomique et de Cosmologie, Université Joseph Fourier and CNRS/IN2P3 and Institut National Polytechnique de Grenoble, Grenoble, France
- ⁵⁶ Department of Physics, Hampton University, Hampton VA, United States of America
- ⁵⁷ Laboratory for Particle Physics and Cosmology, Harvard University, Cambridge MA, United States of America
- ⁵⁸ ^(a)Kirchhoff-Institut für Physik, Ruprecht-Karls-Universität Heidelberg, Heidelberg; ^(b)Physikalisches Institut, Ruprecht-Karls-Universität Heidelberg, Heidelberg; ^(c)ZITI Institut für technische Informatik, Ruprecht-Karls-Universität Heidelberg, Mannheim, Germany
- ⁵⁹ Faculty of Applied Information Science, Hiroshima Institute of Technology, Hiroshima, Japan
- ⁶⁰ Department of Physics, Indiana University, Bloomington IN, United States of America
- ⁶¹ Institut für Astro- und Teilchenphysik, Leopold-Franzens-Universität, Innsbruck, Austria

- ⁶² University of Iowa, Iowa City IA, United States of America
⁶³ Department of Physics and Astronomy, Iowa State University, Ames IA, United States of America
⁶⁴ Joint Institute for Nuclear Research, JINR Dubna, Dubna, Russia
⁶⁵ KEK, High Energy Accelerator Research Organization, Tsukuba, Japan
⁶⁶ Graduate School of Science, Kobe University, Kobe, Japan
⁶⁷ Faculty of Science, Kyoto University, Kyoto, Japan
⁶⁸ Kyoto University of Education, Kyoto, Japan
⁶⁹ Instituto de Física La Plata, Universidad Nacional de La Plata and CONICET, La Plata, Argentina
⁷⁰ Physics Department, Lancaster University, Lancaster, United Kingdom
⁷¹ ^(a)INFN Sezione di Lecce; ^(b)Dipartimento di Fisica, Università del Salento, Lecce, Italy
⁷² Oliver Lodge Laboratory, University of Liverpool, Liverpool, United Kingdom
⁷³ Department of Physics, Jožef Stefan Institute and University of Ljubljana, Ljubljana, Slovenia
⁷⁴ School of Physics and Astronomy, Queen Mary University of London, London, United Kingdom
⁷⁵ Department of Physics, Royal Holloway University of London, Surrey, United Kingdom
⁷⁶ Department of Physics and Astronomy, University College London, London, United Kingdom
⁷⁷ Laboratoire de Physique Nucléaire et de Hautes Energies, UPMC and Université Paris-Diderot and CNRS/IN2P3, Paris, France
⁷⁸ Fysiska institutionen, Lunds universitet, Lund, Sweden
⁷⁹ Departamento de Fisica Teorica C-15, Universidad Autonoma de Madrid, Madrid, Spain
⁸⁰ Institut für Physik, Universität Mainz, Mainz, Germany
⁸¹ School of Physics and Astronomy, University of Manchester, Manchester, United Kingdom
⁸² CPPM, Aix-Marseille Université and CNRS/IN2P3, Marseille, France
⁸³ Department of Physics, University of Massachusetts, Amherst MA, United States of America
⁸⁴ Department of Physics, McGill University, Montreal QC, Canada
⁸⁵ School of Physics, University of Melbourne, Victoria, Australia
⁸⁶ Department of Physics, The University of Michigan, Ann Arbor MI, United States of America
⁸⁷ Department of Physics and Astronomy, Michigan State University, East Lansing MI, United States of America
⁸⁸ ^(a)INFN Sezione di Milano; ^(b)Dipartimento di Fisica, Università di Milano, Milano, Italy
⁸⁹ B.I. Stepanov Institute of Physics, National Academy of Sciences of Belarus, Minsk, Republic of Belarus
⁹⁰ National Scientific and Educational Centre for Particle and High Energy Physics, Minsk, Republic of Belarus
⁹¹ Department of Physics, Massachusetts Institute of Technology, Cambridge MA, United States of America
⁹² Group of Particle Physics, University of Montreal, Montreal QC, Canada
⁹³ P.N. Lebedev Institute of Physics, Academy of Sciences, Moscow, Russia
⁹⁴ Institute for Theoretical and Experimental Physics (ITEP), Moscow, Russia
⁹⁵ Moscow Engineering and Physics Institute (MEPhI), Moscow, Russia
⁹⁶ Skobeltsyn Institute of Nuclear Physics, Lomonosov Moscow State University, Moscow, Russia
⁹⁷ Fakultät für Physik, Ludwig-Maximilians-Universität München, München, Germany
⁹⁸ Max-Planck-Institut für Physik (Werner-Heisenberg-Institut), München, Germany
⁹⁹ Nagasaki Institute of Applied Science, Nagasaki, Japan
¹⁰⁰ Graduate School of Science, Nagoya University, Nagoya, Japan
¹⁰¹ ^(a)INFN Sezione di Napoli; ^(b)Dipartimento di Scienze Fisiche, Università di Napoli, Napoli, Italy
¹⁰² Department of Physics and Astronomy, University of New Mexico, Albuquerque NM, United States of America
¹⁰³ Institute for Mathematics, Astrophysics and Particle Physics, Radboud University Nijmegen/Nikhef, Nijmegen, Netherlands
¹⁰⁴ Nikhef National Institute for Subatomic Physics and University of Amsterdam, Amsterdam, Netherlands
¹⁰⁵ Department of Physics, Northern Illinois University, DeKalb IL, United States of America
¹⁰⁶ Budker Institute of Nuclear Physics, SB RAS, Novosibirsk, Russia
¹⁰⁷ Department of Physics, New York University, New York NY, United States of America
¹⁰⁸ Ohio State University, Columbus OH, United States of America
¹⁰⁹ Faculty of Science, Okayama University, Okayama, Japan
¹¹⁰ Homer L. Dodge Department of Physics and Astronomy, University of Oklahoma, Norman OK, United States of America
¹¹¹ Department of Physics, Oklahoma State University, Stillwater OK, United States of America
¹¹² Palacký University, RCPTM, Olomouc, Czech Republic
¹¹³ Center for High Energy Physics, University of Oregon, Eugene OR, United States of America
¹¹⁴ LAL, Univ. Paris-Sud and CNRS/IN2P3, Orsay, France
¹¹⁵ Graduate School of Science, Osaka University, Osaka, Japan
¹¹⁶ Department of Physics, University of Oslo, Oslo, Norway

- ¹¹⁷ Department of Physics, Oxford University, Oxford, United Kingdom
¹¹⁸ ^(a)INFN Sezione di Pavia; ^(b)Dipartimento di Fisica, Università di Pavia, Pavia, Italy
¹¹⁹ Department of Physics, University of Pennsylvania, Philadelphia PA, United States of America
¹²⁰ Petersburg Nuclear Physics Institute, Gatchina, Russia
¹²¹ ^(a)INFN Sezione di Pisa; ^(b)Dipartimento di Fisica E. Fermi, Università di Pisa, Pisa, Italy
¹²² Department of Physics and Astronomy, University of Pittsburgh, Pittsburgh PA, United States of America
¹²³ ^(a)Laboratorio de Instrumentacao e Fisica Experimental de Particulas - LIP, Lisboa, Portugal; ^(b)Departamento de Fisica Teorica y del Cosmos and CAFPE, Universidad de Granada, Granada, Spain
¹²⁴ Institute of Physics, Academy of Sciences of the Czech Republic, Praha, Czech Republic
¹²⁵ Faculty of Mathematics and Physics, Charles University in Prague, Praha, Czech Republic
¹²⁶ Czech Technical University in Prague, Praha, Czech Republic
¹²⁷ State Research Center Institute for High Energy Physics, Protvino, Russia
¹²⁸ Particle Physics Department, Rutherford Appleton Laboratory, Didcot, United Kingdom
¹²⁹ Physics Department, University of Regina, Regina SK, Canada
¹³⁰ Ritsumeikan University, Kusatsu, Shiga, Japan
¹³¹ ^(a)INFN Sezione di Roma I; ^(b)Dipartimento di Fisica, Università La Sapienza, Roma, Italy
¹³² ^(a)INFN Sezione di Roma Tor Vergata; ^(b)Dipartimento di Fisica, Università di Roma Tor Vergata, Roma, Italy
¹³³ ^(a)INFN Sezione di Roma Tre; ^(b)Dipartimento di Fisica, Università Roma Tre, Roma, Italy
¹³⁴ ^(a)Faculté des Sciences Ain Chock, Réseau Universitaire de Physique des Hautes Energies - Université Hassan II, Casablanca; ^(b)Centre National de l'Energie des Sciences Techniques Nucleaires, Rabat; ^(c)Faculté des Sciences Semlalia, Université Cadi Ayyad, LPHEA-Marrakech; ^(d)Faculté des Sciences, Université Mohamed Premier and LPTPM, Oujda; ^(e)Faculté des Sciences, Université Mohammed V- Agdal, Rabat, Morocco
¹³⁵ DSM/IRFU (Institut de Recherches sur les Lois Fondamentales de l'Univers), CEA Saclay (Commissariat a l'Energie Atomique), Gif-sur-Yvette, France
¹³⁶ Santa Cruz Institute for Particle Physics, University of California Santa Cruz, Santa Cruz CA, United States of America
¹³⁷ Department of Physics, University of Washington, Seattle WA, United States of America
¹³⁸ Department of Physics and Astronomy, University of Sheffield, Sheffield, United Kingdom
¹³⁹ Department of Physics, Shinshu University, Nagano, Japan
¹⁴⁰ Fachbereich Physik, Universität Siegen, Siegen, Germany
¹⁴¹ Department of Physics, Simon Fraser University, Burnaby BC, Canada
¹⁴² SLAC National Accelerator Laboratory, Stanford CA, United States of America
¹⁴³ ^(a)Faculty of Mathematics, Physics & Informatics, Comenius University, Bratislava; ^(b)Department of Subnuclear Physics, Institute of Experimental Physics of the Slovak Academy of Sciences, Kosice, Slovak Republic
¹⁴⁴ ^(a)Department of Physics, University of Johannesburg, Johannesburg; ^(b)School of Physics, University of the Witwatersrand, Johannesburg, South Africa
¹⁴⁵ ^(a)Department of Physics, Stockholm University; ^(b)The Oskar Klein Centre, Stockholm, Sweden
¹⁴⁶ Physics Department, Royal Institute of Technology, Stockholm, Sweden
¹⁴⁷ Departments of Physics & Astronomy and Chemistry, Stony Brook University, Stony Brook NY, United States of America
¹⁴⁸ Department of Physics and Astronomy, University of Sussex, Brighton, United Kingdom
¹⁴⁹ School of Physics, University of Sydney, Sydney, Australia
¹⁵⁰ Institute of Physics, Academia Sinica, Taipei, Taiwan
¹⁵¹ Department of Physics, Technion: Israel Inst. of Technology, Haifa, Israel
¹⁵² Raymond and Beverly Sackler School of Physics and Astronomy, Tel Aviv University, Tel Aviv, Israel
¹⁵³ Department of Physics, Aristotle University of Thessaloniki, Thessaloniki, Greece
¹⁵⁴ International Center for Elementary Particle Physics and Department of Physics, The University of Tokyo, Tokyo, Japan
¹⁵⁵ Graduate School of Science and Technology, Tokyo Metropolitan University, Tokyo, Japan
¹⁵⁶ Department of Physics, Tokyo Institute of Technology, Tokyo, Japan
¹⁵⁷ Department of Physics, University of Toronto, Toronto ON, Canada
¹⁵⁸ ^(a)TRIUMF, Vancouver BC; ^(b)Department of Physics and Astronomy, York University, Toronto ON, Canada
¹⁵⁹ Institute of Pure and Applied Sciences, University of Tsukuba,1-1-1 Tennodai,Tsukuba, Ibaraki 305-8571, Japan
¹⁶⁰ Science and Technology Center, Tufts University, Medford MA, United States of America
¹⁶¹ Centro de Investigaciones, Universidad Antonio Narino, Bogota, Colombia
¹⁶² Department of Physics and Astronomy, University of California Irvine, Irvine CA, United States of America
¹⁶³ ^(a)INFN Gruppo Collegato di Udine; ^(b)ICTP, Trieste; ^(c)Dipartimento di Chimica, Fisica e Ambiente, Università di Udine, Udine, Italy

- ¹⁶⁴ Department of Physics, University of Illinois, Urbana IL, United States of America
¹⁶⁵ Department of Physics and Astronomy, University of Uppsala, Uppsala, Sweden
¹⁶⁶ Instituto de Física Corpuscular (IFIC) and Departamento de Física Atómica, Molecular y Nuclear and Departamento de Ingeniería Electrónica and Instituto de Microelectrónica de Barcelona (IMB-CNM), University of Valencia and CSIC, Valencia, Spain
¹⁶⁷ Department of Physics, University of British Columbia, Vancouver BC, Canada
¹⁶⁸ Department of Physics and Astronomy, University of Victoria, Victoria BC, Canada
¹⁶⁹ Waseda University, Tokyo, Japan
¹⁷⁰ Department of Particle Physics, The Weizmann Institute of Science, Rehovot, Israel
¹⁷¹ Department of Physics, University of Wisconsin, Madison WI, United States of America
¹⁷² Fakultät für Physik und Astronomie, Julius-Maximilians-Universität, Würzburg, Germany
¹⁷³ Fachbereich C Physik, Bergische Universität Wuppertal, Wuppertal, Germany
¹⁷⁴ Department of Physics, Yale University, New Haven CT, United States of America
¹⁷⁵ Yerevan Physics Institute, Yerevan, Armenia
¹⁷⁶ Domaine scientifique de la Doua, Centre de Calcul CNRS/IN2P3, Villeurbanne Cedex, France
^a Also at Laboratorio de Instrumentacao e Fisica Experimental de Particulas - LIP, Lisboa, Portugal
^b Also at Faculdade de Ciencias and CFNUL, Universidade de Lisboa, Lisboa, Portugal
^c Also at Particle Physics Department, Rutherford Appleton Laboratory, Didcot, United Kingdom
^d Also at TRIUMF, Vancouver BC, Canada
^e Also at Department of Physics, California State University, Fresno CA, United States of America
^f Also at Novosibirsk State University, Novosibirsk, Russia
^g Also at Fermilab, Batavia IL, United States of America
^h Also at Department of Physics, University of Coimbra, Coimbra, Portugal
ⁱ Also at Università di Napoli Parthenope, Napoli, Italy
^j Also at Institute of Particle Physics (IPP), Canada
^k Also at Department of Physics, Middle East Technical University, Ankara, Turkey
^l Also at Louisiana Tech University, Ruston LA, United States of America
^m Also at Department of Physics and Astronomy, University College London, London, United Kingdom
ⁿ Also at Group of Particle Physics, University of Montreal, Montreal QC, Canada
^o Also at Department of Physics, University of Cape Town, Cape Town, South Africa
^p Also at Institute of Physics, Azerbaijan Academy of Sciences, Baku, Azerbaijan
^q Also at Institut für Experimentalphysik, Universität Hamburg, Hamburg, Germany
^r Also at Manhattan College, New York NY, United States of America
^s Also at School of Physics, Shandong University, Shandong, China
^t Also at CPPM, Aix-Marseille Université and CNRS/IN2P3, Marseille, France
^u Also at School of Physics and Engineering, Sun Yat-sen University, Guangzhou, China
^v Also at Academia Sinica Grid Computing, Institute of Physics, Academia Sinica, Taipei, Taiwan
^w Also at DSM/IRFU (Institut de Recherches sur les Lois Fondamentales de l'Univers), CEA Saclay (Commissariat à l'Energie Atomique), Gif-sur-Yvette, France
^x Also at Section de Physique, Université de Genève, Geneva, Switzerland
^y Also at Departamento de Fisica, Universidade de Minho, Braga, Portugal
^z Also at Department of Physics and Astronomy, University of South Carolina, Columbia SC, United States of America
^{aa} Also at Institute for Particle and Nuclear Physics, Wigner Research Centre for Physics, Budapest, Hungary
^{ab} Also at California Institute of Technology, Pasadena CA, United States of America
^{ac} Also at Institute of Physics, Jagiellonian University, Krakow, Poland
^{ad} Also at LAL, Univ. Paris-Sud and CNRS/IN2P3, Orsay, France
^{ae} Also at Department of Physics and Astronomy, University of Sheffield, Sheffield, United Kingdom
^{af} Also at Department of Physics, Oxford University, Oxford, United Kingdom
^{ag} Also at Institute of Physics, Academia Sinica, Taipei, Taiwan
^{ah} Also at Department of Physics, The University of Michigan, Ann Arbor MI, United States of America
^{ai} Also at Laboratoire de Physique Nucléaire et de Hautes Energies, UPMC and Université Paris-Diderot and CNRS/IN2P3, Paris, France
^{*} Deceased